

https://dspace.org/

Biodiesel production with waste product cycling

Makhale, Itumeleng

2018

https://hdl.handle.net/10539/26729

Makhale, Itumeleng Katlego, (2018) Biodiesel production with waste product cycling, University of the Witwatersrand, Johannesburg, https://hdl.handle.net/10539/26729.

Downloaded from a DSpace repository. https://dspace.org/

M.Sc. submission

BIODIESEL PRODUCTION WITH WASTE PRODUCT CYCLING

By Itumeleng Makhale
0604451y

For the degree: Master of Science in Microbiology & Biotechnology

Student:		Itumeleng Makhale
Supervisor:		Dr. Karl Rumbold
Co-Supervisor:		Dr. Dirk Swanevelder
Advisor:		Prof. Vince Gray

BIODIESEL PRODUCTION WITH WASTE PRODUCT CYCLING

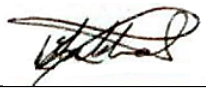
Itumeleng Makhale

A Dissertation submitted to the Faculty of Science, University of the Witwatersrand, in fulfilment of the requirements for the degree of Master of Science

Johannesburg, 2016

1 DECLARATION

I declare that this Dissertation is my own, unaided work. It is being submitted for the Degree of Master of Science at the University of the Witwatersrand, Johannesburg. It has not been submitted before for any degree or examination at any other University.



(Signature of candidate)

22 day of August 2018

in Germiston.

2 ABSTRACT

Bio-derived fuels such as biodiesel and bioethanol have gained considerable attention as liquid transport fuels. Economic viability for large-scale bio-based fuel production in South Africa remains a contentious issue. This study aims to describe an enzymatic biodiesel production process, with a greater goal to stimulate small-scale biodiesel production in and around the country.

The possibility of using an *E. coli* host strain to develop a bacterial-biodiesel generating system was considered utilising a synthetic lipase for the trans-esterification of sunflower oil. The conditions for expression were evaluated with induction trials at 30 and 37 °C respectively; the concentration of IPTG was adjusted in 0.25 mM increments from 0 to 1 mM. The ideal concentration of IPTG was 0.75 mM, and the ideal temperature was 37 °C. The lipase's hydrolytic capacity was further evaluated on para-Nitrophenol palmitate, and the catalytic amount necessary was determined to be below 0.00729 µg for the substrate concentrations employed.

3 ACKNOWLEDGEMENTS

I sincerely wish to thank my supervisor, Dr. Karl Rumbold, for giving me the opportunity to do this research work, and for offering me an endless number of facilities since the beginning. There have been many frustrations along the way, but I sincerely thank him for always believing that my work was worth the effort.

Appreciation is also forwarded in spades to my co-supervisor, Dr. Dirk Swanevelder without whom the writing process would have been a minefield. Despite the workload he has, he always took the time to make himself available where his expertise was needed.

I would like also thank the ladies of Chrissie's Lab – Mmaabo, Imah (Imanu), Sarah, Helen. I appreciate all the lighter moments we've shared. I thank you all as well for your expertise and advice. To the School of Molecular & Cell Biology, and the people therein, thank you for your support.

And an overwhelming thanks to Nomusa Khoza. Without you, I wouldn't have gotten this far.

Contents

1 DECLARATION iii
2 ABSTRACT iv
3 ACKNOWLEDGEMENTS v
4 LIST OF FIGURES viii
5 LIST OF TABLES xiii
6 ABBREVIATIONS xiv
7 LITERATURE REVIEW 1
7.1 Biofuels & the National Biofuels Industrial Strategy of South Africa 1
7.1.1 Biodiesel production 4
7.1.2 Whole-cell biocatalysts for biodiesel production 11
7.2 Glycerol 12
7.2.1 The glycerol "glut" 13
7.2.2 Value-added uses for crude glycerol 14
7.3 Tandem conversions 23
7.3.1 "E-diesel" 26
7.4 Research aim 27
8 MATERIALS & METHODS 28
8.1 Lipase selection 28
8.2 Preparing LipA and LipB from GenScript pUC57 29
8.2.1 LipB 29
8.2.2 LipA PCR amplification from pUC57 30
8.2.3 pETDuet-1 vector and features 31
8.2.4 pETDuet with LipA (MCS1) and LipB (MCS2) 32
8.2.5 Sequencing of pETDuet with inserts by Inqaba Biotechnical Industries (Pty) Ltd 32
8.3 Protein Expression 32
8.3.1 Transforming into *E. coli* BL21 (DE3) 32
8.3.2 Induction pETDuet with LipA, with LipA and LipB, and with LipB only 33
8.3.3 Preliminary tests for enzyme activity 34
9 RESULTS 35
9.1 Lipase and chaperone 35
9.1.1 Chaperone (LipA) 36
9.1.2 Lipase (LipB) (Figure 12) 37

9.1.3 Cloning 38
9.1.4 pETDuet with LipA at MCS1 & pETDuet with LipB at MCS2 – cloning verification through sequence analysis 41
9.1.5 Induction trials 46
9.1.6 Preliminary tests for activity 51
10 DISCUSSION 55
11 REFERENCES 60
12 APPENDIX 72
12.1 Gene optimisation and syntheses 72
12.2 LipA sequences 72
12.3 LipB sequences 73

4 LIST OF FIGURES

Figure 1: Reaction mechanism of triglyceride transesterification. Here, one triglyceride molecule reacts with 3 moles of alcohol to produce 1 mole of glycerol and 3 moles of FAAE with the help of a catalyst. Triglycerides refer to plant/animal oils and/or fats. Catalysts may be enzymes (e.g. lipase) or chemicals (e.g. potassium hydroxide (KOH) or sodium hydroxide (NaOH)). Adapted from (Pereira *et. al.*, 2014). 5

Figure 2: (A) Lack of interfacial activation in *Streptococcus equi* ssp. *equi* catalyzed hydrolysis of vinyl propionate compared against the activity of a lipase (adapted fromXie *et. al.* (2008)). (B) The catalytic mechanism of a lipase with the surface loop, ("lid") regulating catalysis, (left) closed conformation (inactive); (right) open conformation (active form) at a hydrophobic interface where interfacial activation occurs (image sourced from: http://www.icp.csic.es/biocatalisis/web3/Palomoweb/uusframe/lipases.html). 8

Figure 3: Uses of pure glycerol by volume percentage in the market. Redrawn from ABG Inc. (2013). 13

Figure 4: U.S. refined glycerol prices from 1980 - 2007. Prices indicate a marked decline from the premium charged in 2005 (ABG Inc., 2013), to an all-time low of 30 c/lb in 2008 for the refined product and lower for technical grades (Graff, 2009). Prices marginally increased to 45 c/lb in 2015 the U.S., with technical grades up to 73 c/lb (Institute for Supply Management, 2015). Figure from (ABG Inc., 2013) 14

Figure 5: A representation of the value-chain from glycerol to valued fine chemicals (redrawn from Pagliaro *et. al.*, 2007). 16

Figure 6: Aerobic glycerol catabolism in the cytoplasm leading to the formation of DHAP or dihydroxyacetone-3-P, as described in the text. 18

Figure 7: Schematic diagram of a combined bioprocess of production biodiesel by lipase with microbial production of 1,3-propanediol by *K. pneumoniae*. Adapted from Mu *et. al.*, (2008)..... 25

Figure 8: pETDuet with features of interest shown. The Duet series of vectors are designed with co-expression in E. coli in mind, which may increase protein solubility and yields (EMD Biosciences, 2012).The pETDuet-1 vector carries the ColE1 replicon, T7 promoter and two cloning sites with multiple restriction sites, each under the control of a T7lac promoter, and an antibiotic resistance marker (ampicillin). The promoters are flanked by ribosome binding sites and a T7 terminator. The vector also provides options for protein purification in the form of His•Tag® and S•Tag™ sequences, or to produce unfused proteins (EMD Biosciences, 2012).. 31

Figure 9: (A) Gene map, (B) construct map, (C) 5' construct features, (D) 3' construct features. gene map of LipA (A) as received from GenScript® (in pUC57), with a number of restriction sites shown including BamHI (5') and NotI (3') sites included as ordered. The line below the map and highlighted in orange is an indication of the orientation of the ORF, which is 950bp in size. (B) shows a construct map of the pETDuet-LipA, indicating where the ORF was cloned into the vector. Restriction enzyme sites of interest are indicated (BamHI, NotI). LipA was cloned in-frame with the HIS-tag to facilitate downstream purification. Vector features are also indicated (refer to section 5.2.3). (C) shows the 5' end of the pETDuet-LipA construct, highlighting that LipA was cloned in-frame at pETDuet MCS1 (shown in blue). Adjacent sites of importance shown (selected restriction enzyme sites, RBS – ribosome binding site, start codon of ORF (ATG), 6x HIS tag, 1 letter codes of amino acid sequence). (D) shows the 3' end of the gene. Sequencing primer binding sites are shown (Duet UP2, DuetDown1). Images produced with SnapGene® Version 3.3.3. 36

Figure 10: (A) Gene map, (B) construct map, (C) 5' construct features, (D) 3' construct features. Gene map of LipB, (A) as received from GenScript® (in pUC57), with a number of restriction sites shown including BamHI (5') and NotI (3') sites included as ordered. The line below the map and highlighted in orange is an indication of the orientation of the ORF, which is 1022 bp in size. (B) shows a construct map of the pETDuet-LipB, indicating where the ORF was cloned into the vector. Restriction enzyme sites of interest are indicated (NdeI, XhoI). LipB was cloned in-frame with the S-tag to facilitate downstream purification. Vector features are also indicated (selected restriction enzyme sites, RBS – ribosome binding site, start codon of ORF (ATG), S tag, 1 letter codes of amino acid sequence) (ref er to section 5.2.3). (C) shows the 3' end of the pETDuet-LipB construct, highlighting that LipB is fused with the S-tag as the only stop codon is following the tag pETDuet MCS2 (LipB sequence highlighted in blue). (D) shows the 3' end of the gene. Sequencing primer binding sites are shown (T7 terminator) 37

Figure 11: Image Left (A): LipA touch-down PCR from GenScript pUC57 performed in duplicate. Lane 1 – GeneRuler 1kb plus marker, Lane 2 – touch-down sample 1, Lane 3 – touch-down sample 2. Image Right (B): BamH1 and Not1 digest of LipA amplicon from A which was ligated to pETDuet at a 1:2 and 1:3 vector:insert ratio. Lane 1 – GeneRuler 1Kb plus marker, Lane 2 – uncut pETDuet, Lane 3 -BamH1 & Not1 digest of pETDuet and LipA 1:2 ratio, Lane 5 - uncut pETDuet, Lane 6 – BamH1 & Not1 digest of pETDuet and LipA at 1:3 ratio ligation, Lane 7 – GeneRuler 1 Kb plus marker. Band sizes (in bp) have been displayed using the GelDoc ImageLab software. 38

Figure 12: Ligation screen of prior gel purified LipB amplicon in pETDuet at MCS2 with (A) gene- and (B) vector-specific primers. Left image (A): Lane 1 – Marker, Lane 2 - negative control, Lane 3 - R1, Lane 4 - R2, Lane 5 - R3, Lane 6 - R4, Lane 7 – Marker. 39

Figure 13:pETDuet with LipA and LipB Colony PCR (Colony 1 screen, with LipB specific primers)). Lane 1 – Marker, Lane 2 - negative control, Lane 3 – Background control, Lane 4 - R1, Lane 5 - R2, Lane 6 - R3, Lane 7 - R4. For pETDuet MCS2 specific primers: Lane 9 - negative control, Lane 10 – Background Control, Lane 11 - R1, Lane 12 - R2, Lane 13 - R3, Lane 14 - R4. 40

Figure 14: pETDuet with LipA and LipB Colony PCR (Screen of colony 2): Lane 1- Marker, Lane 2 – negative Control, Lane 3 – Blank, Lane 4 - R1, Lane 5 - R2, Lane 6 - R3, Lane 7 -R4. Colony PCR with LipB specific primers (lanes 8 – 15): Lane 8 – negative Control, Lane 9 –Blank, Lane 10 -R1, Lane 11 - R2, Lane 13 - R3, Lane 14 - R4 (pETDuet MCS2 specific primers) 40

Figure 15: LipA cloned in-frame at pETDuet MCS1 with adjacent sites of importance shown (selected restriction enzyme sites, RBS – ribosome binding site, start codon of ORF (ATG), 6x HIS tag, 1 letter codes of amino acid sequence). Trace data not shown (image produced with SnapGene® Version 3.3.3. 41

Figure 16: 3’ end of LipB in pETDuet at MCS2. Gene fusion region with S-tag shown (image produced with SnapGene® Version 3.3.3). 42

Figure 17: Translation of LipB and secondary structure prediction. Amino acid sequence of *P. mendocina* PK12CS lipase shown with 1-letter code (image produced with CLC Main Workbench® 7). 43

Figure 18: BLASTP of LipA showing high sequence similarity with *P. mendocina.* Consensus sequence and conservation regions shown. Green indicates regions of high sequence similarity (image produced with CLC Main Workbench® 7). 44

Figure 19: BLASTP of LipB showing sequence similarity with *P. mendocina*. Consensus sequence and conservation regions shown. Green indicates regions of high sequence similarity (image produced with CLC Main Workbench 7). 45

Figure 20: 30 °C induction. Sample A (0 – 1 mM). Lane 1: Marker, Lane 2 - 4: 0, Lane 5 -7: 0.25, Lane 8 - 9: 0.5, Lane 10 - Marker, Lane 11 - 13: 0.75, Lane 14 - 16: 1. Marker = BioRad Kaleidescope. WC – Whole Cell fraction, S – Soluble fraction, Ins – insoluble fraction. 46

Figure 21: 37 °C induction sample A. (Lanes from left to right): Lane 1- Marker, Lane 2 - 4: 0, Lane 5 - 7: 0.25, Lane 8 - 10: 0.5, Lane 11 - Marker, Lane 12 - 14: 0.75, Lane 15 - 17: 1. Marker = PageRuler BR unstained. WC – Whole Cell fraction, S – Soluble fraction, Ins – insoluble fraction... 47

Figure 22: 30 °C induction. Sample AB (0 – 1 mM). Lane 1 - Marker, Lane 2 - 4: 0, Lane 5-7:0.25, Lane 8 - 10:0.5, Lane 11 - Marker, Lane 12 - 14:0.75, Lane 15 - 17: 1. Marker=BioRad Kaleidescope. WC – Whole Cell fraction, S – Soluble fraction, Ins – insoluble fraction..... 48

Figure 23: 37 °C induction trial. Sample AB (0 – 1mM). (From left to right): Lane 1 - Marker, Lane 2 - 4: 0, Lane 5 - 7: 0.25, Lane 8 - 10: 0.5, Lane 11 - Marker, Lane 12 - 14: 0.75, Lane 15 - 17:1. Marker = PageRuler BR Unstained. WC – Whole Cell fraction, S – Soluble fraction, Ins – insoluble fraction. 48

Figure 24: 30 °C induction. Sample B" (0 – 1mM). Lane 1 - Marker, Lane 2 - 4: 0, Lane 5 - Marker, Lane 6 - 8: 0.25, Lane 9 - 11: 0.5, Lane 12 - 14: 0.75, Lane 15 - Marker, Lane 16 - 18: 1. Marker = BioRad Kaleidescope. WC – Whole Cell fraction, S – Soluble fraction, Ins – insoluble fraction. 49

Figure 25: 37 °C induction trial. Sample AB (0 – 1mM). (From left to right): Lane 1 - Marker, Lane 2 - 4: 0, Lane 5 - 7: 0.25, Lane 8 - 10: 0.5, Lane 11 - Marker, Lane 12 - 14: 0.75, Lane 15 - 17:1. Marker = PageRuler BR Unstained. WC – Whole Cell fraction, S – Soluble fraction, Ins – insoluble fraction. 50

Figure 26: Effect of concentration of pNPP on the initial reaction rate of hydrolysis of pNPP catalysed by the lipase of *P. mendocina* at 0.729 µg enzyme.....51

Figure 27: Initial rate vs. substrate concentration for 0.00729 µg enzyme.....53

Figure 28: Initial rate vs. substrate concentration for 0.0729 µg enzyme.....53

Figure 29: Log-plot of V_0 vs. [S] for 0.0729 and 0.00729 µg lipase. Image obtained using Wolfram Mathematica 10.3.....54

Figure 30: V_0 vs [S] for 0.0729 and 0.00729 µg enzyme respectively. Velocities were plotted on the same set of axes to emphasize the difference in reaction rates.....54

5 LIST OF TABLES

Table 1: Protein Quantification of purified protein (AB, 0.75 mM) 50

6 ABBREVIATIONS

1,3-PDOH - 1,3-propanediol dehydrogenase

1,3-PDO - 1,3 –propanediol

3-HPA - 3- hydroxypropionaldehyde

Acetyl-CoA - Acetyl coenzyme A

ADP - adenosine diphosphae

AlSBA-15 - aluminated SBA-15 silica

ATP - adenosine triphosphate

CO - carbona monoxide

C-C - carbon-carbon

CO_2 - carbon dioxide molecule

c/lb - cents per pound

DHA – Dihydroxyacetone

DhaK - dihydroxyacetone kinase

dNTP - dinucleotide triphosphate

EMBL - European Molecular Biology Laboratory

FAAE - fatty acid alkyl ester

FAD - Flavin adenine dinucleotide

FAME - fatty acid methyl ester

G3P - glycerol-3-phosphate

GlpABC - Glycerol dehydrogenase operon

GlpF - glycerol uptake facilitator

GlpK - glycerol kinase

GlpO - Glycerol oxidase

Glycerol-3-p – glycerol 3-phosphate

H^+ - hydrogen ion

H_2O_2 - hydrogen peroxide

IPTG - Isopropyl β-D-1-thiogalactopyranoside

KOH - Potassium hydroxide

K_2CO_3 - potassium carbonate

KAc - potassium acetate

kb - kilo base

kbp - kilo base-pairs

kDa - Kilo Daltons

K_2SiO_3 - potassium silicate

mM - milli molar

NAD - nicotinamide adenine dinucleotide

NADH - Protonated nicotinamide adenine dinucleotide

NaOH - Sodium Hydroxide

NO_3^- - Nitrate ion

NO_x - nitrous oxide compound

O_2 - Oxygen molecule

PBR - packed bed reactor

PCR - plymerase chain reaction

PEP - phosphoenol pyruvate

Pi - phosphate

PYR - pyruvate

SBA-15 - Santa Barbara Amorphous Silica silica nanoparticles (type 15)

SDS-PAGE - Sodium dodecyl sulphate polyacrylamide gel electrophoresis

TAE - trisacetate Ethylenediaminetetraacetic acid

v/v - volume for volume

w/v - weight per volume

7 LITERATURE REVIEW

7.1 Biofuels & the National Biofuels Industrial Strategy of South Africa

Bio-derived fuels, such as biodiesel and bioethanol, have gained considerable attention as liquid transport fuels mainly due to environmental concerns of fossil fuel combustion (Ragauskas *et. al.*, 2006). Bioethanol and biodiesel have been shown to yield more energy than is required to produce them, i.e. positive net energy balances of 25% and 93% respectively (Hill *et. al.*, 2006). These energy balance calculations are based on analyses of the respective life cycles of the fuels, on farm yield data, commodity and fuel prices, farm energy and chemical inputs, plant production efficiencies, co-product generation, greenhouse gas emissions and other environmental effects (Hill *et. al*., 2006). The significant impact is on greenhouse gas emissions: biodiesel emissions reduce these by 41% and ethanol by 12% respectively when compared to their fossil fuel counterparts (Hill *et. al.*, 2006). These results demonstrate the environmental advantages that biofuels, like biodiesel, have over conventional fossil fuels.

In line with global developments, South Africa developed its own biofuels development programme in 2007: the National Biofuels Industrial Strategy of the Republic of South Africa (the NBIS) (Department of Minerals and Energy, 2007). The NBIS planned to achieve a 400 million litres per annum biofuels penetration, specifically bioethanol and biodiesel, into the country's liquid fuel supply over a 5 years period, starting from 2007. This would have contributed 30% to the national renewable energy target for 2013 (Department of Minerals and Energy, 2007). For bioethanol production, the NBIS recommended sugar cane, sorghum and sugar beet as feedstock sources, at a blending ratio of E8 (8%) bioethanol (Department of Minerals and Energy, 2007). Maize and jatropha were specifically excluded for food security and environmental reasons respectively. Feedstock's recommended by the NBIS for biodiesel production are soybean, canola and sunflower, at a blending ratio of 2% biodiesel (Department of Minerals and Energy, 2007).

The 'Regulations regarding the mandatory blending of biofuels with petrol and diesel', which were gazetted on August 23, 2012, and would come into effect on October 1, 2015 (Department of Minerals and Energy, 2014) were formulated to control the mandatory blending of biodiesel (and bioethanol) with diesel (or petrol) to produce a biofuel blend that would be sold in South Africa. According to Section 3 of the regulations, all petrol and diesel supplied to a petroleum blending facility must allow for the blending of biofuels with a minimum concentration of 5% for biodiesel since, according to the country's Regulations regarding Petroleum Products Specifications and Standards, biodiesel may be blended at different concentrations into conventional (mineral) diesel, right from 5% biodiesel (B5) even up to 100% biodiesel (B100).

The price of fuel in South Africa is determined by many different costs that together constitute the petrol/diesel price. Chiefly, this price is determined by the market movements of 3 main constituents: the basic fuel price (affected by costs of shipping, insurance, storage, etc.), retail and distribution margins (fuel station owners/distributors), and fuel levies that are collected on every litre of fuel sold. The levies are of interest to this discussion. The fuel levies are divided between the Fuel Levy, Road Accident Fund levy, and customs and excise duties levies. The Fuel Levy is treated as a general tax that is collected and administered by the National Treasury annually; the customs and excise duties are collected by SARS (South African Revenue Service) according to provisions of the Customs and Excise Act, 1964 (Act No. 91 of 1964) (AASA Public Affairs, 2016).

Amongst the many criticisms against the NBIS (African Centre for Biosafety, 2008; Food Agriculture and Natural Resources Policy Analysis Network, 2009), including frustration at the lack of progress by investors (Greve, 2015) are the economic incentives proposed for biofuel production (Letete & Blottnitz, 2009). The NBIS proposed the use of a producer support mechanism to balance the difference in fuel tax support to biodiesel (and bioethanol) by setting a fixed margin price (Department of Minerals and Energy, 2007). With this strategy, biodiesel should receive a 50% fuel levy exemption, i.e. effectively R0.53 per litre based on 2007 prices (Letete & Blottnitz, 2009). However, working with 2008 commodity and energy prices, it was shown that the proposed biofuel tax support system would result in losses for the biofuel producer of R 3.70, R 3.13 and R 0.36 per litre for soybean, sunflower and canola derived biodiesel respectively (Letete, 2009). This prevented an economical solution and the strategy was not realised.

In a revision, 'The Biofuels Production Incentive' was established to balance the risks associated with biofuel production with the initial capital cost hurdles and thus stimulate biofuel production (Department of Energy, 2007). The incentives proposed relied on the costs of a hypothetical, world-scale biofuels plant based in South Africa, and would compensate manufacturers via the (general) Fuel Levy for movements in feedstock's output prices that occur monthly (Department of Energy, 2013). These rebates would provide a firm 15% return on investment for biofuels manufacturers and would come into effect on 1 October 2015. They were proposed to be between 4.5 cents per litre and 6.5 cents per litre for 20 years (Gilder & Mamkeli, 2014). In the Minister of Finance's 2013 Budget Review, the incentives were revised to afford biodiesel manufacturers a subsidy through a levy imposed on petrol and diesel that ranged from 3.5 to 4.5 cents per litre (Department of Minerals and Energy, 2014).

The regulations governing the framework for the financial support programme intended for biofuels manufacturers were further intended to be revised from those proposed in 2007 (Department of Energy, 2014), detailed in the 'Draft Position Paper on the South African Biofuels Regulatory Framework'. This document, which governs the pricing and subsidy mechanism of the biofuels

industry, was gazetted on January 15, 2014. The 'Final Position Paper' was reported to be published by May or June 2014 by the Department of Energy. The deadline was missed; and unfortunately, to date, the document has still not been published (Greve, 2015).

The biofuels pricing mechanism for biodiesel was also since revised in the 'Draft Position Paper on the South African Biofuels Regulatory Framework' (Department of Minerals and Energy, 2014). Here, biodiesel falls within the general fuel tax net (i.e. Fuel Levy) and thus biodiesel manufacturers would not be 50% tax exempt as previously proposed, but rather receive a rebate of 50% on the Fuel Levy, and further be afforded accelerated depreciation on their manufacturing facilities as tax incentives at a 50:30:20 ratio. This would effectively mean in the first year producers would be taxed a million rand. In the second year R500 000, in the third R300 000, and in the fourth R200 000. The differences between 50% tax exemption and 50% tax rebate are contentious for biofuel manufacturers/companies however. For example, the benefits of a 50% tax exemption include that only 50% of the income will be taxed. However, questions such as which amounts would qualify for the exemption and whether all the income or only a portion is exempt remain unanswered. For the rebate, questions include how the rebate will be calculated considering that a rebate is dependent on the income and expenses of the company. The accelerated depreciation as well will only apply to the qualifying assets of the company/manufacturer, which begs the question what of the other income the company/manufacturer can expect?

In contrast to biodiesel, a similar rebate could not be established for bioethanol as it falls outside the fuel tax net and therefore will not qualify for a rebate (Department of Minerals and Energy, 2012; Department of Energy, 2013; Department of Minerals and Energy, 2014). However, only those biofuel manufacturers that are licensed, in terms of the Manufacturing Licences Regulations, would be eligible for the financial support by the Levy (Gilder & Mamkeli, 2014). Turning the South African biofuels industry into an attractive investment opportunity, then, remains to be seen. One of the ways this effort was envisaged was through the regulatory environment, where the Mandatory Blending of Biofuels with Petrol and Diesel would be used as a legal instrument. This, in effect, would guarantee the uptake of the biofuels supplied by licensed manufacturers to manufacturers of petroleum products and their wholesalers to purchase and blend all the biofuels made available to them (Department of Minerals and Energy, 2014).

Indeed, the large-scale economic viability for sunflower oil-derived biodiesel remains a quarrelsome issue in South Africa. This situation is due to the requirement of significant government subsidisation or imposed legislation to reach the mandated 2% penetration level (Nolte, 2007), which to date has been marginal (Department of Minerals and Energy, 2013). While a 2% penetration of biofuels has been the target for biofuel introduction/blending in the national fuel pool, it has been acknowledged by the government that the practicality of every litre of fuel in South Africa containing 2% biofuels is

unrealistic for various reasons (Department of Minerals and Energy, 2014). It has thus been proposed that flexibility is considered in the concentration of biofuels, to vary between, say, 5% and 10% of a certain portion of the geographic fuel pool, most likely in close proximity to the biofuels manufacturing plants (Department of Minerals and Energy, 2014). The lack of impetus has further been contributed to by the high input costs, improvements in conversion technologies (Caesar *et. al.*, 2007) logistical and blending considerations/pricing framework.

In the interim, an opportunity for farmers to reduce their production costs would be well received, especially since limited fuel production without licencing is allowed. Fuel costs account on average for 15% of a grain/oilseed farmer's production costs (Joubert, 2012). The whole value chain, i.e. the production of the oil seed crop, its seed processing, oil extraction and the conversion thereof into biodiesel, have been shown to be economically viable at a farm-scale by the Vermont Bioenergy Initiative (White & Callahan, 2013). Indeed, they have demonstrated that oilseed crops, when grown in rotation with other grains, and fodder, are a sustainable means of producing renewable fuel to power the Vermont's agricultural sector at community scale, while generating livestock feed and food-grade oil as well (White & Callahan, 2013).

Processing oil into biodiesel is based on the use of a process which utilises acid or base catalysis (see 7.1.1.1). This study aims to describe a "greener" method of processing sunflower oil into biodiesel. If the method is feasible, and can be adopted along with the economic model suggested by the Vermont Bioenergy Initiative in the South African context, it would be able to empower the agricultural community (i.e. areas and communities targeted by the National Biofuels Industrial Strategy) and stimulate small-scale biodiesel production in and around the country. This would be a move in line with Nolte (2007), who determined, in a preliminary economic feasibility study, that for commercial biodiesel production to be a success, production should not be centralized but rather should happen through a greater number of relatively small-scale operations located in oilseed producing regions.

7.1.1 Biodiesel production

Biodiesel refers to the fatty acid alkyl esters (FAAEs) that are produced from the esterification of fatty acids or the transesterification of plant or animal oils/fats (triglycerides) (fig. 1) with short-chain alcohols (Tan *et. al.*, 2010). They are also produced from the pyrolysis or micro-emulsification of these sources (Ranganathan *et. al.*, 2008). Whereas esterification involves the reaction of an acid with alcohol to produce an ester and water, transesterification involves displacement of one alcohol by another from an ester. Pyrolysis refers to the decomposition of a compound by the use of high temperatures (also referred to as "cracking"). Micro-emulsification is an improvement on the mass transfer limitations of esterification/transesterification reaction conditions whereby the interfacial

surface area for the reaction is dramatically increased through the use of various intensification methods such as ultrasonic and microwave irradiation, hydrodynamic cavitation, addition of co-solvents or mass transfer catalysts (Veljković *et. al.*, 2012). The most popular method for the production of FAAEs is transesterification owing to the relative ease and cost-effective conversion process, which will be discussed in a following section.

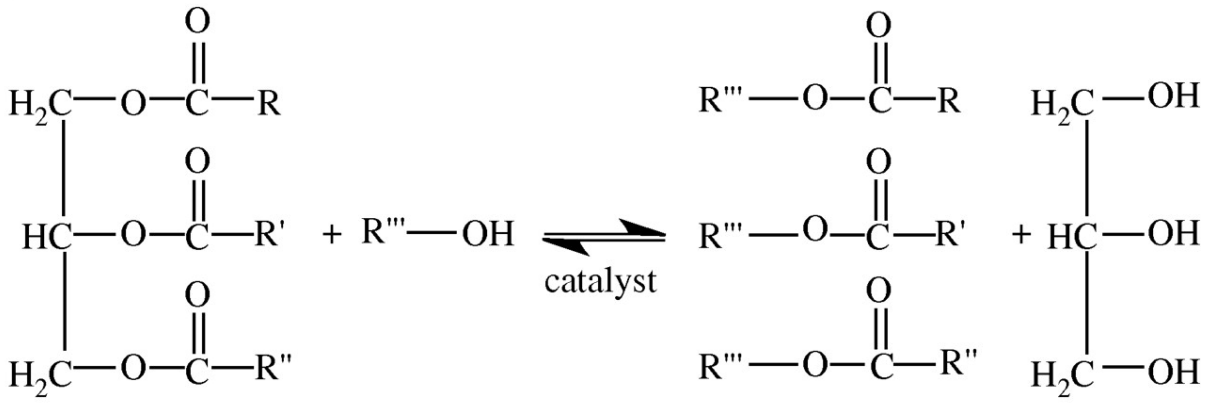


Figure 1: Reaction mechanism of triglyceride transesterification. Here, one triglyceride molecule reacts with 3 moles of alcohol to produce 1 mole of glycerol and 3 moles of FAAE with the help of a catalyst. Triglycerides refer to plant/animal oils and/or fats. Catalysts may be enzymes (e.g. lipase) or chemicals (e.g. potassium hydroxide (KOH) or sodium hydroxide (NaOH)). Adapted from (Pereira *et. al.*, 2014).

7.1.1.1 Transesterification

Transesterification involves the displacement of an alcohol moiety from an ester by another alcohol which acts as an acyl acceptor (fig. 1). The process can be catalysed chemically, using liquid acids or bases; by solid catalysts, which can be homogenous or heterogeneous; enzymatically using an esterase/lipase, or the alcohol and substrate in supercritical conditions (severe temperatures and pressures) (Ranganathan *et. al.*, 2008; Sivasamy *et. al.*, 2009). In industry, chemical catalysis - specifically liquid base catalysis (e.g. KOH and NaOH) - is often preferred due to the high conversion rates, lower cost of additives, short reaction times and relatively lower operating temperatures (Fukuda *et. al.*, 2008; Sivasamy *et. al.*, 2009). However, this process is subject to soap and pigment formation under high moisture content and requires extensive pre-treatment steps to reduce the water or fatty acid content. Issues of catalyst recovery and the treatment of catalyst-containing wastewater are yet more considerations for the liquid base catalysis method. Another complication is the vast amount of energy required to recover or remove the by-product glycerol (Fjerbaek *et. al.*, 2009; Fukuda *et. al.*, 2008; Sivasamy *et. al.*, 2009; Szczęsna Antczak *et. al.*, 2009).

Solid catalysts are gaining preference in industry since they enable the design of continuous processes with high reaction rates and good methyl ester yields while being insensitive to free fatty acids (Sani *et. al.*, 2014). Chief among these are the solid acid catalysts, which have found favour due to being amenable to esterification and transesterification of high free fatty acid containing feedstocks, and have been shown to be more economical than alkali and homogenous acid catalysts, as well as supercritical processes (West *et. al.*, 2008). Further advantages include improved production process economics and simplified post-treatment processes since soaps are not produced as by-products (Islam *et. al.*, 2013; Lam *et. al.*, 2010).

Xie & Fan (2014), for example, developed a solid base catalyst in which tetra-alkylammonium hydroxide-functionalized SBA-15 materials (SBA-15-pr-NR3OH) were prepared by anchoring dimethyloctadecyl [3-(trimethoxysilyl)propyl] ammonium hydroxides onto the surface of mesoporous SBA-15 silica. The catalyst was then utilised in the transesterification of soybean oil with methanol (methanol/oil molar ratio of 12:1) and the catalytic activity was determined. With a reaction time of 30 min and with methanol reflux, the methyl ester yield was 99.4% with a negligible loss of catalyst activity after several cycle runs. Chen *et. al.* (2011) developed a series of solid base catalysts based on potassium salts (K_2CO_3,K_2SiO_3 and KAc) supported on mesoporous silicas (SBA-15 and AlSBA-15) to catalyse the transesterification of jatropha oil with methanol. A biodiesel yield of 95% was obtained (using the K_2SiO_3/AlSBA-15 catalyst) at a methanol/jatropha oil molar ratio of 9:1, at a reaction temperature 60 °C for 150 min. The K_2SiO_3/AlSBA-15 catalyst maintained steady catalytic activity compared with traditional KOH and K_2CO_3 catalysts; and only led to 6% decrease in biodiesel yield after 5 cycles. Wang *et. al.* (2013) used chemical synthesis to prepare a solid base catalyst containing $Ca_{12}Al_{14}O_{33}$ and CaO for the transesterification of rapeseed oil with methanol. Methyl ester content reached 90% after 3 hours at 65 °C with a methanol/oil molar ratio of 15:1 and a stirring rate of 270 rpm. The catalyst could be reused at least 7 times with the methyl ester content at over 87%. Wang *et. al.* (2012) achieved 98.1% conversion with a lithium orthosilicate (Li_4SiO_4) catalyst during the transesterification of soybean oil with methanol, at a methanol/oil molar ratio of 18:1, and a reaction temperature of 65 °C for 2 hours.

Solid catalysts, however, are very sensitive to the presence of water and free fatty acids, which deactivate the catalyst (in the case of a heterogeneous base), or require higher temperatures and higher catalyst loads to achieve reasonable yields of FAAEs (for heterogeneous acid catalysts) (Sivasamy *et. al.*, 2009). Additionally, a number of other chemical (e.g. leaching, reusability, calcination temperature) and physical factors (pore structure, surface area, mechanical strength) affect the FAAE yield, process life as well as the catalysts productivity (Islam *et. al.*, 2013). High bioreactor costs, especially specialist reactors required due to the nature of the reactions, are a key hindrance to further industrial-scale biodiesel production using solid catalyst technologies (Lam *et. al.*, 2010).

7.1.1.2 Enzymatic biodiesel production

Enzymatic biodiesel production is an alternative to biodiesel production by chemical catalysts. The enzymatic process offers significant advantages with respect to FAAE generation because enzymes are more tolerant to variations in the feedstock (Sivasamy *et. al.*, 2009). Additionally, the lack of adverse reactions and higher crude glycerol yield, make enzymes particularly suited to biodiesel production compared to conventional catalysts (Lam *et. al.*, 2010). Furthermore, enzymatic conversion provides a single-step production process that utilises less energy and produces less polluting by-product (Fjerbaek *et. al.*, 2009; Fukuda *et. al.*, 2008).

Considering these benefits, industrial-scale use has been hampered due to the fact that enzymes are typically much more expensive compared to chemical catalysts, and prone to comparatively lower reaction rates and shorter re-usability schedules, i.e. usage is typically limited 100 days of operation (Lam *et. al.*, 2010). Efforts to circumvent these have been on-going, and immobilization of enzymes to improve stability in industrial processes has found great application in this regard as this allows for repeated use of the catalyst (Tan *et. al.*, 2010). The enzymes themselves may be immobilized by 3 primary methods: adsorption onto a carrier (supports such as polysaccharide derivatives, synthetic polymers and even glass), encapsulation (utilising polymers like collagen, cellulose, k-carrageenan, or liposomes and microcapsules) within a carrier or via cross-linkage (carrier-free; utilising bi/multifunctional reagents such as glutaraldehyde, bisdiazobenzidine and hexamethylene di-isocyanate) (Datta *et. al.*, 2012; Sheldon & van Pelt, 2013). Lipases are the principal enzymes involved in enzymatic biodiesel production.

7.1.1.2.1 Lipases: enzymes of considerable industrial potential

Lipases (E.C. 3.1.1.3) are defined as carboxylesterases which catalyse the hydrolysis and synthesis of long-chain acylglycerols (fig. 1 and fig. 2) (Jaeger *et. al.*, 1999). These enzymes are ubiquitous among plants, animals, and microorganisms, and are among a group of lipolytic enzymes which catalyse the conversion of lipids, along with phospholipases (E.C. 3.1.4.3), cutinases (E.C. 3.1.1.74) and esterases (E.C. 3.1.1) (Joseph *et. al.*, 2008; Pauwels, 2008). Lipases catalyse many important industrial reactions, and possess unique specificities and properties (e.g. thermo- and organic solvent-stability) (Hasan *et. al.*, 2009). Consequently they have found extensive applications in oleochemistry, organic synthesis, detergent formulations and nutrition (Hasan *et. al.*, 2006; Sharma *et. al.*, 2001).

Lipases were initially kinetically defined by the observation of a phenomenon termed “interfacial activation” (fig. 2 A), and structurally by the presence of a “lid” (fig. 2 B) (Jaeger *et. al.*, 1999). The former term describes the enriched catalytic activity of the enzyme when the substrate concentration

exceeds the critical micelle concentration and forms an emulsion. The latter term refers to a loop located on the surface of the molecule which moves to expose the active site upon contact with the interface (Jaeger *et. al.*, 1999; Pauwels, 2008). Since then, exceptions to these rules have been discovered and the enzymes have subsequently been redefined by substrate preference (Jaeger *et. al.*, 1999; Pauwels, 2008).

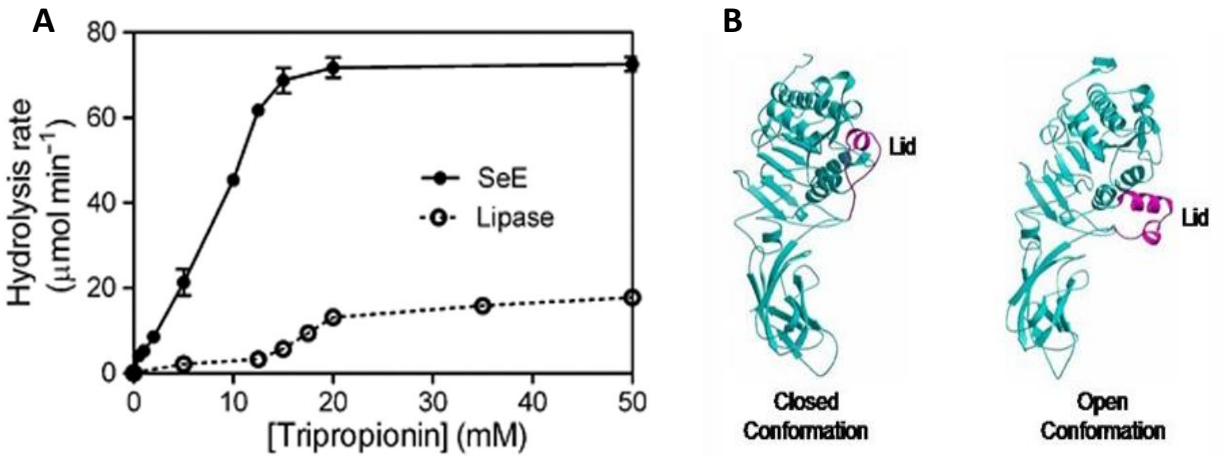


Figure 2: (A) Lack of interfacial activation in *Streptococcus equi* ssp. *equi* catalyzed hydrolysis of vinyl propionate compared against the activity of a lipase (adapted fromXie *et. al.* (2008)). **(B)** The catalytic mechanism of a lipase with the surface loop, ("lid") regulating catalysis, (left) closed conformation (inactive); (right) open conformation (active form) at a hydrophobic interface where interfacial activation occurs (image sourced from: http://www.icp.csic.es/biocatalisis/web3/Palomoweb/uusframe/lipases.html).

Whilst no strict definition for the term "long-chain" exists, lipase substrates are generally regarded as glycerolesters with a chain length greater than 10 carbon atoms (Jaeger *et. al.*, 1999). Esterases (E.C. 3.1.1.1), whilst being a group of carboxylesterases which hydrolyse water-soluble esters as well (Rosenau & Jaeger, 2000), are distinct from lipases in that they show a preference for glycerolesters with acyl chain lengths shorter than 10 carbon atoms (Jaeger *et. al.*, 1999).

7.1.1.2.2 Microbial-derived lipases

Most commercially available lipases are derived from bacteria and fungi (Hara *et. al.*, 1997; Hasan *et. al.*, 2006; Jaeger *et. al.*, 1999), with a handful of mammalian origin (Schmid & Verger, 1998). Examples are the lipases produced by *Mucor miehei* (Lipozyme), *Candida antarctica* (Novozyme 435), *Aspergillus niger*, *Pseudomonas* and *Burkholderia* species. The latter have been extensively characterized because of their ability to function in extreme conditions (Pauwels, 2008). Of the known

variety of lipases from both Gram-positive and Gram-negative bacteria, the majority are produced by Gram-negative bacteria. The most important Gram-negative genus in this regard is *Pseudomonas*, with at least seven different lipase-producing species and five lipases characterized originating from *P. aeruginosa* alone (Jaeger *et. al.*, 1994). The prototype enzyme of this group is the lipase from *P. aeruginosa*. PAO1, which has also provided the basis of a classification system of lipases (Jaeger *et. al.*, 1994). Due to the high yields possible, the variety of catalytic activities available and rapid growth on inexpensive media, microbial enzymes are often more useful than enzymes derived from plants or animals (Hasan *et. al.*, 2006). Microbial enzymes are also more stable than their corresponding plant and animal enzymes and their production is more convenient and safer (Hasan *et. al.*, 2006). Bacterial strains are generally more used as sources of enzymes as they offer higher activities compared to yeasts, and their enzymes tend to have industrially relevant properties, such as neutral or alkaline pH optima and, often, thermostability (Hasan *et. al.*, 2006). Furthermore, the genetic tools for their manipulation already exist (Datta, 1985) and are relatively simpler to apply.

Bacterial lipases are relevant as the most important group of biocatalysts in industry, considering their stability in organic solvents, the non-requirement of cofactors, their broad substrate specificity and high enantioselectivity. They are used for a number of biotechnological applications which make use of these properties, such as in the synthesis of biopolymers and biodiesel, the production of enantiomerically pure pharmaceuticals, agrochemicals, and flavour compounds (Hasan *et. al.*, 2006; Jaeger *et. al.*, 1999).

7.1.1.2.3 Classification of lipases

A comparison of amino acid sequence conservation and fundamental biological properties of lipases by Arpigny & Jaeger (1999) led to lipases being classed into 8 distinct families, with true lipases forming family I, that is further sub-divided into 6 sub-families (Arpigny & Jaeger, 1999). Since 2002, family I now comprise at least 30 lipases partitioned into 7 subfamilies, of which I.1, I.2 and I.3 are Gram-negative bacterial lipases (Jaeger & Eggert, 2002). The discussion is limited to family I lipases in *Pseudomonas* as a *Pseudomonas* sp.-derived enzyme is employed in this study. Lipases from subfamily I.1 include those secreted by *P. aeruginosa* and *P. fragi*, both with a molecular weight of approximately 30 kDa. Subfamily I.2 is represented by lipases produced by *B. glumae* and *B. cepacia*, which have an approximate molecular weight of 33 kDa and show about 60% amino acid sequence identity to those of family I.1 (Jaeger & Eggert, 2002; Arpigny & Jaeger, 1999). In contrast to subfamilies I.1 and I.2, subfamily I.3 lipases have a molecular weight of ~50 kDa and they show poor sequence similarities to either subfamily I.1 or I.2 (Angkawidjaja & Kanaya, 2006). Lipases produced by Gram-positive bacteria belong to subfamilies I.4 – I.7.

Lipases from subfamilies I.1 and I.2 contain a di-sulphide bridge that contribute to the stability of the protein, and require an additional gene product, the so-called lipase-specific foldase or Lif, for correct folding and secretion. These proteins have themselves garnered considerable interest (Rosenau & Jaeger, 2000; Rosenau *et. al.*, 2004). They have been classed into four distinct families based on sequence similarity with only 8 conserved amino acid residues in all known Lifs analogous to the classification of lipases (Rosenau *et. al.*, 2004). Family I comprises of Lifs from *P. aeruginosa*, *P. mendocina*, *P. wisconsinensis* and *P. alcaligenes*; family II comprises Lifs from *B. cepacia*, *B. glumae*, *P. fragi*, *Xanthomonas fastidosa* and *Ralstonia metallidurans*, and family III Lifs from *Acinetobacter calcoaceticus*. Lifs from *Pseudomonas* sp. strain KFCC10818, *Vibrio cholerae* and *V. vulnificus* form family IV, because these proteins differ significantly from all other Lifs in size (279, 284 and 280 amino acids) and amino acid sequence.

7.1.1.2.4 Industrial applications of lipases

The first commercially significant application of lipases was in the detergent industry with the introduction of Lipolase™ by Novo Nordisk which originated from the fungus *Thermomyces lanuginosus* (Jaeger, 1998). This was followed by Unilever which obtained a patent for the *B. glumae* lipase resulting in decreased washing temperatures, and surfactant use for the removal of fat stains, once added to their range of washing powders (Pauwels, 2008). Lipases have also been applied for the treatment of fat-containing wastewater and for the removal of 'pitch' (mainly triglycerides and waxes originating from wood) in the paper industry (Jaeger, 1998).

There is growing interest in the hydrolytic power of lipases. In the dairy industry, lipases contribute to cheese ripening and flavour development. In the baking industry, lipases degrade polar wheat lipids to produce emulsifier substitutes or supplement traditional emulsifiers. In oleochemistry, lipases are used to produce non-ionic surfactants (mono- and di-glycerides) which are further applied for emulsification in food, cosmetics and drug preparations (Schmid & Verger, 1998). In industrial production, lipases are superior to classical chemical catalyst processes because they operate in milder reaction conditions and exhibit improved substrate specificity (Sheldon & van Pelt, 2013). In addition, the enzymes' stability under non-aqueous conditions, and versatile catalytic activities, has made them highly valued biocatalysts in organic chemistry (Datta *et. al.*, 2012). Lipases are also renowned for their regio- and enantio-selectivity, as well as their promiscuity for substrates. They find extensive use in the resolution of racemic acids and alcohols, and can accept a variety of both water soluble and emulsified esters (Jaeger *et. al.*, 1994).

Lipases are also known for their catalysis in the transesterification of oils and fats. Lipase-catalysed transesterification of less valuable oils such as palm oil can produce more desirable species, e.g. cocoa

butter (Hasan *et. al.*, 2006; Jaeger *et. al.*, 1994) which is extensively used in all types of chocolates; as a base for medicinal suppositories, and as a popular ingredient in products for the skin such as soaps and lotions (Hasan *et. al.*, 2006). Cocoa butter is solid at room temperature and has a melting point of 34 – 38 ºC due to the high proportion of stearates (Hasan *et. al.* 2006). When added to food, e.g. chocolate, this addition results in chocolate which is solid when sold, but readily melts in the mouth when ingested, depending on the crystal structure of the cocoa butter established during tempering (Jaeger *et. al.*, 1994; Svanberg *et. al.*, 2013).

The synthesis of fatty compounds through the use of lipases has the potential to reduce the ecological impact of production since the reaction conditions are less stringent and toxic. This has the added advantage of eliminating the need for the various chemical steps usually employed, leaving only the product of interest further reducing processing expenditure (Schmid *et. al.*, 1999). The high quality products produced from utilising lipases in industrial processes are particularly well suited for uses in the cosmetic and pharmaceutical industries (Pauwels, 2008). Polyunsaturated free fatty acids also have a biomedical and nutritional role, where they are used to produce a number of anti-cholesterolaemic, anti-inflammatoric and anti-thrombolytic pharmaceuticals (Hasan *et. al.*, 2006; Jaeger *et. al.*, 1994).

7.1.2 Whole-cell biocatalysts for biodiesel production

In an effort to improve the cost-effectiveness of production processes utilising enzymes, whole-cell biocatalysts have found great application in industrial biotransformations (Straathof *et. al.*, 2002). These are applied in the food, pharma and agro sectors. They are particularly used in the fine chemicals sector for the production of fine chemicals where enantiomerically pure products are significant (Straathof *et. al.*, 2002). Whole cells are more popularly used than (partly) isolated enzymes in redox biotransformations; however, their use in non-redox biotransformations is also prominent (Straathof *et. al.*, 2002).

Whole-cell biocatalysts circumvent the disadvantages associated with enzyme preparations, which include costly purification steps and the re-use and recovery of the catalyst (Fukuda *et. al.*, 2008). Optimal environments for enzyme function are already provided - i.e. all co-factor and regeneration networks are maintained within the organism and the catalyst itself is protected from the extracellular environment (Jose *et. al.*, 2012). Several studies have reported the use of yeasts, bacteria and filamentous fungi for triglyceride conversion to biodiesel in this manner (Ban *et. al.*, 2001; Fujita *et. al.*, 2002; Narita *et. al.*, 2006; Xiao *et. al.*, 2011). Ban *et. al.* (2001) investigated the methanolysis of soybean oil with immobilized *Rhizopus oryzae* cells that expressed a 1,3-positional specificity lipase. The cells were immobilized within biomass support particles. When methanolysis was carried out

with stepwise additions of methanol, the methyl ester content in the reaction mixture reached 90% in the presence of 15% water. Narita *et. al.* (2006) developed an *Escherichia coli* cell surface display system by employing PgsA as an anchoring motif, and displayed α-amylase from *Streptococcus bovis* 148, and lipase B (CALB) from *C. antarctica*. CALB-displaying *E. coli* cells successfully catalysed enantio-selective transesterification. Xiao *et. al.* (2011) used a strain of *A. niger*, immobilized within polyurethane biomass support particles, for enzymatic lipase transesterification of palm oil to biodiesel in a packed-bed reactor (PBR). High FAME yield (>90%) in the PBR after 72 hours of reaction time at a flow rate of 15 $L.h^{-1}$, and a water content of 15% was achieved following the addition of glutaraldehyde solution (0.5 vol.%) to stabilize lipase activity. A high conversion rate (>85%) was further maintained after four palm oil batch conversion cycles in the PBR.

Whole-cells benefit production of the lipase in a simplified, cost-effective and durable system that shows stability in non-conventional media. However mass-transfer effects, lower reaction rates and yields, are detriments (Fukuda *et. al.*, 2008).

7.2 Glycerol

Glycerol is a viscous, sweet tasting, clear hygroscopic liquid that is odourless, non-toxic, water soluble and biodegradable, and is a structural component of all fats and oils (Ayoub & Abdullah, 2012). It is a very versatile molecule owing to its 3 reactive hydroxyl groups, and has many end uses (> 1500) (Ayoub & Abdullah, 2012). Pure glycerol is mainly used as an additive with little to no structural modification largely in food (e.g. as a sweetener in candies and cakes) and beverages manufacture; as a humectant in tobacco, in pharmaceuticals, in the pulp, paper and textile industries; in personal care products including toothpastes, hair and skin-care products as well as in soaps (fig. 3) (Kenar, 2007; Paulo *et. al.*, 2009). Its industrial uses also include: synthesis of polyethers, polyols and alkyd resins, production of detergents, cellophane, triacetin, urethane foams, synthetic resins and explosives, among others.

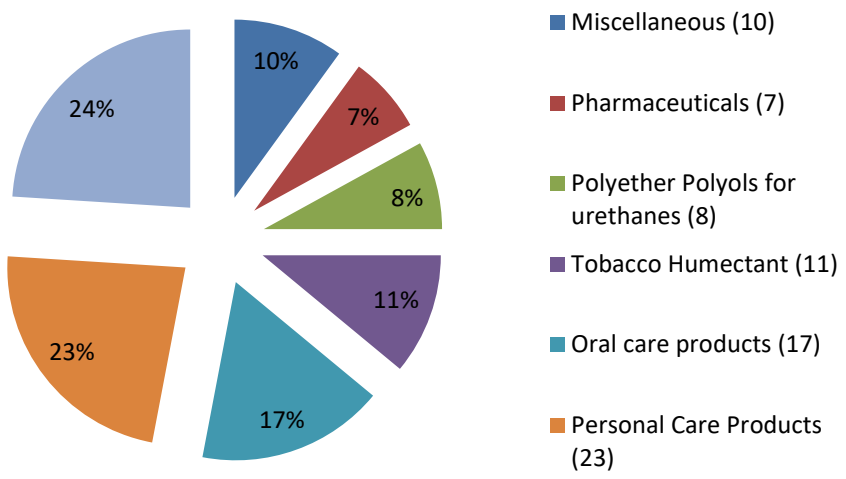


Figure 3: Uses of pure glycerol by volume percentage in the market. Redrawn from ABG Inc. (2013).

7.2.1 The glycerol "glut"

An inevitable by-product of the transesterification process in biodiesel production is the production of impure (crude) glycerol, i.e. a glycerol with approximately 80% purity that depends on the production process. Large tax support programmes from US and European governments, and mandated use in road fuels, have significantly increased the production of biodiesel in recent years, leading to a surplus of the commodity to flood traditional (refined glycerol) markets (Johnson & Taconi, 2007). Initially this crude product could fetch decent prices in the market, but this is not the case anymore and currently only negligible prices are offered (IncBio, 2016). Consequently, many companies involved in the manufacture of refined glycerol from petro-chemical sources have ceased operations (da Silva *et. al.*, 2009; Dharmadi, 2006). The flood of crude glycerol has thus caused massive volatility in the sale prices of refined glycerol (fig. 4) (Miller-Klein Associates, 2006).

The global refined glycerol market is valued at $1 billion annually (ABG Inc., 2013), and grew to $1.64 billion in 2014 and projected to grow at 6.5 – 7.9% by 2022 (Radiant Insights Inc., 2016), on the back of increasing demand for technical and higher grades (IncBio, 2016). Prices for refined glycerol in the United States however showed a pronounced reduction: from around $1543/tonne prior to biodiesel market expansion, to $661/tonne in 2007 (fig. 4) (Miller-Klein Associates, 2006; Wang *et. al.*, 2001; Yang *et. al.*, 2012), while demand has increased in Europe as a result of increased application in the cosmetics industry, suggesting growth and stability of the market (Radiant Insights Inc., 2016).

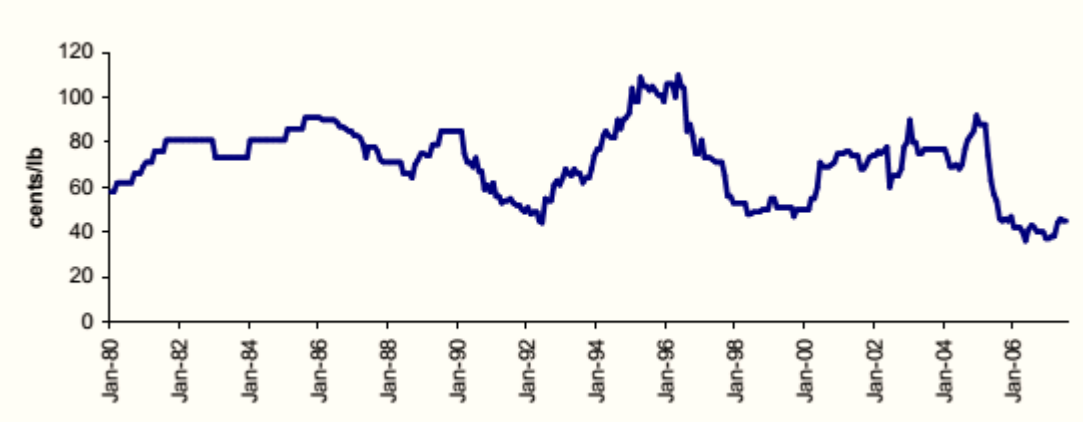


Figure 4: U.S. refined glycerol prices from 1980 - 2007. Prices indicate a marked decline from the premium charged in 2005 (ABG Inc., 2013), to an all-time low of 30 c/lb in 2008 for the refined product and lower for technical grades (Graff, 2009). Prices marginally increased to 45 c/lb in 2015 the U.S., with technical grades up to 73 c/lb (Institute for Supply Management, 2015). Figure from (ABG Inc., 2013)

Glycerol market trends in South Africa are largely unknown. However, an output of about 40,000 litres of glycerol monthly is reported, of which a maximum of 3% is used as an additive in animal feed, and also in local soap industries, and to produce antifreeze with the remainder either stored, sold or disposed (Babajide, 2013). Despite the uncertainty, it is assumed that local market trends follow international developments.

The personal care industry is reported to have shown an increasing demand for the product, owing to consumers' desire for more natural and eco-friendly products (Ayoub & Abdullah, 2012). Other markets dependant on polyols derived from petrochemical sources represent the most promising avenues to absorb refined glycerol, such as anti-freeze for the automobile industry (ethylene glycol, propylene glycol and pentaerythritol), aircraft defrosters and alkyd resins (Kenar, 2007). With the advent of the biodiesel industry the influx of inexpensive impure/crude glycerol to the market, this so called "glycerol glut" has compelled academia and industry to seek value-added alternatives, or additional fields of application, for glycerol in its available forms, and its derivatives (Yang *et. al.*, 2012).

7.2.2 Value-added uses for crude glycerol

As a commodity, crude glycerol from biodiesel production is a potential financial and environmental liability, for which currently operating facilities, and small-scale biodiesel producers, are faced with limited options (Johnson & Taconi, 2007). Biodiesel producers have the option to sell the crude glycerol to a glycerol refinery as a way to defray the high capital costs of production (70 – 95% of

production cost is raw material), but this is not a very economically attractive option (Paulo *et. al.*, 2009; Yazdani & Gonzalez, 2007). Crude glycerol typically contains impurities depending on the production method, such as alcohol, salts, heavy metals, and water, and must be purified and refined before subsequent use in conventional applications at cost (Ayoub & Abdullah, 2012), typically by vacuum distillation and subsequent fractional distillation (Katryniok *et. al.*, 2011). Moreover, the biodiesel producer is also responsible for freight costs, which can easily match or exceed the value of the crude glycerol (Johnson & Taconi, 2007). Conversion of crude glycerol into value-added products has been touted as a valuable opportunity for the biodiesel industry to increase revenue and expand its product market (fig. 5) (Johnson & Taconi, 2007; Paulo *et. al.*, 2009; Yazdani & Gonzalez, 2007).

Glycerol can be converted to chemicals of commercial interest by a number of reaction types, including chemical or biochemical reduction or oxidation reactions, bond breaking, and polymerization reactions which generate alternative three-carbon compounds (Johnson & Taconi, 2007; Kenar, 2007; Pagliaro *et. al.*, 2007). Selective oxidation of glycerol produces glycerol oxygenates, which have considerable practical value (Zhou *et. al.*, 2008). Oxidation of the hydroxy groups yields glyceric, tartronic acids, dihydroxyacetone (DHA) mesoxalic acid (or ketomalonic acid). Etherification can be used to produce fuel oxygenates, such as glycerol tertiary butyl ether, which when incorporated in standard aromatic diesel fuel, leads to significantly reduced emissions of particulate matter, hydrocarbons, carbon monoxide and unregulated aldehydes (Pagliaro *et. al.*, 2007). Hydrogenolysis produces propylene glycol (1,2-propanediol); dehydration produces acrolein, reforming produces syngas, and microbial fermentation produces 1,2- and 1,3-propanediol (Johnson & Taconi, 2007; Pagliaro *et. al.*, 2007).

Glycerol carbonate (4-hydroxymethyl-1,3-dioxolan-2-one) is a relatively new material in the chemical industry, reportedly with a large potential as a novel component of gas-separation membranes, a solvent for several types of materials, a biolubricant (owing to its adhesion to metallic surfaces and resistance to oxidation), hydrolysis, and pressure, and polymer precursor (Johnson & Taconi, 2007). It can be prepared directly and in high yield from renewable glycerol and dimethyl carbonate or urea in a reaction catalysed by lipases, or in a reaction with carbon dioxide under supercritical conditions (Kenar, 2007).

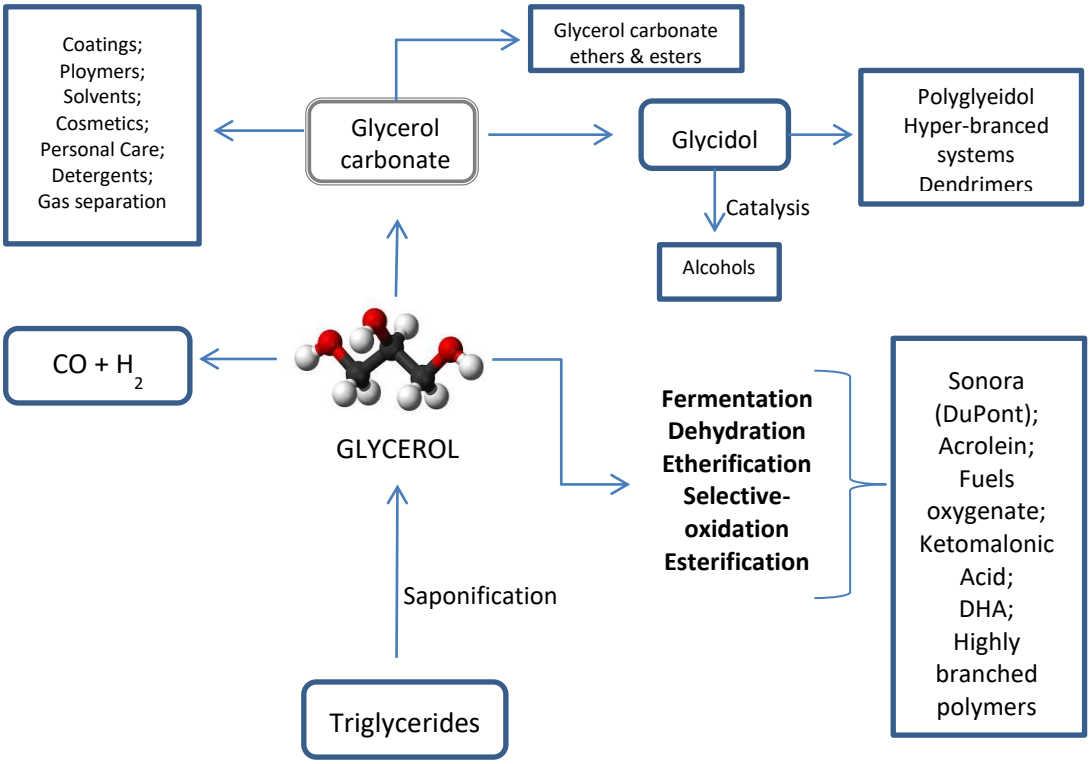


Figure 5: A representation of the value-chain from glycerol to valued fine chemicals (redrawn from Pagliaro *et. al.*, 2007).

High crude oil prices have also made glycerol an attractively priced substitute for many petro-derived chemicals (Miller-Klein Associates 2006; Transparency Market Research, 2013). In the manufacture of epichlorohydrin for example (a chemical intermediate in epoxy resin manufacture, in paints and coatings, composites, adhesives, pulp and paper chemicals, water treatment and others); or in poly-(trimethylene terephthalate) manufacture, a polymer fibre with properties related to nylon and polyethylene terephthalate, are produced from 1,2-propanediol, or 1,3-propanediol, which are derived from glycerol (Kenar, 2007; Ragauskas *et. al.*, 2006). Production of these compounds has resulted in companies such as Archer Daniel Midland (ADM), Solvay, Cargill, Huntsman, and Dow Chemical Co., and others, shifting to using glycerol as their main feedstock in industrial transformations reliant on microbial fermentation processes (Kenar, 2007; Miller-Klein Associates, 2006; TransparencyMarketResearch, 2013).

7.2.2.1 Bioconversion of glycerol

The excess amounts of glycerol generated from biodiesel production represent too large a surplus product which the existing glycerol market cannot economically accommodate (Miller-Klein Associates, 2006). Thus new markets and applications for crude glycerol are required to ensure long-term market sustainability. Crude glycerol is an inexpensive and abundant carbon source for industrial

microbiology (Kenar 2007; Fakas *et. al.*, 2009). Many known microorganisms are able to naturally utilize glycerol as a sole carbon and energy source (Yazdani & Gonzalez, 2007), and these have attracted attention for the use of glycerol from biodiesel in bioconversion to obtain, for example, reduced chemicals such as succinate, 1,3-propanediol, ethanol, xylitol, propionate, hydrogen, etc. at higher yields than those obtained using sugars (Paulo *et. al.*, 2009; Yazdani & Gonzalez, 2007). While promising, the limitation with these applications however is that the crude glycerol which the microorganisms are grown on often contains impurities such as water, alcohols, heavy metals, salts, which inhibit their growth and productivity (Johnson & Taconi, 2007).

7.2.2.1.1 Microbial catabolism of glycerol: aerobic & anaerobic pathways

Glycerol's uptake/incorporation across the cytoplasmic membrane of *E. coli* is facilitated via a transport mechanism and mediated by the glycerol uptake facilitator protein, GlpF. Once entry into the cell is established, a number of catabolic pathways are used to metabolise the compound depending on the prevailing environmental conditions (aerobic, microaerobic or anaerobic).

Aerobic glycerol catabolism

There are two major pathways involved in aerobic glycerol catabolism: the phosphorylation pathway, which is the most common, and the oxidation pathway. The phosphorylation pathway involves glycerol phosphorylation by glycerol kinase (GlpK) to yield glycerol-3-P, which is then oxidized to dihydroxyacetone-3-P (or DHAP) by an NAD-linked dehydrogenase (Courtright, 1976; Sprague & Cronan, 1977). In *Enterobacter faecalis*, this reaction is catalysed by glycerol-3-P oxidase (GlpO), which uses molecular oxygen as an electron acceptor thus forming H_2O_2 in the process (Bizzini *et. al.*, 2010). In the oxidative pathway, glycerol is first oxidized to yield dihydroxyacetone, which is then phosphorylated by DHA-kinase to produce again 3-P-dihydroxyacetone (Morgan, 2013). Both pathways lead to the formation of DHAP, a glycolysis intermediate (fig. 6).

It has generally been accepted that microorganisms use either the phosphorylation or oxidative pathways to assimilate glycerol depending on anaerobic or anaerobic environmental conditions. In *E. faecalis* it was established that the GlpK and GlyD pathways operate under aerobic conditions, whereas the GlyD-DhaK pathway is used exclusively under anaerobic conditions (Bizzini *et. al.*, 2010).

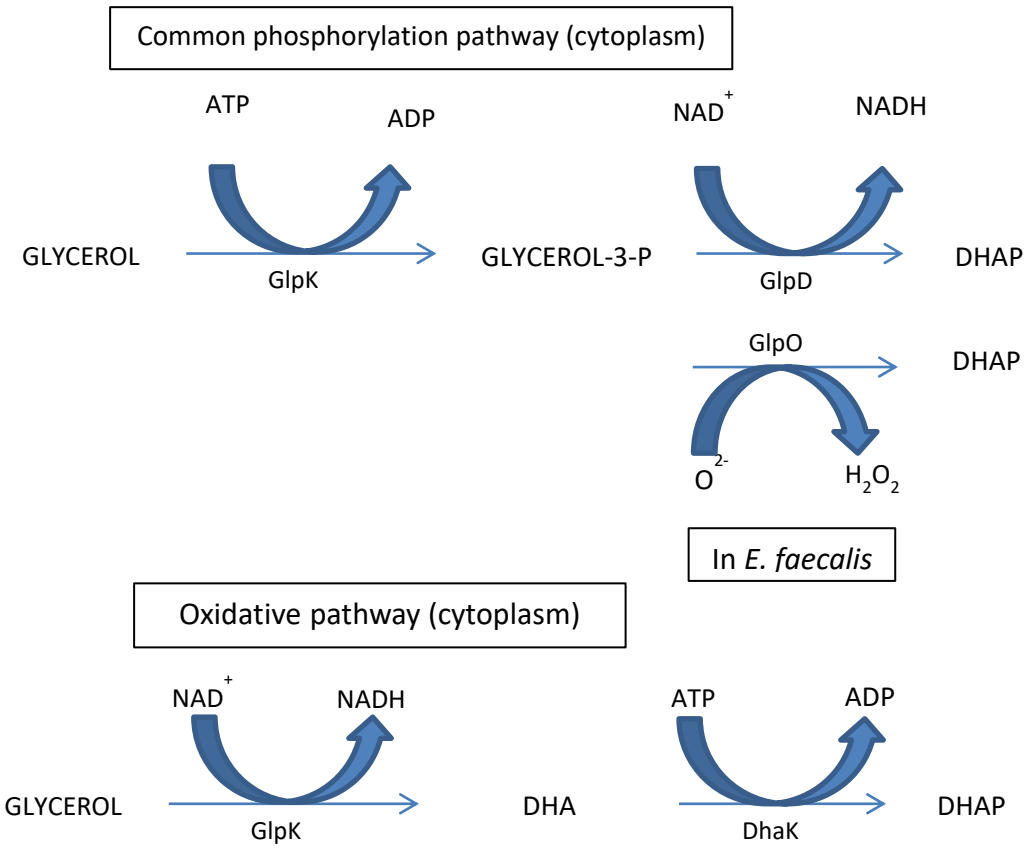


Figure 6: Aerobic glycerol catabolism in the cytoplasm leading to the formation of DHAP or dihydroxyacetone-3-P, as described in the text.

In *Neurospora crassa* both pathways operate; and in some microorganisms, alternative pathways are considered in which glycerol is oxidized by a NADP-linked dehydrogenase to glyceraldehyde, which may then be converted to 3-P glyceraldehyde or glycerate, and then 3-P-glycerate (Tom *et. al.*, 1978). Yet another pathway for glycerol catabolism operates in strains of *Aspergillus*, *Neurospora*, and *Penicillium*, and involves glycerol oxidase that oxidizes glycerol to D-glyceraldehyde and hydrogen peroxide using molecular oxygen (Fakas *et. al.*, 2009). The glycerol oxidase pathway has the unique feature that glycerol oxidation is not coupled to the reduction of NAD or FAD (Fakas *et. al.*, 2009). Whichever pathway is used, glycerol is finally transformed to intermediates of the glycolytic pathway. Then, the second branch of glycolytic pathway is employed to transform these intermediates to pyruvic acid and hence to acetyl-CoA. Assuming that glycerol is catabolized by one of the major pathways, the overall stoichiometry of glycerol catabolism is:

Glycerol + 2NAD+ ADP+ Pi -> Pyruvate + 2NADH+ 2H + ATP (Fakas, *et. al.*, 2009)

Thus one mole each ATP and pyruvate are produced per mole of glycerol consumed, while two moles of each ATP and pyruvate are produced per mole of glucose consumed. The produced pyruvate is further metabolized to acetyl-CoA, which is the biosynthetic precursor of various microbial products (e.g. citric acid, lipids). ATP is produced through oxidative phosphorylation, thus bioprocesses are required to be well aerated.

7.2.2.1.2 Anaerobic pathways

Microorganisms are able to convert glycerol through fermentation (i.e. in the absence of terminal electron acceptors such as NO_3^- and O_2) generating useful organic compounds as redox consuming products. These compounds are used primarily as monomers for polyester synthesis. Of those able to perform these conversions, a number belong to the *Enterobacteriaceae* family. *Klebsiella pneumoniae*, *Citrobacter freundii*, *Clostridium butyricum*, as well as species of the genera *Lactobacillus*, *Enterobacter*, *Bacillus*, *Propionibacterium* are known fermenters of glycerol (Gonzalez *et. al.*, 2008; Murarka *et. al.*, 2008; Trinh & Srienc, 2009). These genera produce 1,3-propanediol as a product (Drożdżyńska *et. al.* 2011; Barbirato *et. al.* 1996). The production of 1,2-propandiol is described later.

In these species, glycerol fermentation produces ethanol via a redox-balanced pathway which produces ATP via substrate-level phosphorylation, where one molecule of ATP is generated per molecule of glycerol converted to ethanol (Gonzalez *et. al.*, 2008; Yazdani & Gonzalez, 2007). Fermentation is facilitated by an oxidative and reductive pathways as with aerobic dissimilation (fig. 7) (Gonzalez *et. al.*, 2008; Drożdżyńska *et. al.*, 2011; Gupta *et. al.*, 2009), resulting in the synthesis of dihydroxyacetone-phosphate (DHAP) and 1,3-propanediol (1,3-PDO) respectively (Drożdżyńska *et. al.* 2011). Glycerol is dehydrogenated to dihydroxyacetone (DHA) by a type I, NAD-linked glycerol dehydrogenase (glyDH-I) in the oxidative branch. DHA then becomes phosphorylated by ATP- or PEP-dependent DHA kinases (DHAK) to DHAP (Gonzalez *et. al.*, 2008; Gupta *et. al.*, 2009; Paulo *et. al.*, 2009). In the alternate reductive branch, glycerol is dehydrated by the coenzyme B12-dependent glycerol dehydratase to form 3-hydroxypropionaldehyde (3-HPA). 3-HPA is then reduced to 1,3-PDO by the NADH-linked 1,3-PDO dehydrogenase (1,3-PDODH), regenerating NAD+ in the process (Gupta *et. al.* 2009; Paulo *et. al.* 2009; Drożdżyńska & Czaczyk 2011).

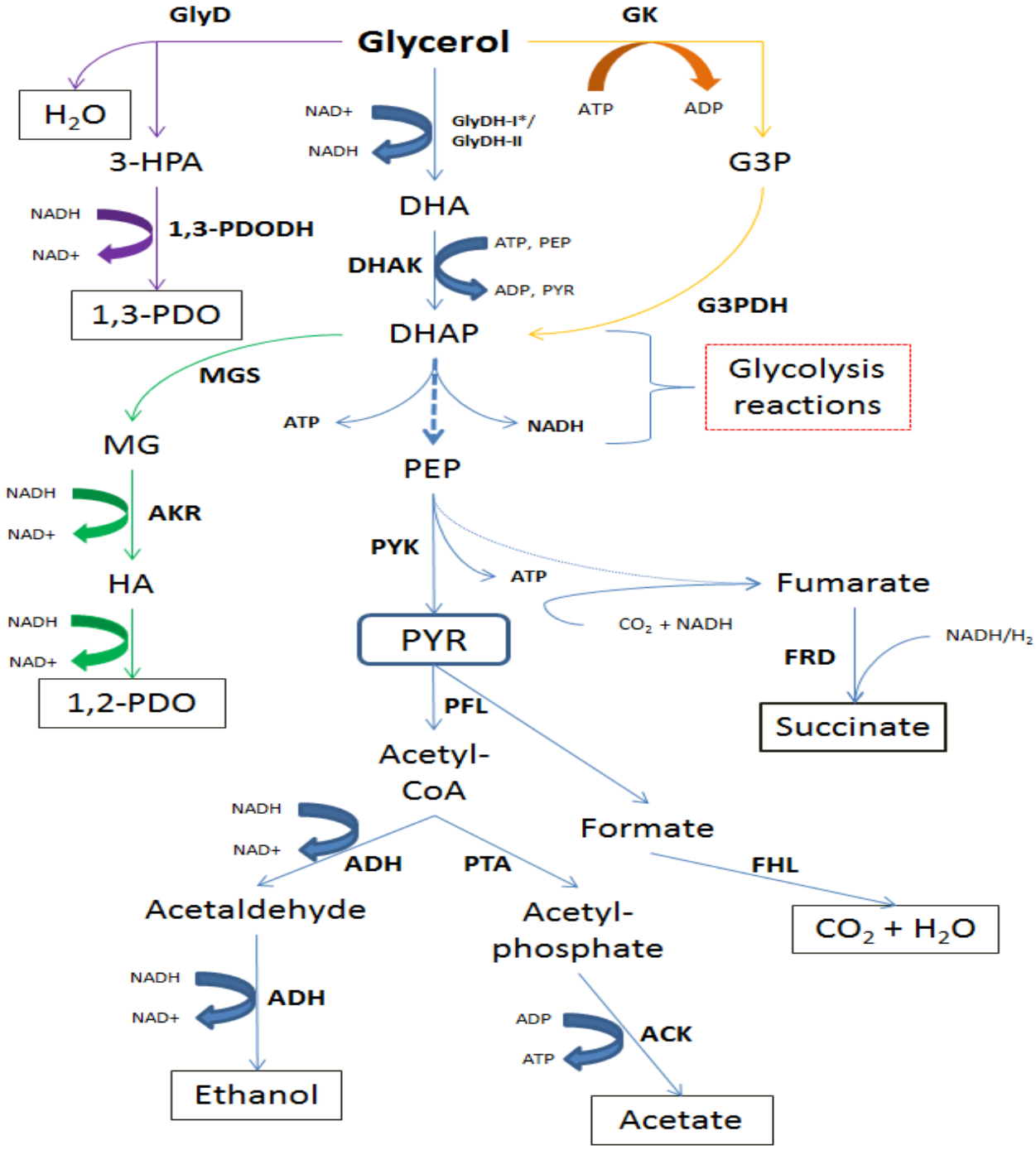


Figure 7: Glycerol metabolism in *E. coli* and other members of Enterobacteriaceae family. Diagram indicates major products of fermentation (encircled with black boxes). Purple and orange pathways are the oxidative and reductive pathways of the Enterobacteriaceae respectively. In green and blue are the pathways used by *E. coli*, as described in the text. Enzymes responsible for reactions are shown in caps beside the respective reaction. Abbreviations: ACK – acetylkinase; ADH – acetaldehyde dehydrogenase; AKR – aldo-keto reductases; DHAK – dihydroxyacetone kinase; FRD – fumarate dehydrogenase; GDH – glycerol dehydrogenase; PFL – pyruvate formate lyase; PYK – pyruvate kinase; MGS – methylglyoxal synthase; G3PDH – glycerol-3-dehydrogenase; GK – glycerol kinase; 1,3-PDODH – 1,3-PDO dehydrogenase; GlyD – glycerol dehydratase; GlyDH-I – glycerol dehydrogenase type 1; GlyDH-II – glycerol dehydrogenase type 2. 1,3-PDO - 1,3-propanediol; 3-HPA - 3-hydroxypropionaldehyde; DHA - dihydroxyacetone; DHAP – dihydroxyacetone phosphate; G3P – glycerol-3-phosphate; G3PDH - glycerol-3-phosphate dehydrogenase; HA - hydroxyacetone; MG - methylglyoxal; PEP – phosphoenolpyruvate; PYR – pyruvate. Image constructed from the following references: (Gonzalez *et. al.*, 2008; Blankschien *et. al.*, 2010; Yazdani & Gonzalez 2008; da Silva *et. al.*, 2009).

7.2.2.1.3 Glycerol fermentation in *E. coli*

Glycerol fermentation activity was thought to be absent within *E. coli* given the lack of a native 1,3-propanediol pathway that acts as an electron sink under anaerobic conditions (Gonzalez *et. al.*, 2008; Trinh & Srienc, 2009). This hypothesis was modelled on *in vitro* studies of two membrane-bound dehydrogenases, glycerol-3-phosphate dehydrogenase (encoded by *glpD*), which is coupled to glycerol metabolism in the presence of oxygen, and the *GlpABC* operon, that transfers electrons to fumerate or nitrate in anaerobic conditions (fig. 8). *E. coli* contains two glycerol-3-phosphate dehydrogenases encoded by the *glpABC* and *glpD* genes. GlpABC is required for anaerobic growth with glycerol or glycerol-3-phosphate and fumarate as the terminal electron acceptor, while GlpD is required for aerobic growth with glycerol (or glycerol-3-phosphate) (Cole *et. al.*, 1988).

These are involved in the conversion of glycerol-3-phosphate (G3P), a product following phosphorylation of glycerol by glycerol kinase to the intermediate dihydroxyacetone-phosphate (DHAP), which is subsequently converted to pyruvate via glycolysis (Dharmadi, 2006; Gonzalez *et. al.*, 2008). Therefore, subsequent efforts to ensure aerobic glycerol metabolism by this microorganism depended on the canonical addition of external electron acceptors to the medium (e.g. nitrate, nitrite, fumerate, dimethyl sulfoxide or trimethylalamine-*N*-oxide). Metabolic engineering events which balance the redox potential, such as introducing the 1,3-propanediol pathway from one of the other members of the *Enterobacteriaceae* family if anaerobic metabolism was essential (Trinh & Srienc, 2009) would also be employed.

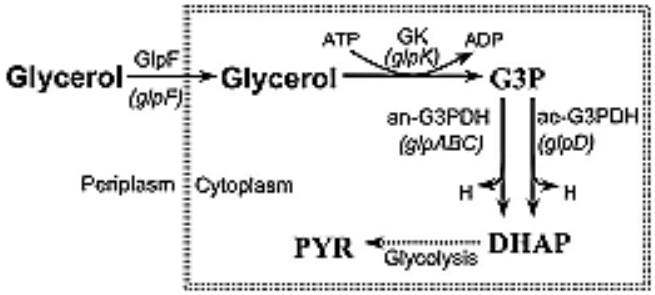


Figure 8: Aerobic glycerol metabolism in *E. coli*. In the presence of electron acceptors, glycerol is metabolised by an ATP-dependant glycerol kinase (GK) and two respiratory enzymes, aerobic G3PDH (ae- G3PDH) and the electron transporter (an-G3PDH). H – Reducing equivalent (NADH/NADPH/FADH2); DHAP – dihydroxyacetone phosphate; G3P – glycerol-3-phosphate; PYR – pyruvate (Murarka *et. al.*, 2008).

Anaerobic metabolism of glycerol in the absence of externally supplied electron acceptors was recently demonstrated in *E. coli* with controlled environmental conditions (Dharmadi, 2006). In late fermentation samples with glycerol as the sole carbon source, 1,2-PDO was formed alongside the major fermentation products (Murarka *et. al.*, 2008). In an advanced report, the pathways responsible for the anaerobic utilisation of glycerol in *E. coli* were identified and characterised, and a new model

for this process suggested. This model suggests that glycerol fermentation results in 1,2-PDO via a dormant, native pathway, instead of the common 1,3-PDO pathway as with other enteric bacteria. This process is described as follows (fig. 7): Glycerol is dehydrogenised to dihydroxyacetone (DHA) by glyDH-II; DHA is phosphorylated by DHA kinase (DHAK) to generate DHAP and DHAP is then reduced to methylglyoxal by methylglyoxal synthase. Methylglyoxal is further reduced to hydroxyacetone by three aldo-keto reductases, encoded by *yeaE, yghZ, yafB,* and generating NAD^+ in the process. Hydroxyacetone is then reduced further to 1,2-PDO by NADH-linked glycerol dehydrogenase generating another NAD^+ molecule (Gonzalez *et. al.*, 2008).

Despite the potential and promise for amenability, industrial-level application of most of these microorganisms, i.e. *K. pneumonia* and *C. butyricum*, is limited. This is primarily due to issues of pathogenicity, the lack of genetic tools for their manipulation, and the requirement for rich nutrient supplements (Murarka *et. al.*, 2008). However, of these, *E. coli* is a most promising glycerol converter, since most genetic tools for manipulation already exist for this model organism (Datta, 1985).

The case for an aerobic glycerol conversion process

E. coli is a metabolically versatile facultative anaerobic bacterium that is able to grow in the presence and absence of oxygen. Depending on the availability of electron acceptors, different modes are used for energy production: respiration or fermentation.

In the presence of O_2, aerobic respiration allows the complete oxidation of a growth substrate (usually sugars), and therefore is the most productive and hence the preferred metabolic mode. During aerobic metabolism, the glycolytic conversion of a substrate to pyruvate and the oxidative decarboxylation of pyruvate by the pyruvate dehydrogenase complex, leads to the formation of acetyl-CoA and carbon dioxide. Two ATP and two NADH molecules are also formed (Förster & Gescher, 2014; Partridge *et. al.*, 2006) which feeds the citric acid cycle. The expression of pyruvate dehydrogenase is influenced by NADH/NAD ratio as well as the pyruvate concentration (Förster & Gescher 2014).

Where O_2 is available, oxidation of the acetyl units generates reducing equivalents that are transferred to O_2 via aerobic electron transport chains, creating proton gradients that can be used to generate ATP and drive other essential activities (Partridge *et. al.*, 2006).

In the absence of O_2, two alternative metabolic modes are available: anaerobic respiration and fermentation. If a terminal electron acceptor, such as NO_3^-, is present, then anaerobic respiration is possible. During anaerobic respiration the role of the pyruvate dehydrogenase complex is assumed by

pyruvate formate-lyase, which catalyses the formation of acetyl-CoA and formate and prevents the release of NADH during pyruvate consumption. The citric acid cycle is repressed, and the metabolic flow in the C_4 section of the citric acid cycle is reversed, and acetyl-CoA is converted to the main product acetate. Anaerobic respiration yields less energy than aerobic respiration because the substrate is only partially oxidized (Förster & Gescher, 2014; Partridge *et. al.*, 2006).

Under fermentative conditions, energy is conserved by substrate level phosphorylation, and redox balance is achieved by the formation of acetate, ethanol, H_2, CO_2, formate, and succinate. This process occurs through the action of alcohol dehydrogenase catalysing acetyl-CoA to ethanol, consuming two NADH molecules in the process. Lactate production occurs through the reduction of pyruvate by lactate dehydrogenase, a process which consumes one NADH molecule. In the formation of succinate, oxaloacetate is formed from the carboxylation of phosphoenolpyruvate by PEP-carboxylase, followed by the activities of malate dehydrogenase, fumerase reductase and fumerase (Förster & Gescher 2014). Anaerobic respiration is more productive than fermentation (Partridge *et. al.*, 2006).

A redox balance analysis further explains the observed results in the fermentative utilisation of glycerol. During fermentation, the incorporation of glycerol in cellular biomass results in the generation of reducing equivalents, which are consumed by the generation of ethanol as the major product, as its synthesis from glycerol takes place through a redox-balanced pathway (Durnin *et. al.*, 2009). Energetically however, the process is not as efficient as the aerobic process and yields less energy and further produces more by-products.

7.3 Tandem conversions

The conversion of vegetable oil to methyl- or other short-chain alcohol esters can be catalysed in a transesterification reaction using lipases in organic solvents or in aqueous systems as discussed previously (Jaeger & Eggert, 2002). This process results in a glycerol by-product and the biodiesel product of interest. While potential applications of the by-product are numerous, of progressive interest is a combined bioprocess approach, where the by-product is directly utilised in a further reaction to produce useful compounds. This approach to bio-catalysis is more common in organic synthesis, where whole-cells are exploited to produce such desired products as alcohols, acids and acid derivatives, amino acids and amines, for C-C bond formation, for the synthesis of nucleosides, nucleotides and their derivatives, oligosaccharides, glycoconjugates, etc. In such applications the cells' metabolic networks have been engineered to minimize the diversion of substrate for their normal metabolic requirements (Oroz-Guinea & García-Junceda, 2013). Isolated enzymes involved in the processes themselves may also be used in tandem reactions allowing precise control of

parameters. Doing so leaves the enzymes vulnerable to performance issues and co-factor dependence, among other problems (Oroz-Guinea & García-Junceda, 2013).

Interesting applications for tandem reactions include multi-enzyme biofuel cells, i.e. the production of hydrogen, and ethanol (Oroz-Guinea & García-Junceda, 2013). Sotenko *et. al.* (2012) reported on the conversion of codeinone to oxycodone using consecutive biological and chemical catalysis in 1-(3-hydroxypropyl)-3-methylimidazolium glycolate ionic liquid by Walker & Bruce (2004), and on Liu *et. al.* (2007) who demonstrated fermentation of glycerol to 1,3-propanediol using *C. butyricum*, followed by direct use of the fermentation broth to produce secondary amines using hydrogen transfer catalysis in a biphasic system (an unpurified fermentation broth with the catalyst dissolved in an ionic liquid). Sotenko *et. al.* (2012) used tandem transformation of purified waste glycerol from biodiesel production via microbial fermentation and membrane-supported *Rhizomucor miehei* lipase esterification in a continuous system, in which 1,3-propanediol was produced at an optimised productivity of 2.4 $g.L^{-1}.h^{-1}$, and was further esterified in a biphasic system to achieve an ester yield of up to 75%.

More recently, the tandem approach was used in the production of biodiesel using a lipase (lipozym 435) as the transesterification catalyst, secured onto a macroporous resin support with a diameter of 0.3 – 0.9 mm (fig. 9). The combined bioprocess avoids enzyme inhibition by glycerol, reduces the production cost and raises productivity for biodiesel and the product alternatives produced from glycerol fermentation (Mu *et. al.*, 2008). Plant oils are trans-esterified by a lipase to produce FAME (biodiesel) and glycerol, where the glycerol by-product is further used as a substrate for microbial whole-cell fermentation thereafter. Whilst most publications focus on using glycerol as a component of a media formulation, few have focused on using glycerol as the sole carbon source with tandem production in mind. Mu *et. al.* (2008) reported biodiesel production in this manner with microbial production of 1,3-propanediol (1,3-PD) using *K. pneumoniae*. In this report, glycerol was directly converted to 1,3-PD by *K. pneumoniae*, and after 20 hours the methyl ester yield was 84%, and the molar yield and productivity of 1,3-PD were 0.47 $mol.mol^{-1}$ and 1.7 $g.l^{-1}.h^{-1}$, respectively. The study considered a hollow-fibre membrane through which glycerol would pass through during transesterification and enter the fermentative cycle. The experimental setup was as below:

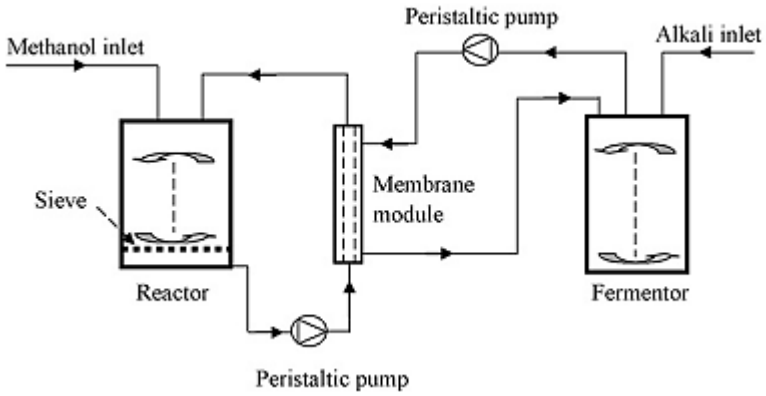


Figure 7: Schematic diagram of a combined bioprocess of production biodiesel by lipase with microbial production of 1,3-propanediol by *K. pneumoniae*. Adapted from Mu *et. al.*, (2008)

In a similar approach to Mu *et. al.* (2008), this work aims to utilise a tandem approach in the transesterification of sunflower oil catalysed by a lipase, and to utilise whole-cell fermentation of the glycerol waste product to produce biodiesel.

Problem statement:

As discussed, *E. coli* has the ability to produce ethanol in an anaerobic environment, from glycerol. Lipase from a glycerol carbon source can also be produced. Additionally, ethanol can replace methanol in the production of biodiesel. This leaves the following scenario:

Reaction 1

10 oil + ethanol → 10 biodiesel + glycerol (where the catalyst is a lipase). Ratios are 10:1 oil:ethanol → 10:1 biodiesel:glycerol (ratios shown here are molar ratios)

This reaction is reversible. In practice the reaction is pushed forward with high levels of methanol / ethanol.

Reaction 2

Glycerol → lipase catalyst. Here, the lipase is produced by *E. coli* when utilising glycerol as the carbon source.

Reaction 3:

Glycerol → ethanol. Glycerol is converted to ethanol by *E. coli* through anaerobic production.

When these three reactions are put together, the overall reaction is as below:

Oil + Ethnaol → biodiesel + {Glycerol → lipases +Ethanol, *E. coli* derived}

The overall reaction is therefore pushed forward since:

1. The by-product glycerol is removed
2. Ethanol is produced, one of the key reactions

The question of how many ethanol molecules could be formed from a glycerol molecule, while maintaining sufficient energy for cell growth and lipase production remains.

As a supplement, the below section is included should there be a surplus/excess ethanol in the system.

7.3.1 "E-diesel"

Ethanol as an additive in diesel fuel is not a new proposition, and has been considered since ethanol was used in petroleum blends (Ribeiro *et. al.*, 2007). Ethanol addition to diesel reportedly decreases the flash point, increases the vapour formation potential, decreases cetane number (a quantity indicating the ignition properties of diesel fuel relative to cetane as a standard), heating value, aromatic fractions, kinematic viscosity and changes distillation temperatures. Ethanol solubility in diesel, however, is affected by temperature (which can be improved by the addition of surfactants and co-solvents), the hydrocarbon composition of diesel, and water content in the blend (Kousoulidou *et. al.*, 2008).

Lee & Lee (2007) evaluated the effects of different ethanol–diesel blends, from 0% ((E0-D) to 20% (E20–D)), on the performance and emissions of diesel engines to find the optimum percentage of ethanol that gives simultaneously better performance and lower emissions. Among the other parameters evaluated, it was found that fuel consumption increased with an increase of ethanol contents in the blended fuel at overall operating conditions. Smoke (including CO and NOx), however, and particulate matter emissions decreased for every grade of blend, especially with E10–D and E15–D (Lee & Lee, 2007). Since the blending of ethanol and diesel fuel results in a decrease of the cetane number and alters the physiochemical properties of the latter, an additive is usually used for compensating the deterioration in fuel characteristics (He *et. al.*, 2003). Researchers have thus considered ethanol-biodiesel-diesel blends (EB-Diesel), where petroleum diesel is used as an amphiphile to stabilise ethanol and biodiesel blends which tend to separate at low temperatures. This approach is exemplified in the study by Shi *et. al.* (2006) in which their EB-Diesel contained ethanol, methyl soyate and diesel fuel at a ratio of 5:20:75. Reports of the effects on engine parameters and emissions however vary widely according to the conditions under which the fuel is used (speed, load, test cycle, engine size and engine design) (Kousoulidou *et. al.*, 2008).

7.4 Research aim

From the presented review it was shown that *E.coli* is able to: 1. use glycerol as a carbon source; 2. produce ethanol anaerobically; and 3. grow and produce lipsases with glycerol as a carbon source. Since ethanol can replace methanol in the production of biodiesel, and the reaction could be catalysed by lipases, the following biodiesel production system is proposed:

Oil + ethanol → biodiesel, with

Glycerol → lipases + Ethanol (*E.coli* derived).

The reactions are therefore pushed forward since the by-product glycerol is removed, while the one substrate, ethanol is being produced as one of the key reactions.

This work aims to:

1. Determine the feasibility of this reaction by theoretically determining the molecular ratios, of ethanol formed from glycerol molecules, while having sufficient energy for cell growth and lipase production.
2. Obtain lipase expression in *E. coli* as the first step to test this hypothesis.
3. Propose to use the whole cell to express lipase under aerobic conditions and then further ferment glycerol when placed in anaerobic conditions.

8 MATERIALS & METHODS

8.1 Lipase selection

The lipase gene sequence was sought on the BRENDA database (www.brenda-enzymes.info) at the instruction of Dr. K. Rumbold. The following parameters were considered, influenced by the potential operating conditions of the system: mesophillic; solvent tolerant (ethanol); operating pH 6 – 7; expressable in *E. coli*; high turnover. From the list returned, the following candidates were considered:

Aspergillus niger: Mycelium-bound lipase with optimal activity in pH range 3.0 – 6.5, with two pH optima at 4 and 7. High catalytic activity between 4 – 8 °C. Highly stable in reaction mixtures containing methanol and ethanol with 100% activity following exposure to ethanol for 1 hour (Romero *et. al.*, 2007).

Acinetobacter baylyi: enzyme expressed maximum activity at 60 °C and pH 8.0 with p-nitrophenyl palmitate as a substrate; stable in pH range 6.0 - 9.0, and temperature range 60 - 80 °C. Enzyme could hydrolyse a wide range of p-nitrophenyl esters, but preferentially medium length acyl chains (C(8)-C(12)) (Uttatree *et. al.*, 2010).

Aspergillus fumigatus CGMCC 2873: preference for short carbon chain p-nitrophenyl esters, especially toward C2 p-nitrophenyl ester. Optimum pH and temperature: 8.5 and 65 °C, respectively. The lipase was stable in the pH range 6.0 - 8.5 for 16 h (at 4 °C) and at 30 - 50 °C for 1 hour (Shangguan *et. al.*, 2011).

Pseudomonas mendocina M-37: lipase was optimally active at pH 9.0, temperature of 50 °C and was found to be stable between pH 7.0-11.0. Enzyme has 100% activity at 20% (v/v) ethanol (Dahiya *et. al.*, 2010).

A candidate was found that suitably matched the criteria. It was chosen on the basis that a bacterial lipase was preferred due to the influence of codon bias, and the under the operating conditions of the system was deemed to be the most preferred candidate. This was the *Pseudomonas mendocina* (PK-12CS) lipase. The lipase was reported with maximum activity at 37 °C and pH 8; and 82.69% activity in ethanol (Jinwal *et. al.*, 2003). The lipase, however, required a chaperone. The sequences of both enzyme (LipB) and chaperone (LipA) were retrieved from GenBank (https://www.ncbi.nlm.nih.gov/genbank/, acc. no.: AY091666.1; LipA protein ID: AAM14701.1, LipB protein ID: AAM14702.1). The DNA sequence for LipB was unavailable, thus the protein sequence was back translated using the EMBL BackTransSeq with *E. coli* K-12 (high) codon table selected. Complete sequences were submitted to GenScript® (Piscataway, NJ, USA) for synthesis with codon optimisation requested to minimise codon bias (Appendix, section 11.3).

Due to the requirement of a chaperone to assist in the enzyme assuming its final active conformation following translation of the enzyme, a system was sought which would enable the dual-expression of the enzyme with its helper protein. Dual-plasmids were undesireable due to the metabolic burden placed on the expression host, and the potential for one of the plasmids to be expelled where dual-selection was not performed. Simplicity of the expression vector and system was further favoured. This was pETDuet (for detailed features of this vector, see section 7.2.3).

8.2 Preparing LipA and LipB from GenScript pUC57

8.2.1 LipB

LipA and LipB were ordered and received from GenScript in pUC57, with BamHI at 5' and NotI at 3' restriction sites (see Appendix, section 11.1). Restriction of the pETDuet vector with Not1 and BamH1 would remove the area between the two cloning sites (see section 7.2.3). This was corrected with primers ordered from Inqaba Biotech to change the restriction sites (5' and 3') of the LipB gene to have a restriction site for NdeI at 5' and XhoI at 3', thus preserving the vector area between MCS1 and MCS2.

PCR amplification of LipB from pUC57

A PCR reaction for LipB was performed with pUC57 containing LipB as template DNA, using the primers Lip B_F10 5'-ATTGATGGTCCATATGTCACGCTCCATCCTGC-3' (NdeI) and LipB_R10 5'-CGCTTAG CGGGTACGGTCCTCGAGGACCCAAT-3' (XhoI). Amplification was performed in a 25 µl reaction volume and consisted of 10 µl nuclease free water, 200 µM of each dNTP (from 10 mM stocks), 0.5 µM forward primer and reverse primer respectively, 0.5 µg template pUC57 plasmid DNA with LipB as insert, 0.02 U/µl Phusion polymerase (Thermo Scientific). PCR was performed using a Biorad PCR T100® thermocycler. The thermal cycler was programmed for 90 s at 95 °C for initial denaturation, followed by 35 cycles of 30 s at 95 °C for denaturation, 30 s at 55 °C for annealing, 90 s at 72 °C for extension, and 5 min at 72 °C for the final extension. An aliquot of the PCR products were resolved by electrophoresis at 80 V for 45 min in a 1% (w/v) agarose gel, which contained 1 µl of a 0.5 µg/ml ethidium bromide solution in 1 x TAE buffer, with the marker being a 1 kb DNA ladder. The electrophoresis gel was then visualised on a Molecular Imager® Gel Doc™ XR System (BioRad).

Band excision (gel), cleaning & insert verification

Following gel visualization, the band was quickly excised under 200nm UV light and cleaned using a Qaigen QIAquick PCR Purification Kit as per the protocol. The LipB amplicon was then double-digested with FastDigest BamH1 and Not1 (Thermo Scientific) in a water bath as per the protocol,

along with a parallel digest of the pETDuet vector at the second multiple cloning site (MCS2) with the same enzymes. An aliquot of this reaction was then set up for ligation in a 1:2 and 1:3 vector:insert ratio according to the protocol overnight at 4 °C, with an aliquot of the reactions saved for gel viewing. A 5 µl aliquot of the ligation mixture was then introduced into 50 µl of pre-prepared competent *E. coli* DH5α cells (F^- *endA1 glnV44 thi-1 recA1 relA1 gyrA96 deoR nupG purB20* φ80d*lacZ*ΔM15 Δ(*lacZYA-argF*)U169, hsdR17($r_K^- m_K^+$), λ^-) using the standard heat-shock technique. A volume of 100 µl of the transformed mixture was spread onto two LB-ampicillin plates (ampicillin was prepared as 1 mg/ml working stock solution and aseptically added to media/agar when the solution(s) had cooled sufficiently) to aid selection. A ligation screen was employed with suitable vector- and gene-specific primers respectively to verify the insert.

8.2.2 LipA PCR amplification from pUC57

A PCR for LipA was set up, with pUC57 containing LipA as template DNA, with primers ordered from Inqaba Biotechnical Industries (Pty) Ltd., with unique restriction sites chosen for MCS 1 (BamH1 & Not1). In previous attempts, various annealing temperatures were used which did not yield adequate results for the amplicon. Thus a touch-down PCR was considered. Primers were: LipAF10 5'-AGCCAGGATCCCATGAATAAAAAAT-3' (BamHI), and LipAR10 5'-GCGGCCGCTCACAGACCAGCATTTT-3' (NotI). Amplification was performed in a 25 µl reaction volume and consisted of 10 µl nuclease free water, 200 µM of each dNTP (from 10 mM stocks), 0.5 µM forward primer and reverse primer respectively, 0.5 µg template pUC57 plasmid DNA with LipA as insert, 0.02 U/µl Phusion polymerase (Thermo Scientific). PCR was performed using a Biorad PCR T100® thermocycler. The thermal cycler was programmed for 5 min at 94 °C for initial denaturation, followed by 24 cycles of 20 s at 92 °C for denaturation, 20 s at 70 °C for annealing, 1 min at 72 °C for extension, and 5 min at 72 °C for the final extension, followed by a hold at 10 °C. The amplicon was prepared for verification similarly to LipB, with the exceptions that BamHI and NotI were the restriction enzymes chosen, and the first multiple cloning site was chosen for ligation with the pETDuet vector (MCS1).

pETDuet (fig. 11) was received as a 10 µg lyophilised pellet and prepared to a final working concentration of 1 µg/µl as per the manufacturer's protocol. The pETDuet vector without inserts at either MCS1 or MCS2 was transformed into competent *E. coli* DH5α cells using the heat-shock technique. A volume of 100 µl of the transformed mixture was spread onto two LB-ampicillin plates to aid selection (fig.11).

8.2.3 pETDuet-1 vector and features

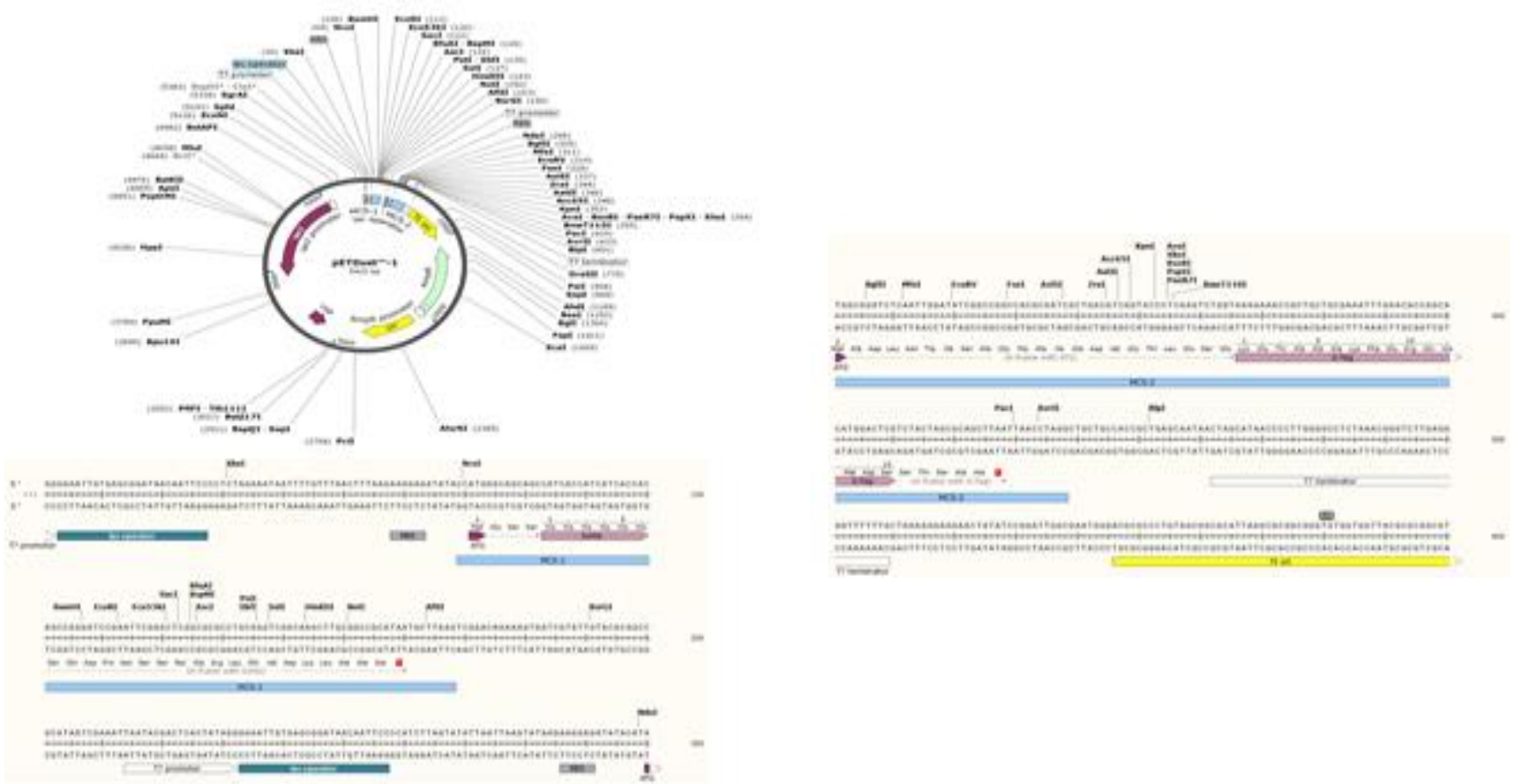


Figure 8: pETDuet with features of interest shown. The Duet series of vectors are designed with co-expression in E. coli in mind, which may increase protein solubility and yields (EMD Biosciences, 2012).The pETDuet-1 vector carries the ColE1 replicon, T7 promoter and two cloning sites with multiple restriction sites, each under the control of a T7lac promoter, and an antibiotic resistance marker (ampicillin). The promoters are flanked by ribosome binding sites and a T7 terminator. The vector also provides options for protein purification in the form of His•Tag® and S•Tag™ sequences, or to produce unfused proteins (EMD Biosciences, 2012)..

8.2.4 pETDuet with LipA (MCS1) and LipB (MCS2)

pETDuet with LipA at MCS1 was double-digested with FastDigest Nde1 and Xho1 according to the manufacturer's protocol, and was viewed alongside pETDuet without inserts for comparison following electrophoresis at 80 V on a 1% agarose gel made up with 1X TAE buffer and containing 1 ug/ml ethidium bromide. The cut vector band was then excised from the gel, cleaned and checked for linearity. The vector linearised at MCS 2 was then ligated with the previously prepared LipB amplicon that was digested with the appropriate enzymes and left overnight at 4 °C. This ligation mixture was transformed into DH5α via heat-shock and plated as per the protocol. Four colonies were selected from this plate, designated R1 – to R4. Each of these colonies were subjected to a screening procedure with LipB (gene-) and MCS2 (vector-specific) primers. An overnight culture of the colony with both inserts was then prepared at 37 °C in standard LB supplemented with ampicillin. The culture was subsequently isolated on a small scale using a Qaigen mini-prep kit (QAIprep Spin Miniprep). An aliquot of the purified plasmid was double-digested with both sets of enzymes respectively to check for the presence of the inserts. Once the inserts were confirmed, the isolated plasmid with insets at both cloning sites was sent for sequencing by Inqaba Biotechnical Industries (Pty) Ltd. LipA (lipase) was cloned into MCS1, in frame with the HIS-tag to aid in downstream purification. LipB (foldase/chaperone) was cloned into MCS 2, in-frame with the S-tag.

8.2.5 Sequencing of pETDuet with inserts by Inqaba Biotechnical Industries (Pty) Ltd

Sequencing of MCS1 and MCS2 was required. Inqaba performed sequencing by the Sanger method, with the Basic Service option selected. Plasmid DNA was supplied (LA3 and LALB6 at 10 µg/µl), and primers were provided to Inqaba at the 10 µM each (pET Upstream primer: 5'-ATGCGTCCGGCGTAGA-3', pETDuet Down1 primer: 5'-GATTATGCGGCCGTGTACAA-3', T7 Terminator primer: 5'-GCTAGTTATTGCTCAGCGG-3', pETDuet UP2 primer: 5'-TTGTACACGGCCGCATAATC-3'). The T_m of the primers was 58.2 °C and 59.3 °C respectively. Expected amplicon size was ~1 kbp. Sequencing reactions, purification and injection were performed on an ABI 3500XL Genetic Analyzer.

8.3 Protein Expression

8.3.1 Transforming into *E. coli* BL21 (DE3)

Once sequencing confirmed the presence of the inserts, pETDuet without inserts, pETDuet with LipA at MCS1; pETDuet with LipB at MCS2, and pETDuet with both LipA and LipB in their respective

cloning sites, were each transformed into competent BL21 cells (F^- *ompT gal dcm lon hsdS*$_B$($r_B^-m_B^-$) λ(DE3 [*lacI lacUV5-T7 gene 1 ind1 sam7 nin5*]) [*malB*$^+$]$_{K\text{-}12}$(λ^S)), prepared in PIPES buffer (100 mmol/l $CaCl_2$, 10 mmol/l PIPES-HCl, 15% glycerol v/v pH 7; cell pellet suspended in the buffer following OD_{600} growth of the culture to between 0.3 and 0.5) via the standard-heat shock technique. This was to be able to determine expression of both genes singly, together and to establish a base-line with regard to expression from the empty vector. A volume of 50 µl of the transformed mixture was plated on LB-ampicillin plates overnight at 37 °C. A colony from each plate (pETDuet with LipA, with LipA and LipB, and with LipB only (two samples)) was further prepared overnight in LB media containing ampicillin (37 °C, shaking at 250 rpm).

8.3.2 Induction pETDuet with LipA, with LipA and LipB, and with LipB only

A volume of 3 ml of the culture was then made up to 100 ml with fresh LB and grown for 1 hour with shaking at 250 rpm. The starting culture at OD_{600} was noted. Thereafter cultures were split into two each containing 50 ml to represent the induced and un-induced populations. Each of the 50 ml cultures was then further split into 10 ml cultures, each marked for addition with a different concentration of IPTG (prepared as a 1M working stock and diluted to relevant concentration as required). Induction was performed with IPTG from 0.25 mM to 1 mM, in 0.25 mM increments. Aliquots of 1 ml were taken periodically (every 1 hour) from the 10 ml samples over the 3 hr. induction course. Induction trials were performed at 37 °C and at 30 °C respectively in 250 ml flasks shaken at 250 rpm. No glucose was added to prevent leaky expression as this was not considered at the time of writing.

Lysis of induced/uninduced samples

The 1 ml aliquots were subsequently centrifuged at 3000*g* for 10 min and the supernatant decanted. Lysis buffer (0.02% sodium azide and 5x sample buffer with 10 mM dithiothreitol or beta-mercaptoethanol (used interchangeably)) was added to the samples. Samples were then placed in a heat block (95 °C, 5 mins) to denature, and allowed to cool. When sufficiently cooled, 5 µl of sample was combined with loading dye and added to the wells of SDS-PAGE gels.

SDS-PAGE Gels

Resolution of the genes LipA and LipB, cloned in-frame under induction with varying concentrations of IPTG at 30 and 37 °C respectively was performed on 12% Laemlli SDS-PAGE gels (running buffer was 10x Tris/Glycine/SDS, pH 8.3 (BioRad), prepared to 1x for use). Samples were loaded as the whole-cell extract, the soluble extract, and the insoluble extracts unless otherwise suggested, from left to right, from un-induced sample, to 0.25 mM IPTG, to 1 mM, in 0.25 mM increments. The

extracts in turn were separated from each other by centrifugation at 12*g* for 2 mins, followed by suspension in 1ml 50 mM Tris-HCL buffer, pH 8. The fractionation procedure may have left soluble proteins in the insoluble fraction, but for rapid visualisation, this was the method of choice for this investigation. Fairbanks staining was used for SDS-PAGE gels and was prepared and used as per the protocol (http://labs.mcdb.lsa.umich.edu/labs/maddock/protocols/protein/fairbanks_staining_of_gels.html), with the exception that Coomasie G-250 was substituted for Coomasie R-250 due to unavailability.

LipA purification

Since LipA was expressed with a His-Tag, His-tag purification was used to obtain samples of LipA. The Zymo® His-Spin protein mini-prep kit was used following the manufacturer's protocol.

Protein quantification

Quantification of proteins was performed via fluorescence, utilising the Qubit 2.0 following the standard protocol.

8.3.3 Preliminary tests for enzyme activity

Enzyme hydrolytic activity was determined with emulsified para-Nitrophenol Palmitate (pNPP) (Sigma Aldrich Co.) using a slightly modified version of the Pencreach & Baratti (1996) protocol. Assays were repeated a substantial number of times to grasp the techniques involved. Only the positive sets of results were documented.

The reaction course was followed by UV-Visible spectrophotometry (Ultraspec 3000, Pharmacia Biotech, Stockholm, Sweden). Assays were performed in aqueous media due to the unavailability of n-heptane. For the reaction, 995 µl of substrate solution was combined with 5 µl of enzyme suspended in a solution of His-Elution buffer (50 mM sodium phosphate buffer pH 7.7, 300 mM sodium chloride, 250 mM imidazole) at concentrations of 0.729, 0.0729, 0.00729 µg/µl LipA. This was done to establish the reaction rate which would not be too fast or too slow to be followed.

The molar extinction co-efficient was determined from a calibration curve with varying amounts of substrate solution (0, 5.6, 11.2, 16.8, 22.4, 28, 33.6, 39.2, 44.8 and 50 µM pNPP) prepared under assay conditions, yielding an absorption range of between 0 and 1. Reaction rate was calculated from the slope of the curve absorbance versus time by using the molar extinction co-efficient. One enzyme unit was the amount of protein liberating one µmole of p-nitrophenol per minute in the above conditions.

9 RESULTS

9.1 Lipase and chaperone

The bacterium is expected to process sunflower oil into biodiesel, and use the formed by-product glycerol as a carbon source in the production of ethanol to produce a biodiesel. Excess ethanol could be combined with the biodiesel resulting in a biodiesel-ethanol product. To this end, a suitable lipase was recruited suited to the conditions the strain would be subjected to, including pH considerations, ethanol tolerance and molar processivity.

Figures below describe a summary of the results from cloning LipA and LipB, from pUC57, into the cloning sites MCS1 and MCS2 in pETDuet-1 respectively (fig. 11 and fig. 12).

9.1.1 Chaperone (LipA)

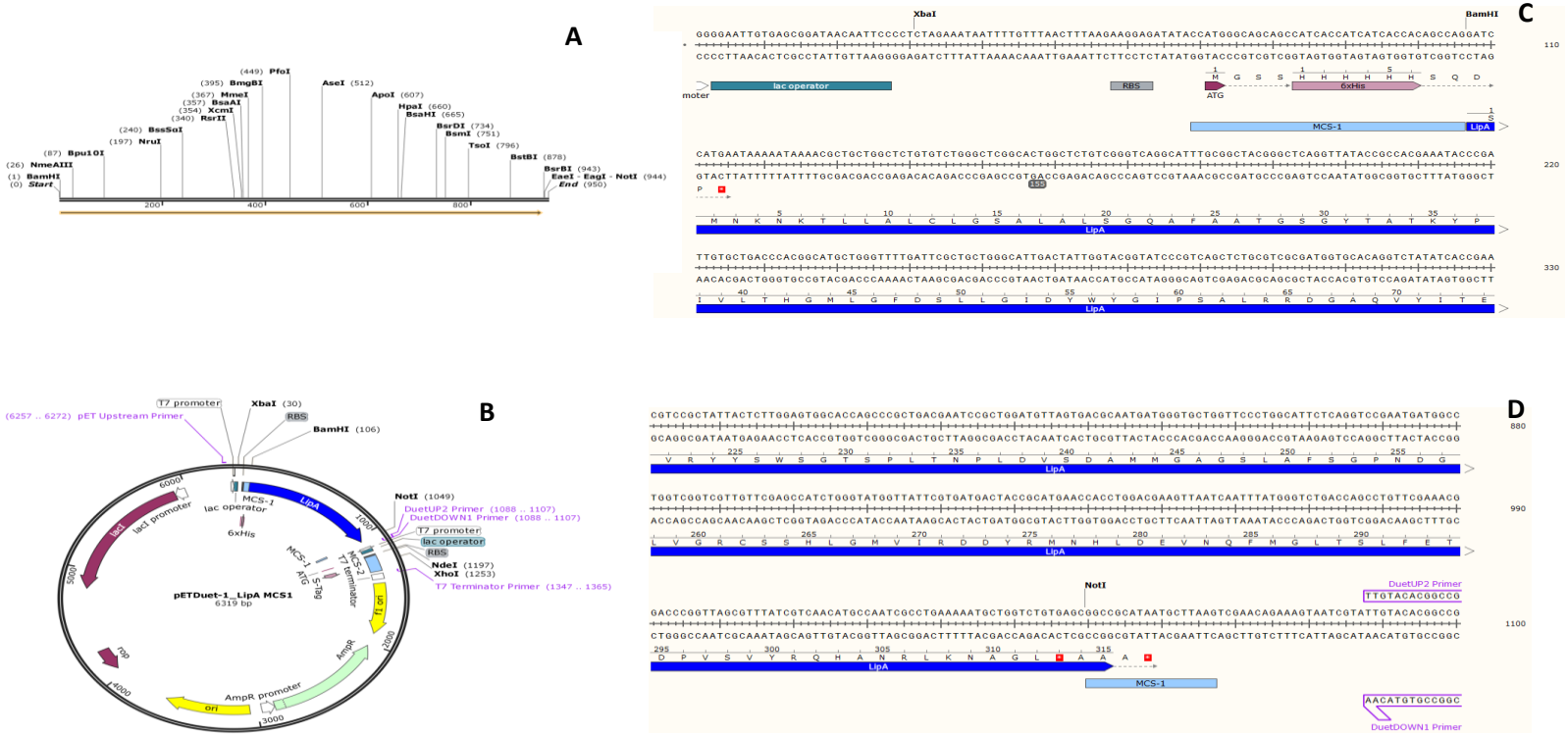


Figure 9: (A) Gene map, (B) construct map, (C) 5' construct features, (D) 3' construct features. gene map of LipA (A) as received from GenScript® (in pUC57), with a number of restriction sites shown including BamHI (5') and NotI (3') sites included as ordered. The line below the map and highlighted in orange is an indication of the orientation of the ORF, which is 950bp in size. (B) shows a construct map of the pETDuet-LipA, indicating where the ORF was cloned into the vector. Restriction enzyme sites of interest are indicated (BamHI, NotI). LipA was cloned in-frame with the HIS-tag to facilitate downstream purification. Vector features are also indicated (refer to section 5.2.3). (C) shows the 5' end of the pETDuet-LipA construct, highlighting that LipA was cloned in-frame at pETDuet MCS1 (shown in blue). Adjacent sites of importance shown (selected restriction enzyme sites, RBS – ribosome binding site, start codon of ORF (ATG), 6x HIS tag, 1 letter codes of amino acid sequence). (D) shows the 3' end of the gene. Sequencing primer binding sites are shown (Duet UP2, DuetDown1). Images produced with SnapGene® Version 3.3.3.

9.1.2 Lipase (LipB) (Figure 12)

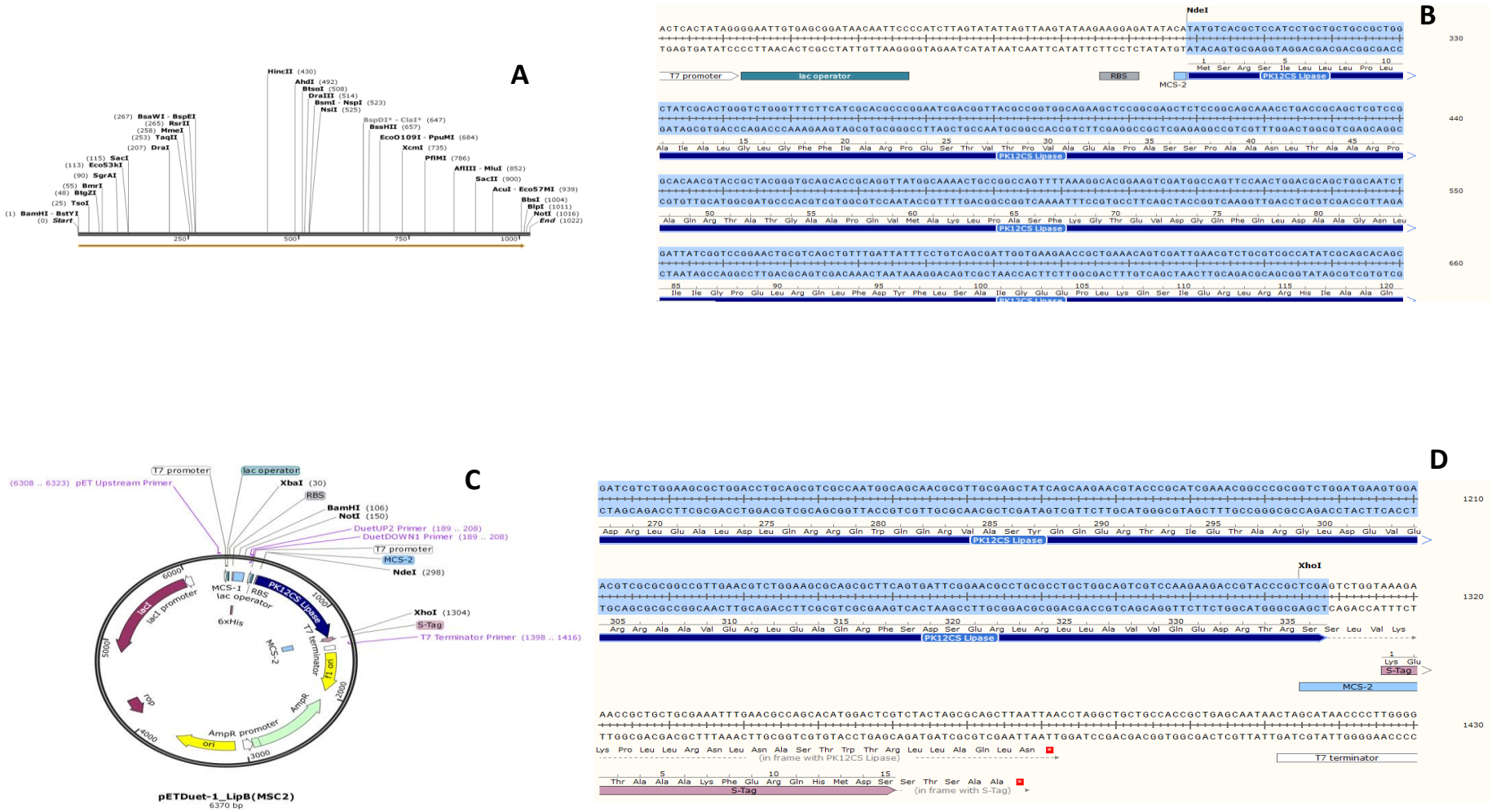


Figure 10: (A) Gene map, (B) construct map, (C) 5' construct features, (D) 3' construct features. Gene map of LipB, (A) as received from GenScript® (in pUC57), with a number of restriction sites shown including BamHI (5') and NotI (3') sites included as ordered. The line below the map and highlighted in orange is an indication of the orientation of the ORF, which is 1022 bp in size. (B) shows a construct map of the pETDuet-LipB, indicating where the ORF was cloned into the vector. Restriction enzyme sites of interest are indicated (NdeI, XhoI). LipB was cloned in-frame with the S-tag to facilitate downstream purification. Vector features are also indicated (selected restriction enzyme sites, RBS – ribosome binding site, start codon of ORF (ATG), S tag, 1 letter codes of amino acid sequence) (ref er to section 5.2.3). (C) shows the 3' end of the pETDuet-LipB construct, highlighting that LipB is fused with the S-tag as the only stop codon is following the tag pETDuet MCS2 (LipB sequence highlighted in blue). (D) shows the 3' end of the gene. Sequencing primer binding sites are shown (T7 terminator)

9.1.3 Cloning

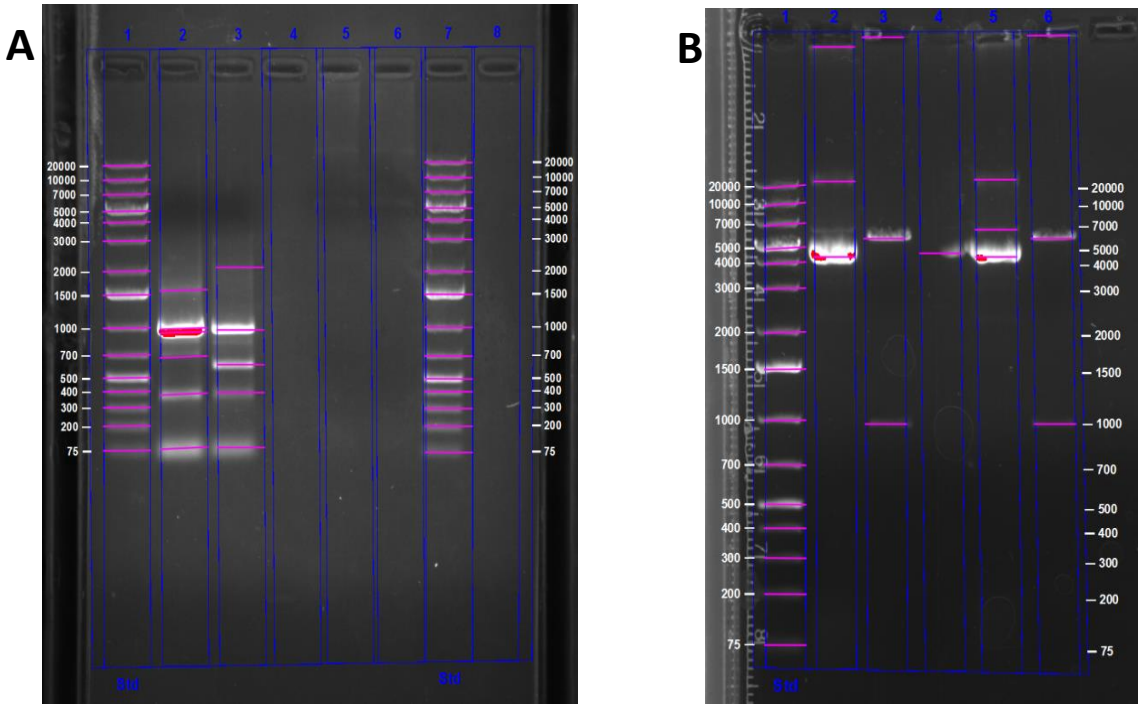


Figure 11: Image Left (A): LipA touch-down PCR from GenScript pUC57 performed in duplicate. Lane 1 – GeneRuler 1kb plus marker, Lane 2 – touch-down sample 1, Lane 3 – touch-down sample 2**. Image Right (B):** BamH1 and Not1 digest of LipA amplicon from A which was ligated to pETDuet at a 1:2 and 1:3 vector:insert ratio. Lane 1 – GeneRuler 1Kb plus marker, Lane 2 – uncut pETDuet, Lane 3 -BamH1 & Not1 digest of pETDuet and LipA 1:2 ratio, Lane 5 - uncut pETDuet, Lane 6 – BamH1 & Not1 digest of pETDuet and LipA at 1:3 ratio ligation, Lane 7 – GeneRuler 1 Kb plus marker. Band sizes (in bp) have been displayed using the GelDoc ImageLab software.

From the Touchdown PCR, LipA was obtained as an amplicon of just under 1kbp (fig. 13A). The amplicon was excised and cleaned, and set up for a ligation with pETDuet, for which the vector was digested with the same restriction enzymes (BamHI and NotI). Following the ligation, LipA was then digested out of the vector to confirm the presence of LipA in pETDuet (fig. 13B), and to verify that the directional cloning was successful.

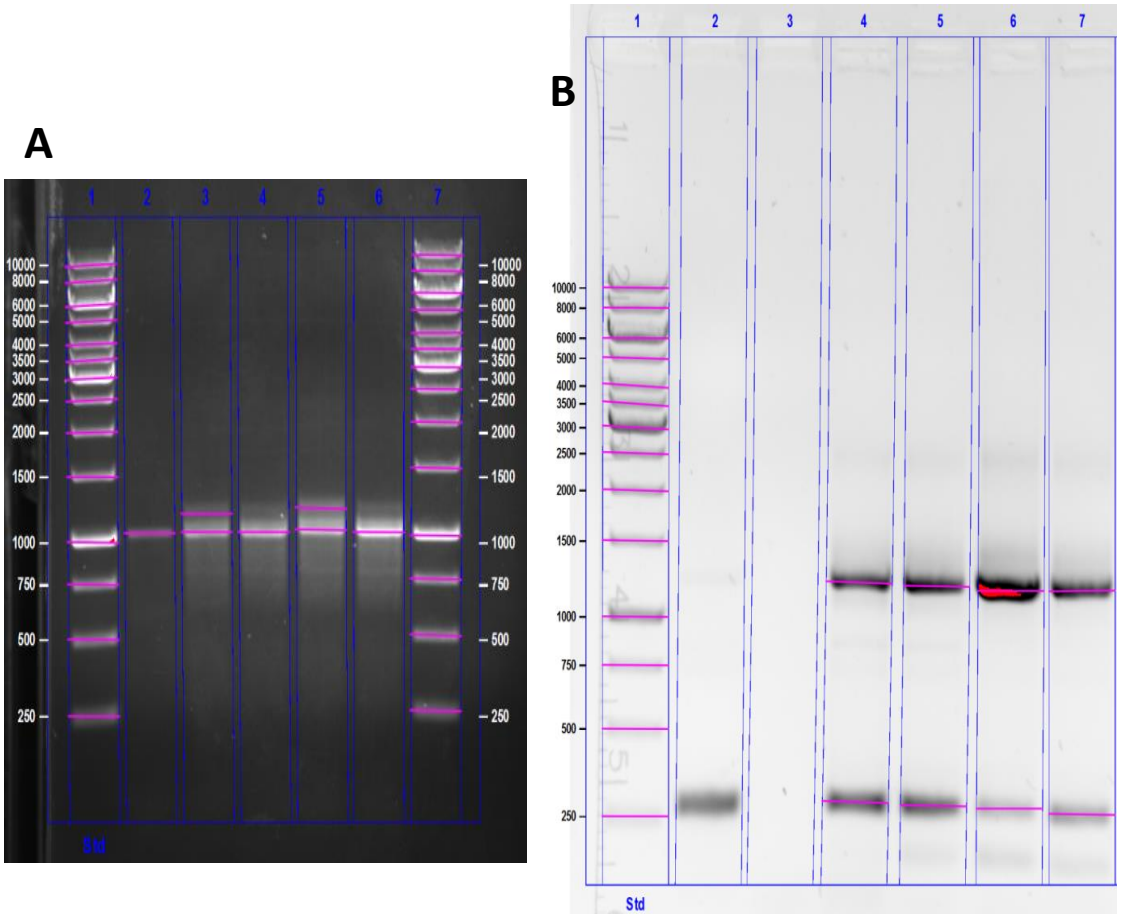


Figure 12: Ligation screen of prior gel purified LipB amplicon in pETDuet at MCS2 with **(A)** gene- and **(B)** vector-specific primers. **Left image (A):** Lane 1 – Marker, Lane 2 - negative control, Lane 3 - R1, Lane 4 - R2, Lane 5 - R3, Lane 6 - R4, Lane 7 – Marker.

Image right (B): Lane 1 – Marker, Lane 2 – background control, Lane 3 - negative control, Lane 4 -R1, Lane 5 - R2, Lane 6 -R3, Lane 7 - R4.

For LipB, a PCR was performed from which the gel-excised and cleaned amplicon was set up for a ligation with pETDuet at MCS2, following a double-digest with XhoI and NdeI. Following the incubation period, the ligation reaction was screened with LipB-gene specific primers to check for the insert (fig. 14A). Since the ligation may have left some of the amplicon un-ligated with the vector, vector specific primers were also used. This generated amplicons of just over 1.5kbp, alluding to the success of the ligation as LipB is 1022bp, with the region between primer sites on the vector being ~520bp (fig. 14B).

pETDuet with LipA was then digested at MCS2 with the relevant enzymes, and LipB was ligated into the site. The construct was then transformed into the DH5α host, for which two colonies were then screened by colony PCR (fig. 15) using gene- and vector specific primers. Gene-specific primers showed no result, whilst vector specific generated a bright band for both colonies (fig. 16). It is likely that the discrepancy was due to the same conditions being used for both sets of primers (both vector- and gene-specific primers used in same machine set up with parameters favouring only one set), for which the results support that the reaction parameters supported the vector specific primers.

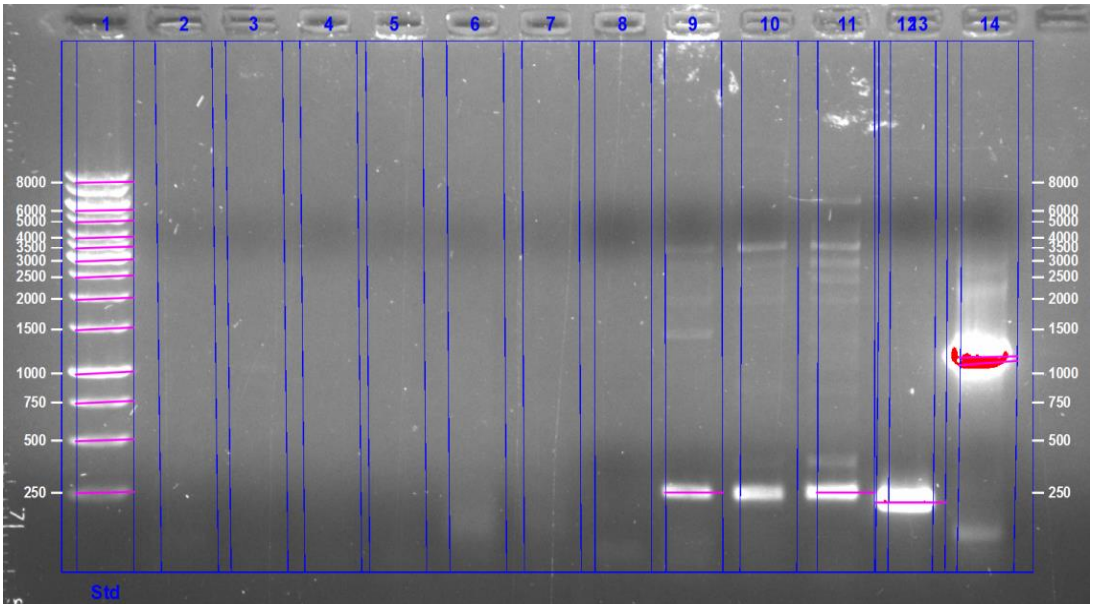


Figure 13:pETDuet with LipA and LipB Colony PCR (Colony 1 screen, with LipB specific primers)). Lane 1 – Marker, Lane 2 - negative control, Lane 3 – Background control, Lane 4 - R1, Lane 5 - R2, Lane 6 - R3, Lane 7 - R4. For pETDuet MCS2 specific primers: Lane 9 - negative control, Lane 10 – Background Control, Lane 11 - R1, Lane 12 - R2, Lane 13 - R3, Lane 14 - R4.

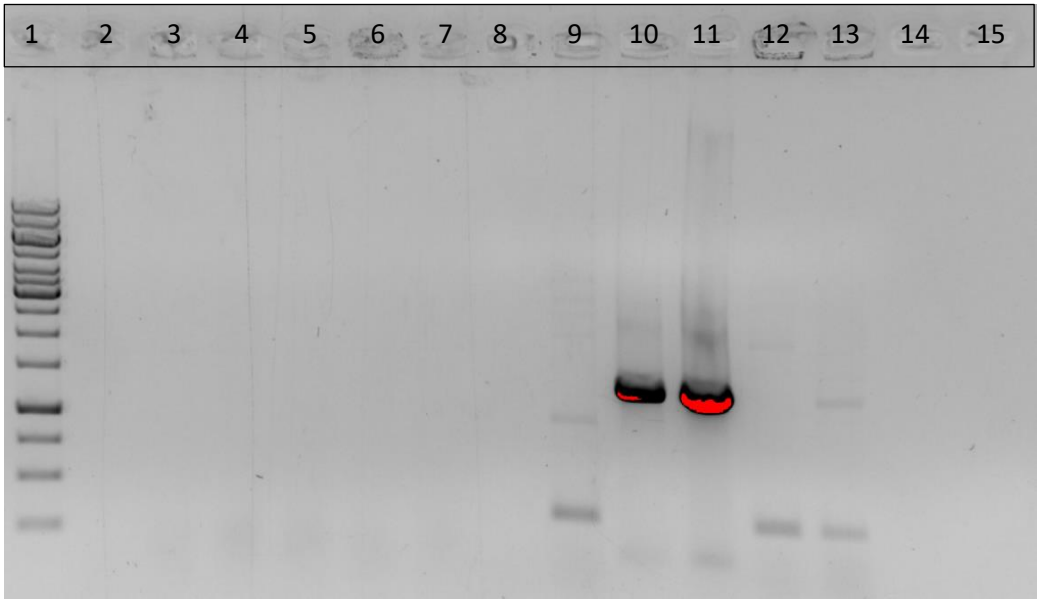


Figure 14: pETDuet with LipA and LipB Colony PCR (Screen of colony 2): Lane 1- Marker, Lane 2 – negative Control, Lane 3 – Blank, Lane 4 - R1, Lane 5 - R2, Lane 6 - R3, Lane 7 -R4. Colony PCR with LipB specific primers (lanes 8 – 15): Lane 8 – negative Control, Lane 9 – Blank, Lane 10 -R1, Lane 11 - R2, Lane 13 - R3, Lane 14 - R4 (pETDuet MCS2 specific primers)

Colonies named R1 and R2 were selected for further analysis of their cloning regions (fig. 16). These were isolated on a small scale, and digested with the enzymes as described in fig. 15. When R1 was

subjected to digest with only one of the enzymes (Lane 3 – Lane 6), only a single band is visible, whereas when double-digested with the enzymes the amplicons are released as expected (Lane 7 and Lane 8). Lane 7 also shows that LipA is smaller than LipB. R1 was then sent for sequencing.

9.1.4 pETDuet with LipA at MCS1 & pETDuet with LipB at MCS2 – cloning verification through sequence analysis

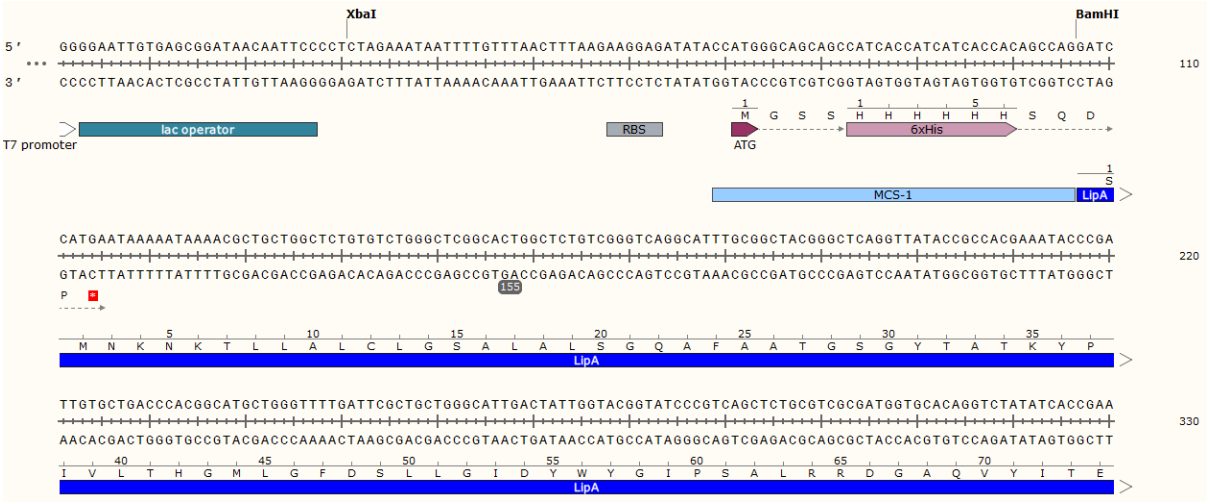


Figure 15: LipA cloned in-frame at pETDuet MCS1 with adjacent sites of importance shown (selected restriction enzyme sites, RBS – ribosome binding site, start codon of ORF (ATG), 6x HIS tag, 1 letter codes of amino acid sequence). Trace data not shown (image produced with SnapGene® Version 3.3.3.

LipA is shown in blue (fig. 17). Sites for the Lac operator and ribosome binding sites, the His tag region (shaded blue adjacent to translation start indicator) are shown. The BamH1 site is also shown for reference. The gene was cloned in-frame without incidence.

LipB was also cloned in-frame. Sequencing revealed however, that at the 3’ end of the gene, the stop codon was omitted, resulting in an alteration to the sequence and further resulting in a fusion region with the S-tag (fig. 18).



Figure 16: 3’ end of LipB in pETDuet at MCS2. Gene fusion region with S-tag shown (image produced with SnapGene® Version 3.3.3).

Lifs are typically composed of 3 main sections: a large hydrophillic C-terminal domain, a proline-rich segment, and a hydrophobic section localised at the N-terminus. From localization studies, the hydrophillic section anchors the Lif to the inner membrane of the host bacterium, leaving the rest of the protein to localise in the periplasm (Jaeger *et. al.*, 1999; Nagradova, 2008). For this study, it was thought that the C-terminus of the protein was modified as a result of a GC-rich primer during the PCR process, resulting in a fusion with the S-tag. However, it was subsequently noted that the primer used in the alteration of the 3’ restriction site omitted the gene’s stop codon. Translation of the ORF and subsequent secondary structure prediction (via CLC Main® Workbench 7) indicated that the region and the first 11 amino acids of the s-tag respectively formed two alpha-helices (fig. 19). Since the gene was altered, it was of interest to investigate whether the changes affected the protein's folding in some way, and thus it's catalytic activity, probably resulting in an expressed but unfolded - and thus non-functional, LipA.

While there is evidence to show that N-terminally truncated or modified Lifs retain their catalytic activity (Nagradova 2008), there is not yet enough evidence to conclude what role that C-terminal modifications have on the chaperone. Ihara *et. al.* (1992) reported that LimL, a lipase foldase of *Pseudomonas* strain 109, could activate the lipase in *E. coli* and that the N-terminal sequence of the lipase was not necessary for the activation of the lipase.

In another study, Shibata *et. al.* (1998a) cloned LipB (a Lif) and LipA from *P. aeruginosa* TE3285, and prepared two forms of truncated Lif mutant proteins: LipB 21-amino acids short on the N-terminal end, and another short of 61 amino acids on the N-terminal end. Experiments showed that

both truncated forms of LipB were able to reactivate stoichiometric amounts of denatured LipA, producing an enzyme with the same level of activity as native LipA. Quyen *et. al.*, (1999), with a Lif from *P. cepacia* ATCC 21808 short 70 and 34 amino acids on the N-terminal end confirmed, along with the prior report, that the truncated forms of the Lifs contained all the functional residues required for reactivation of LipA.

The modified region in this study was changed from polar and charged residues (QEDRTR, before the s-tag) to LESG[(KET] - part of S-tag), to a similar distribution with two hydrophic residues introduced. Although a number of residues are conserved in Lifs (Jaeger *et. al.*, 1994), the last 6 residues are not conserved. Moreover, only two residues have been shown to be highly conserved in Lifs (Tyr-99 and Arg-115) and involved in the interaction with lipase (Jaeger *et. al.*, 1999; Shibata *et. al.*, 1998b). Prediction of Lif structure has been shown to be composed of approximately 70% alpha helices, and 30% random coil elements, along with the indication that all Lifs have similar secondary structure and that this structural arrangement is conserved (Nagradova, 2008) The region however, maintains its secondary structure (fig. 19). Also activity of LipA was unaffected as LipB was able to show catalytic activity against pNPP (fig. 28, 29 and 30 respectively).

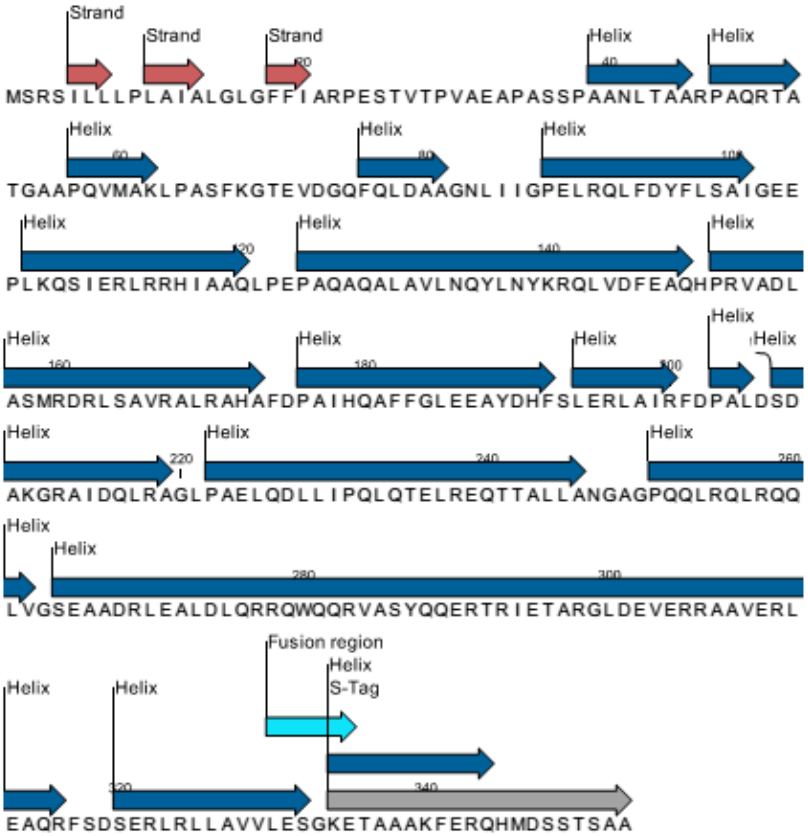


Figure 17: Translation of LipB and secondary structure prediction. Amino acid sequence of *P. mendocina* PK12CS lipase shown with 1-letter code (image produced with CLC Main Workbench® 7).

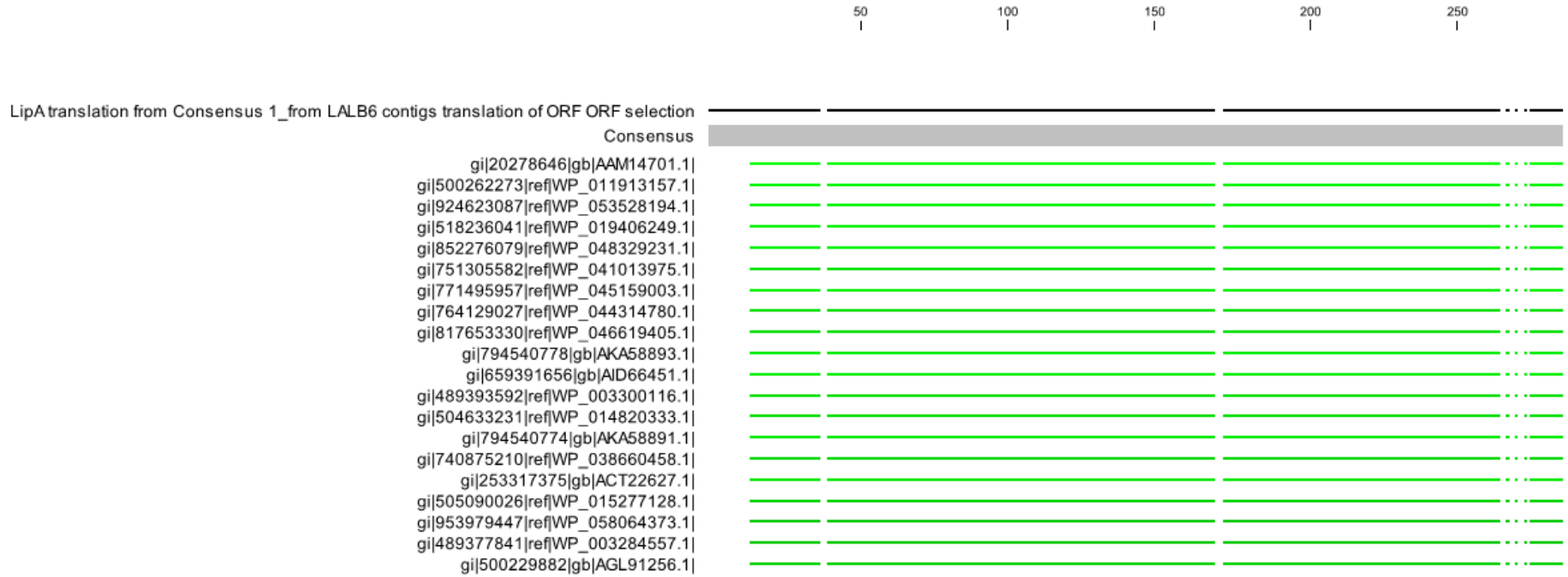


Figure 18: BLASTP of LipA showing high sequence similarity with *P. mendocina*. Consensus sequence and conservation regions shown. Green indicates regions of high sequence similarity (image produced with CLC Main Workbench® 7).

Figures 20 and 21 are BLASTP of LipA and LipB respectively, indicating the high sequence conservation of both proteins despite the introduction of errors as a result of the cloning process.

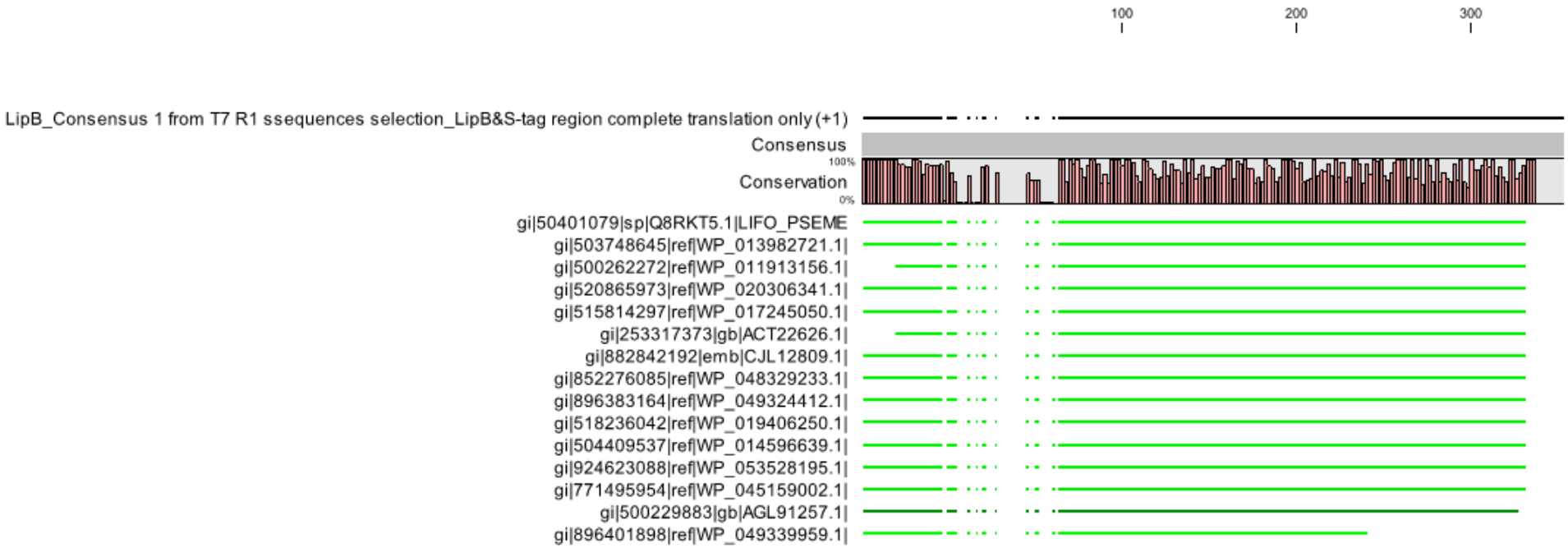


Figure 19: BLASTP of LipB showing sequence similarity with *P. mendocina*. Consensus sequence and conservation regions shown. Green indicates regions of high sequence similarity (image produced with CLC Main Workbench 7).

9.1.5 Induction trials

Observation of all the gels (fig. 22 - 27) suggests that 37 °C was the better, in terms of apparent yield, of the two temperatures for the induction process. This is corroborated by the band intensity, which loosely corresponds to the amount of expressed protein. This trend was also observed for IPTG concentration, for which an increase in band intensity was observed at higher temperature and at increasing IPTG concentrations, than at higher concentrations at lower temperature. The bands also resolved better at 37 °C than at 30 °C, although that could have been a result of the sample preparation process.

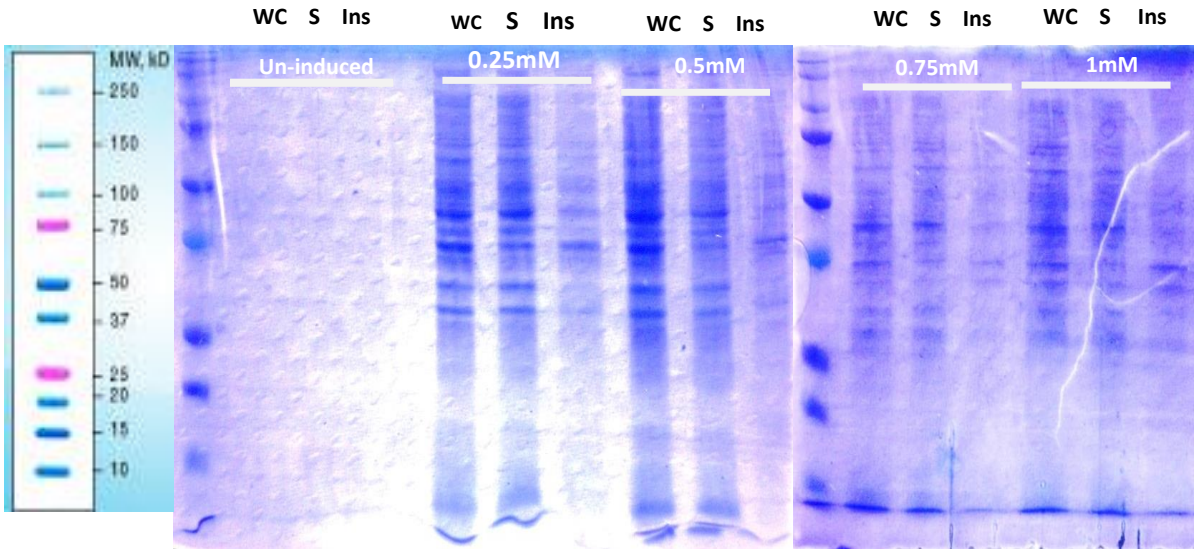


Figure 20: 30 °C induction. Sample A (0 – 1 mM). Lane 1: Marker, Lane 2 - 4: 0, Lane 5 -7: 0.25, Lane 8 - 9: 0.5, Lane 10 - Marker, Lane 11 - 13: 0.75, Lane 14 - 16: 1. Marker = BioRad Kaleidescope. WC – Whole Cell fraction, S – Soluble fraction, Ins – insoluble fraction.

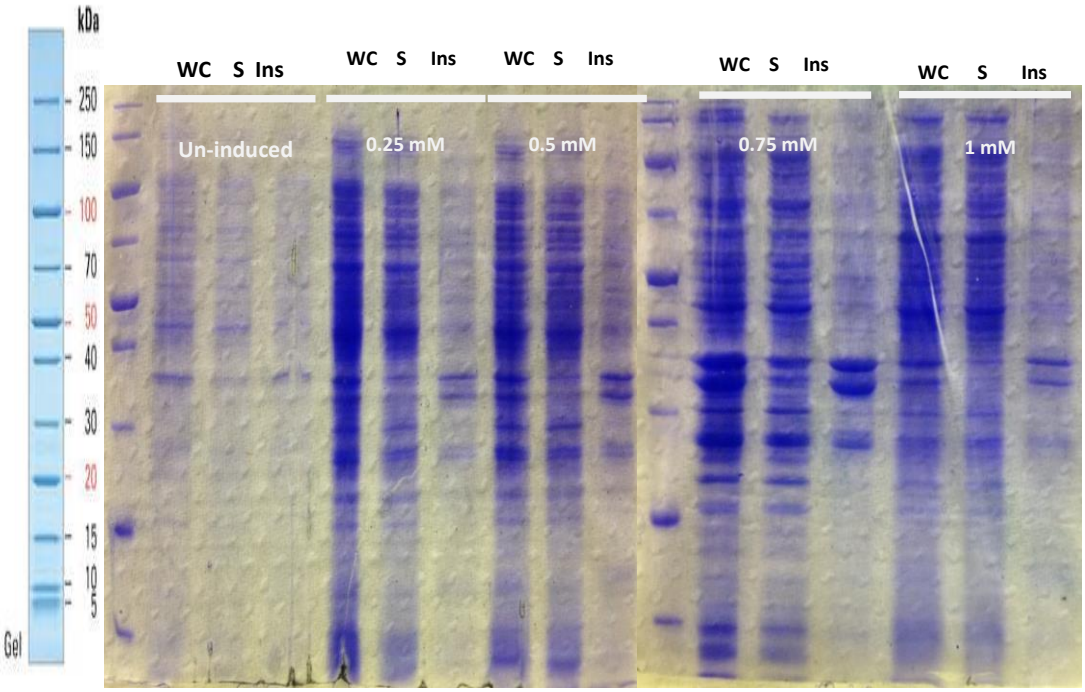


Figure 21: 37 °C induction sample A. (Lanes from left to right): Lane 1- Marker, Lane 2 - 4: 0, Lane 5 - 7: 0.25, Lane 8 - 10: 0.5, Lane 11 - Marker, Lane 12 - 14: 0.75, Lane 15 - 17: 1. Marker = PageRuler BR unstained. WC – Whole Cell fraction, S – Soluble fraction, Ins – insoluble fraction.

Most *Pseudomonas* lipases are reported to have a mass of around 29 – 33 kDa (Gaur *et. al.*, 2008). The bands corresponding to LipA (~34kDa with the His-tag), and LipB (~39 kDa with the S-tag) were difficult to discern from the rest of the cellular milieu proteins however, which led to referral to the un-induced samples to assist in the identification of the putative proteins. At 30 °C, LipA was putatively expressed as evidenced by cell samples at 37 °C (this was more visible in fig. 23 than fig. 22). No un-induced sample was visible possibly due too little sample being loaded (fig. 22). In fig. 23, for the un-induced sample, there is a single band between 30 and 40 kDa, which is also visible in fig. 22 near 37 kDa. This band however becomes a doublet in the induced samples at 37 °C, suggesting that this or the lower band could be LipA (fig. 23): the lower band of the doublet is present from un-induced, suggesting leaky expression, or only the lower band can be considered, which only appears in the induced samples. Both however also become more pronounced with induction until 0.75mM IPTG. Notably, the bands appear most dense, and localise in, the insoluble fraction for all samples. This could have been due to the sample preparation process as suggested previously or from the production of inclusion bodies. In the 30 °C samples, this band is less visible.

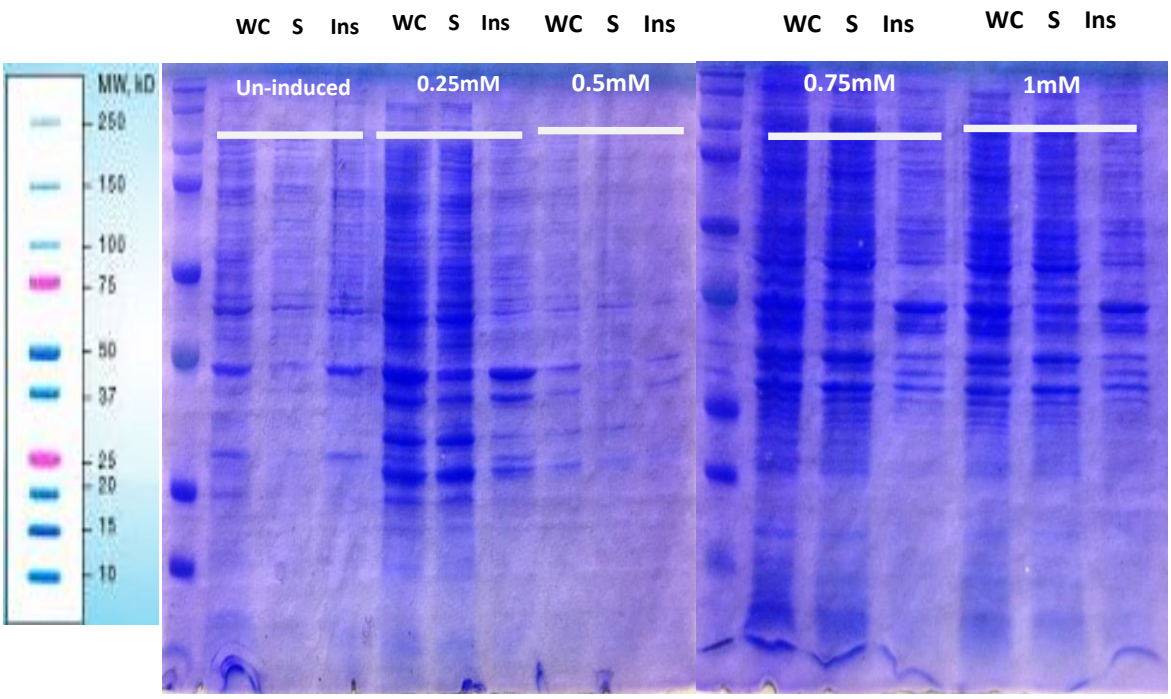


Figure 22: 30 °C induction. Sample AB (0 – 1 mM). Lane 1 - Marker, Lane 2 - 4: 0, Lane 5-7:0.25, Lane 8 - 10:0.5, Lane 11 - Marker, Lane 12 - 14:0.75, Lane 15 - 17: 1. Marker=BioRad Kaleidescope. WC – Whole Cell fraction, S – Soluble fraction, Ins – insoluble fraction.

In sample AB (fig. 24 and 25), these bands are more visible. The doublet of bands at, and below, the band at 37 kDa (fig 24 and 25) are visible from induced samples, and between 40 and 50 kDa (fig. 25), reflecting putative LipA (~34kDa), and LipB (~39 kDa).

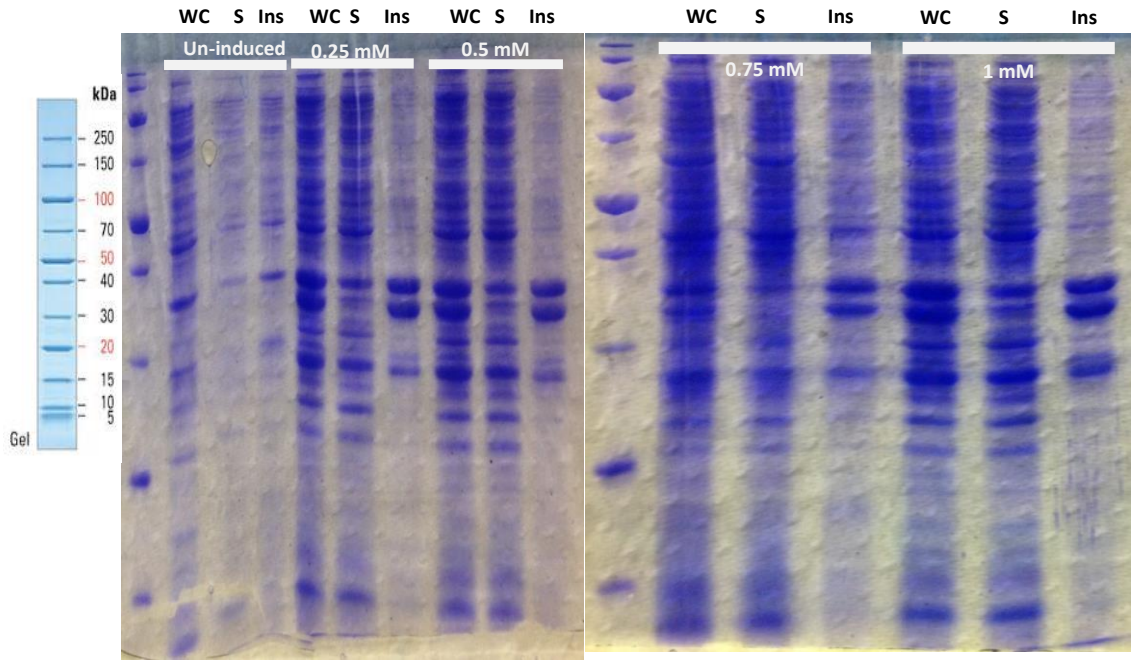


Figure 23: 37 °C induction trial. Sample AB (0 – 1mM). (From left to right): Lane 1 - Marker, Lane 2 - 4: 0, Lane 5 - 7: 0.25, Lane 8 - 10: 0.5, Lane 11 - Marker, Lane 12 - 14: 0.75, Lane 15 - 17:1. Marker = PageRuler BR Unstained. WC – Whole Cell fraction, S – Soluble fraction, Ins – insoluble fraction.

LipB was more difficult to discern in fig. 26 and 27. A comparison of induced vs. un-induced samples at the putative location of the protein (~39 kDa), suggested that the protein was among the poorly resolved set at just below 50 kDa from 0.25 - 1mM at 37 °C (fig. 27). Fewer proteins were expressed at 30 °C (fig. 26) allowing easier identification of the protein. In fig. 26, a doublet band appears at just below and above 50 kDa in induced samples, which do not appear in the un-induced sample. This second band in the doublet also becomes more prominent with the increase in IPTG concentration (fig. 26). The band(s) also appear in all fractions (WC, S, Ins) but more so in the WC and S than the Ins. This trend is also reflected in the samples from 37 °C, although less discernable due the diffuse nature of the proteins' resolution.

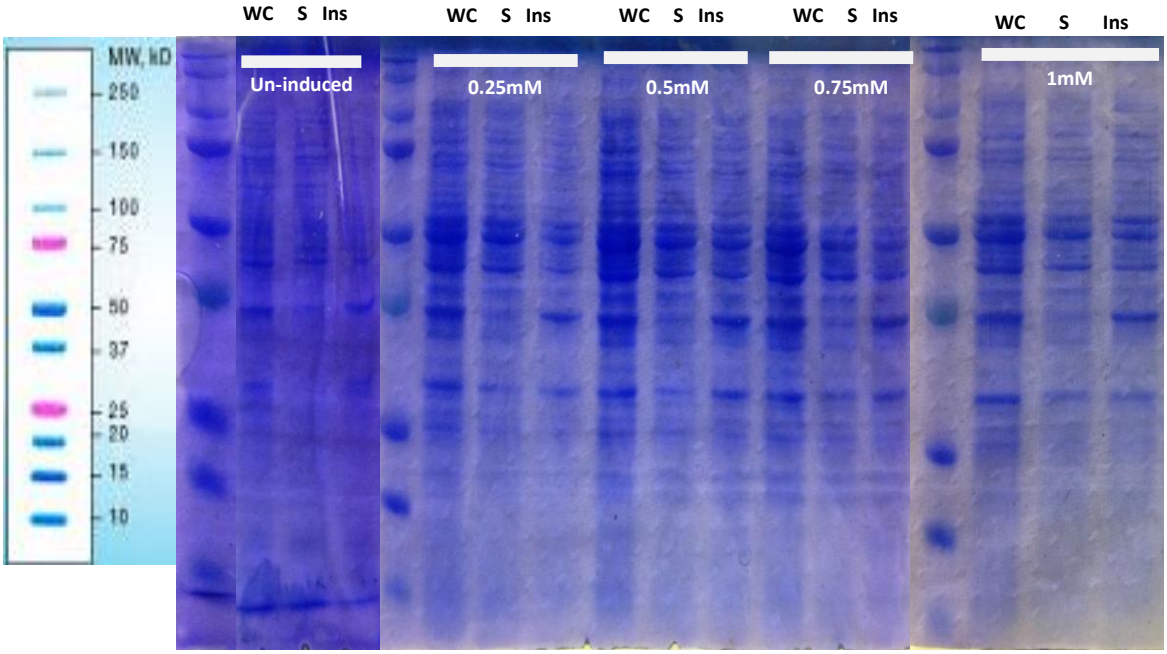


Figure 24: 30 °C induction. Sample B" (0 – 1mM). Lane 1 - Marker, Lane 2 - 4: 0, Lane 5 - Marker, Lane 6 - 8: 0.25, Lane 9 - 11: 0.5, Lane 12 - 14: 0.75, Lane 15 - Marker, Lane 16 - 18: 1. Marker = BioRad Kaleidescope. WC – Whole Cell fraction, S – Soluble fraction, Ins – insoluble fraction.

LipA (from petDuet with LipA and LipB as inserts) was purified with the Zymo His spin column kit, to a concentration of 0.296 µg/µl, from AB37 (Table 1). Approximately 33% of the whole-cell fraction from AB37 loaded into the purification column was purified LipA, compared to approximately 27% in AB30. Not all of the bound protein may have been eluted in either case; however, these results further suggest that more LipA was produced at 37 °C compared to 30 °C.

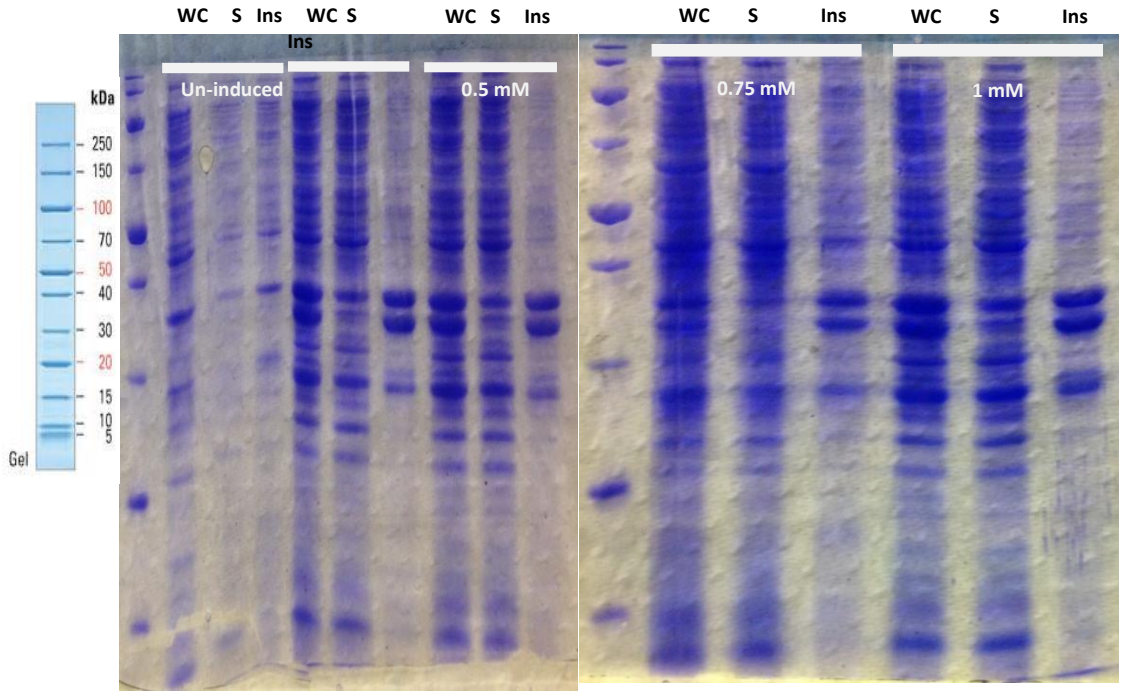


Figure 25: 37 °C induction trial. Sample AB (0 – 1mM). (From left to right): Lane 1 - Marker, Lane 2 - 4: 0, Lane 5 - 7: 0.25, Lane 8 - 10: 0.5, Lane 11 - Marker, Lane 12 - 14: 0.75, Lane 15 - 17:1. Marker = PageRuler BR Unstained. WC – Whole Cell fraction, S – Soluble fraction, Ins – insoluble fraction.

Table 1: Protein Quantification of purified protein (AB, 0.75 mM)

	AB37 (µg/µl)	AB30 (µg/µl)
Flow through	0.880	0.830
Wash 1	0.890	1.07
Wash 2	0.352	0.732
Elute	0.296	0.220

9.1.6 Preliminary tests for activity

Trials to ascertain the activity of the cloned *P. mendocina* lipase were performed, through monitoring hydrolysis of para-Nitrophenol Palmitate (pNPP, Sigma Aldrich Co.). Whilst other reports have used 50 mM pNPP as the saturating amount of substrate, it was found the substrate dissolved poorly at that concentration, even with dissolution in isopropanol. Thus a decreased concentration of pNPP was used from a 16 mM stock, and a decreased amount of enzyme as well to ascertain the catalytic amount necessary for the time-course reaction to be followed. Arbitrary amounts of enzyme were selected, as well as substrate concentrations which would be consistent with Beer's law. Data was processed using Wolfram Mathematica 10.3, and graphs were drawn using the software's automatic least squares regression method, with model fitting set to non-linear models. The molar extinction co-efficient for pNPP was 2.137×10^3 $M^{-1}.cm^{-1}$ using standard solutions of the substrate as described.

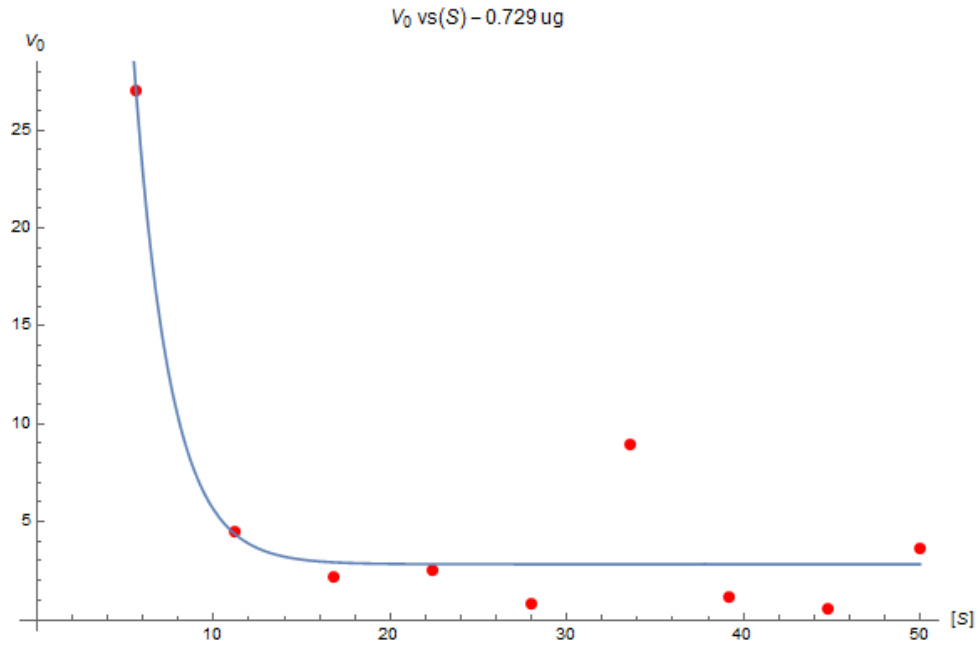


Figure 26: Effect of concentration of pNPP on the initial reaction rate of hydrolysis of pNPP catalysed by the lipase of *P. mendocina* at 0.729 µg enzyme

Fig. 28 shows decreasing rate overall for the substrate concentrations considered (see 5.3.3). Rate starts high at very low substrate concentration, decreases quickly, and is very low as substrate concentrations increase. The amount of enzyme, the rate at which the enzyme hydrolyses the substrate (related to the amount of enzyme used) and how adept the experimenter was at enzyme addition, mixing and starting procedure are considerable factors influencing the results obtained (Bisswanger 2014). For the trend observed, the adeptness at enzyme addition, mixing and starting procedure could have been an issue. The rate is high initially due to the low substrate concentration versus a relatively high enzyme amount, much more than the catalytic amount (relative to 0.0729 µg, and 0.00729 µg).

The enzyme is able to convert the substrate to product very rapidly. Thereafter, the rates are low possibly because by the time the absorbance readings were taken, the reaction was over, thus influencing the calculation of the rates observed. This is especially evident when comparing the rate data from the three enzyme amounts to each other. Whereas the other two show relatively increasing rates as expected, the first shows a decreasing trend

Initial rate vs. substrate concentration for enzyme concentrations

Overall, fig. 30 shows the expected pattern in the rate data, in that as substrate concentration increases so does the reaction rate for that amount of enzyme. The same can be said for fig. 29. The log plot (fig. 31) however shows the general trend is maintained. Plotting 0.0729 and 0.00729 µg rate data against a line of best fit, indicates that the rates under observation were still increasing however, and since no saturating substrate concentration was used, the data is incomplete for any determinations of V_{max}, K_m, K_{cat} or specific activity (A and B).

The data does show however that the catalytic amount of enzyme was close to being found, and was less than 0.00729 µg (fig. 29, 31 and 32). The data supported this observation, as in (fig. 29), where the rate appears to approach a crest at 50 uM PNPP. Also, that increasing the enzyme amount increases the rates observed for the substrate concentrations under consideration (fig. 29 vs. fig. 30). Plotting the best fit of the rate data shows this trend, with the higher enzyme amount having a steeper slope (fig. 32) than the lesser amount.

A

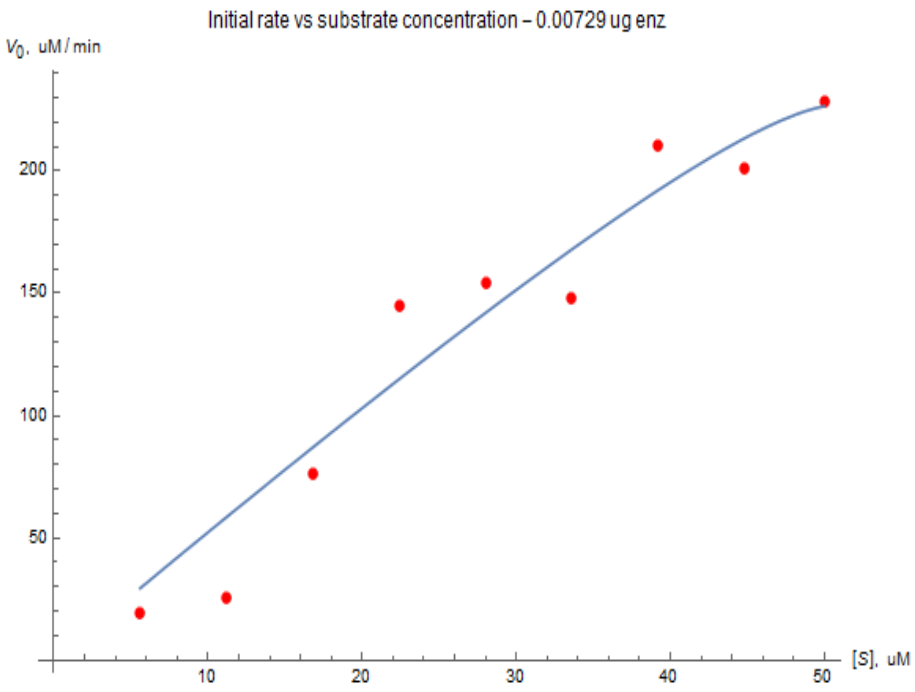


Figure 27: Initial rate vs. substrate concentration for 0.00729 µg enzyme

B

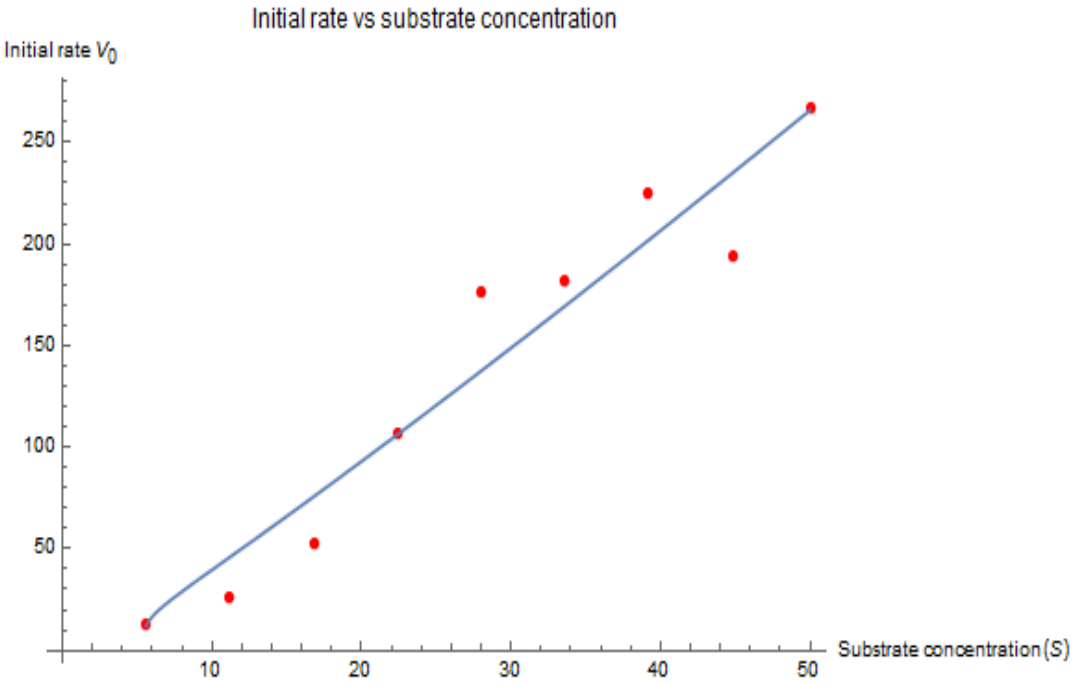


Figure 28: Initial rate vs. substrate concentration for 0.0729 µg enzyme

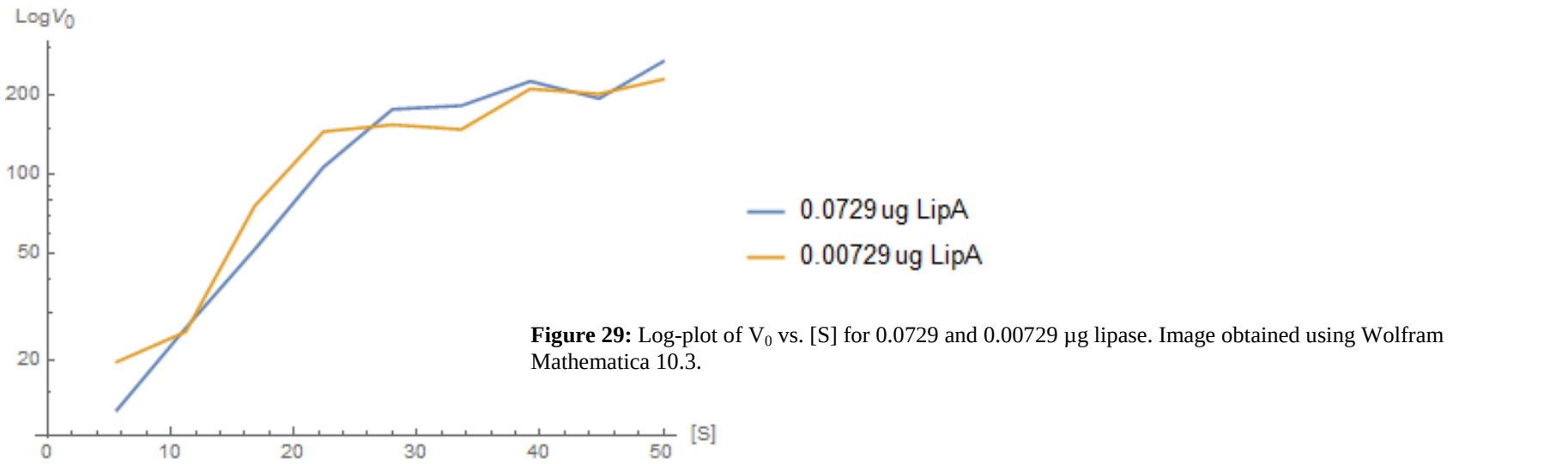


Figure 29: Log-plot of V_0 vs. [S] for 0.0729 and 0.00729 µg lipase. Image obtained using Wolfram Mathematica 10.3.

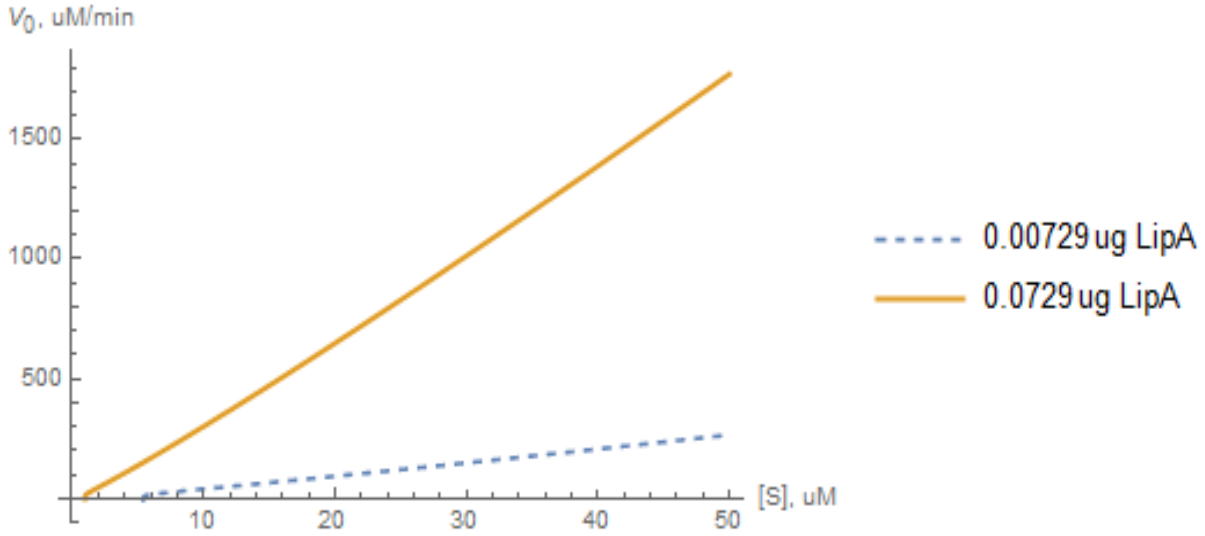


Figure 30: V_0 vs [S] for 0.0729 and 0.00729 µg enzyme respectively. Velocities were plotted on the same set of axes to emphasize the difference in reaction rates.

10 DISCUSSION

A *Pseudomonas* lipase was chosen over a lipase from *E. coli* primarily due to the former being better characterised (Jaeger & Eggert, 2002). Further, the report on *E. coli* lipases was reported on C^{14} substrate (compared to C^{16} as used in this study), and required Ca^{2+} supplementation as well as detergents, for which no activity was reported with Triton X-100 (Nantel & Proulx, 1973).

The lipase from *P. mendocina* requires a chaperone and vector suited to express both the enzyme and its cognate chaperone. pETDuet is well suited to this task as previously described (see 7.2.3). In this respect LipA and LipB genes were introduced into the vector as required, save for the cloning of LipB (see fig. 18 and fig. 19) which did not suffer adverse effects. Areas for consideration however are due to the nature of the vector and its subsequent limitation for this application.

Firstly, the introduced genes are co-expressed in the same molar ratio (i.e. 1:1). The enzyme and chaperone are only required in a 4:1 ratio in the cell (Nagradova, 2008). An inducer is required to begin high-level expression of the target; induction must be performed at the stationary phase of growth; and further, the vector requires specialised cells for expression, i.e. BL21 (DE3). The work ideally requires a subtler method of inducing the expression of the enzyme, and a system that does not rely on plasmids.

Induction

Activity trials were successful in providing an indication that the enzyme was competent in its hydrolysing capacity. The catalytic amount of enzyme was considered to be below 0.00729 µg for the substrate concentrations under consideration (fig. 29). However, the requirement for IPTG induction may not be suitable for the envisaged system (as a consequence of the vector system chosen). Auto-induction media may help alleviate this issue, as the media is designed such that induction is only performed once cells reach the stationary growth phase, the induction point does not need monitoring, cell protein concentrations reach similar levels to IPTG-based induction; higher biomass and thus higher final protein concentrations are achieved (Li *et. al.*, 2011). Also, a more direct method of establishing expression would be beneficial to identify the targets, i.e. purified fractions resolved along with cell fractions, and/or western blotting. Western blotting was not performed due to time contraints.

Enzyme activity & influences

Among the factors influencing enzyme activity, temperature and pH remain highly influential. pH affects the behaviour of an enzyme in two ways: affects the protonation of cofactors and amino acid functional groups involved in the catalytic reaction, and the tertiary structure of the enzyme (Bisswanger, 2014). The *P. mendocina* lipase used in this study was reported to have maximum activity at 37 °C and pH of 8 (Jinwal *et. al.*, 2003). Neither of these two conditions was met. Room temperature was used, which could fluctuate depending of the time of day, location proximity of the assay to exits, etc. The ideal temperature could not be used as the spectrophotometer used in the assays did not have a temperature-control module. It is well-known that the velocity of a chemical reaction increases two or three-fold per 10 °C rise in temperature, and that the behaviour is limited to the thermal stability range, where after denaturation follows even at the maximum temperature the enzyme can withstand (Bisswanger, 2014). Nonetheless, the temperature used in this investigation was not the maximum found for the enzyme and thus the reaction rates would be lower than those reported under similar conditions (assuming 25 °C room temperature).

pH shows a similar effect on enzyme activity. However, the impact of the change in pH from the imidazole from the elution buffer in the Zymo His-spin mini prep kit, which contained the solvent at 250 mM imidazole and a solution pH of 7.7, was minimal. It is reported that addition of an aliquot of the enzyme stock solution to the assay mixture does not affect the assay pH (Bisswanger, 2014). This This is confirmed in this study as one would expect to see the influence of imidazole on the largest concentration of enzyme (0.729 µg/ul) as it would contain the highest concentration of imidazole in the final assay mixture compared to the other two. Since the other two lesser concentrations were diluted in the substrate buffer prior to addition to the assay mixture, the concentration of imidazole in the assay would be negligible in comparison and thus produce even less of an effect. However it is reported that whilst imidazole is useful in the elution of poly-His-tagged proteins it may also result in protein aggregates and affect the activity of the enzyme in question (Young *et. al.*, 2012), as well as influence NMR experiments, competition studies and crystallographic trial (Terpe, 2003). Unfortunately the enzyme stock was not dialysed to remove residual imidazole following purification due to time contraints, which may have helped eliminate this factor.

Enzyme activity could not be quantified due to saturating substrate concentrations being utilised to provide an indication of the maximum rate the enzyme can maintain. The study aimed to establish that enzyme activity was indeed present, and aimed to find the catalytic amount of enzyme prior to investigating the Michaelis-Menten kinetic constants. While the scope of the enzyme activity data is undoubtedly limiting, it does give an indication that purified enzyme is indeed present, catalytically active, and that the amount of enzyme to determine these parameters was less than the least amount investigated in this work (fig. 29). Higher substrate concentrations proved futile to use as they did not

dissolve completely. A water bath was used to help with the substrate's dissolution at 50 mM; however, when the substrate was cooled to room temperature the substrate precipitated out. Furthermore, higher concentrations of the substrate solution were not suitable to use for the calibration curve to establish the molar extinction co-efficient of pNPP in the substrate solution, as absorbance above 50 µM ranged from 1.3 and above.

There was also the chance that the p-nitrophenol absorbance's recorded were some magnitude off the true value since absorbance values were determined at or around the compound's pKa (7.16, at 22 °C). The pH of the substrate solution was not determined, and neither was the enzyme solution nor the assay solution. Lipase assays in other publications which utilised a NaOH extraction step, did so to measure the absorbance of the compound in it's completely deprotonated form, which occurs at alkaline pH which is ≥ 9.12 (Bowers *et. al.*, 1980). The extraction step unfortunately complicates the assay and is laborious for a large test series. No extraction step was performed in this work owing to the buffer pH of 8 to maintain the deprotonated form of p-nitrophenol in the assay mixture.

Hydrolysis was used to establish the enzyme's activity in this work. Lipases however also catalyse another reaction, of interest in the broader scope of this project: transesterification (see 7.1.1.1). The major difference between these two reactions is that one is synthetic (transesterification) while the other is hydrolytic.

Direct comparisons of enzyme activity in aqueous and organic media are rare (Pencreac'h & Baratti, 1996). This was investigated in that study and the lipase from *P. cepacia* was found to only possess only 0.16% of the activity in organic media as compared the activity in water. Vorderwülbecke *et. al.*, (1992) compared the activities of 72 different lipases by different assays and had inconclusive results. (Pencreac'h & Baratti, 2001) compared the hydrolytic activity of 32 different lipase preparations in water and heptane and found that the activities in water and in heptane varied more in water than in heptane. Further, because the researchers found no direct correlation between the activities in both solvents, they introduced a ratio that was a measure of the activity in organic media against that in aqueous media, which they termed $R_{O/A}$ to help characterise the activity in organic media. Using this ratio, they were able to establish that diffusional limitations strongly influence enzyme activity suspended in organic solvents.

Revisions are suggested to focus on incremental developments. For the enzyme, it is essential the Michaelis-Menten constants are determined. Saturating concentrations of the substrate (i.e. > 50 µM pNPP) were not evaluated in this work and thus variables such as V_{max} and K_m are unknown. These have been reported as 430 ± 2µmol of p-nitrophenol.mg^{-1} and 11 ± 0.8 mM, respectively, for *P. cepacia* ATCC 25609 (Dalal *et. al.*, 2008); 2.24 µmol.min^{-1}.mg^{-1} and 70.4 mM on pNPP for *P. aeruginosa* PseA (Gaur *et. al.*, 2008), among others.

The transesterification potential and the rates at which this is achieved for the enzyme would also be necessary to establish as this would help to understand the behaviour of the enzyme under conditions in which the enzyme will be employed, in line with the goals of the study. Once the performance characteristics of the enzyme are established, chromosomal introduction of the lipase (and its chaperone) could be considered for expression of the genes instead of the plasmid system used here. This would potentially alleviate the need for monitored induction and could rectify the molar ratio issue of lipase to chaperone as well.

Additionally, depending on the performance of the enzyme during transesterification, surface display of the enzyme could also be pursued, offering benefits such as enzyme stability, re-use, and avoids issues of catalyst recovery. For example, Narita *et. al*,. (2006) developed an *E. coli* cell surface display system by employing PgsA as an anchoring motif, and displayed α-amylase from *Streptococcus bovis* 148, and lipase B (CALB) from *C. antarctica*. CALB-displaying *E. coli* cells successfully catalyzed enantio-selective transesterification, suggesting that the proposed method is feasible.

Having the lipase expressed this way would further allow for testing of the envisaged system with glycerol present, and changes (metabolic or transcriptional, or both) to the host to increase flux for glycerol and increase ethanol production could be made. These could include changes such as upregulating genes *gldA* and *dhaKLM* (DhaK pathway) as well as *adhE* (Yazdani & Gonzalez, 2008). Monitoring of gene transcription changes could be performed utilising quantitative transcriptomics analyses (Next Generation Sequencing approach) and modelling to determine the main fluxes through the system at a transcript level, thereby identifying key points within the different pathways for subsequent, permanent genetic modifications of the microbial genome in order to have optimal biodiesel production.

Also, a biofilm forming strain, e.g. Nissle 1917, could be considered. Biofilm-growing organisms are self-regenerating, spatially and metabolically well organized, and are in general less affected by toxic substrates and/or products. Their overall robustness makes them attractive living catalysts (Halan *et. al.*, 2012), as they combine the benefits of co-factor regeneration and catalyst stability of whole-cells over free enzymes. *E. coli* Nissle 1917 as a biocatalyst is of interest as the strain is commercially available as probiotic preparation Mutaflor®, and has yet to be used as a biocatalyst. Nissle 1917 is also a typical *E. coli* strain in terms of metabolic capacity (Sonnenborn & Schulze, 2009). Further, a draft assembly of the 5.023-Mbp high-quality draft assembly of the *E. coli* strain Nissle 1917 genome was announced by Cress *et. al.*, (2013). The availability of the data would enable comparative genomics analysis and model-guided predictions of genetic manipulations from re-annotation and metabolic reconstructions.

Conclusion

Design considerations with the intention to determine enzyme activity were sufficient in leading to the reflection that the catalytic amount of enzyme should be below 0.00729 µg for the substrate concentrations employed. Saturating substrate concentrations should be considered to establish the Michaelis-Menten constants for the enzyme under conditions which foster hydrolysis. The lipase's transesterification capacity also needs to be evaluated. The knowledgebase generated from this initial study can be used to explore additional considerations for refinement of how the system can be improved, such as chromosomal introduction of the lipase to regulate expression, surface display of the enzyme, metabolic pathway alterations as well as different strain. With these considerations, the ideal bacterial-biodiesel system could be produced.

11 REFERENCES

AASA PublicAffairs, 2016. Fuel price breakdown - what do you pay for? *Online*, p.1. Available at: https://www.aa.co.za/about/press-room/press-releases/fuel-price-breakdown.html.

ABG Inc., 2013. *U.S. Soybean Export Council Inc.*Online. Available at: http://www.asaimsea.com/download_doc.php?file=Glycerin Market Analysis_Final.pdf.

African Centre for Biosafety, 2008. *Agrofuels in South Africa: projects, players & poverty*. Online. Available at: http://www.globalbioenergy.org/uploads/media/0812_The_African_Centre_for_Biosafety_-_Agrofuels_in_South_Africa.pdf.

Angkawidjaja, C. & Kanaya, S., 2006. Family I.3 lipase: bacterial lipases secreted by the type I secretion system. *Cellular and Molecular Life Sciences CMLS*, 63(23), pp.2804–2817.

Arpigny, J.L. & Jaeger, K.E., 1999. Bacterial lipolytic enzymes: classification and properties. *Biochemical Journal*, 343(Pt 1), pp.177–183.

Ayoub, M. & Abdullah, A.Z., 2012. Critical review on the current scenario and significance of crude glycerol resulting from biodiesel industry towards more sustainable renewable energy industry. *Renewable and Sustainable Energy Reviews*, 16(5), pp.2671–2686.

Babajide, O., 2013. Sustaining biodiesel production via value-added applications of glycerol. *Journal of Energy*, 2013, pp.1–7.

Ban, K. *et. al.*, 2001. Whole cell biocatalyst for biodiesel fuel production utilizing *Rhizopus oryzae* cells immobilized within biomass support particles. *Biochemical Engineering Journal*, 8(1), pp.39–43.

Barbirato, F. *et. al.*, 1996. 3-Hydroxypropionaldehyde: an Inhibitory Metabolite of Glycerol Fermentation to 1,3-Propanediol by Enterobacterial species. *Applied and Environmental Microbiology*, 62(4), pp.3–7.

Bisswanger, H., 2014. Enzyme assays. *Perspectives in Science*, 1(1–6), pp.41–55.

Bizzini, A. *et. al.*, 2010. Glycerol Is Metabolized in a Complex and Strain-Dependent Manner in

Enterococcus faecalis . *Journal of Bacteriology*, 192(3), pp.779–785.

Blankschien, M.D., Clomburg, J.M. & Gonzalez, R., 2010. Metabolic engineering of *Escherichia coli* for the production of succinate from glycerol. *Metabolic engineering*, 12(5), pp.409–19.

Caesar, W.K., Riese, J. & Seitz, T., 2007. Betting on biofuels. *The McKinsey Quarterly*, 2, pp.53–63.

Chen, H.-C. *et. al.*, 2011. Continuous production of lipase-catalyzed biodiesel in a packed-bed reactor: optimization and enzyme reuse study. *Journal of biomedicine & biotechnology*, 2011, pp.5–10.

Cole, S.T. *et. al.*, 1988. Nucleotide sequence and gene-polypeptide relationships of the glpABC operon encoding the anaerobic sn-glycerol-3-phosphate dehydrogenase of *Escherichia coli* K-12. *Journal of bacteriology*, 170(6), pp.2448–2456.

Courtright, J., 1976. Induction of enzymes of the glycerophosphate pathway in leu-5 mutants of *Neurospora crassa*. *Biochemical Genetics*, 14(11–12), pp.1057–1063.

Cress, B., Linhardt, R. & Koffas, M., 2013. Draft genome sequence of *Escherichia coli* Strain Nissle 1917 (serovar O6: K5: H1). *Genome announcements*, 1(2), pp.1–2.

Dahiya, P. *et. al.*, 2010. Characterization of an extracellular alkaline lipase from *Pseudomonas mendocina* M-37. *Journal of Basic Microbiology*, 50(5), pp.420–426.

Dalal, S. *et. al.*, 2008. Purification and properties of the alkaline lipase from *Burkholderia cepacia* A.T.C.C. 25609. *Biotechnology and Applied Biochemistry*, 51(1), pp.23–31.

Datta, N., 1985. *Escherichia coli* as a genetic tool. *The Journal of hygiene*, 95(3), pp.611–8.

Datta, S., Christena, L.R. & Rajaram, Y.R.S., 2012. Enzyme immobilization: an overview on techniques and support materials. *3 Biotech*, 3(1), pp.1–9.

Department of Energy, R. of S.A., 2013. INDUSTRIAL STRATEGY UPDATE ON THE BIOFUELS.

Department of Minerals and Energy, 2007. Biofuels Industrial Strategy of the Republic of South Africa. , (December), pp.1–27.

Department of Minerals and Energy, 2012. *Government Gazette Staatskoerant*,

Department of Minerals and Energy, 2014. *Government Gazette Staatskoerant*,

Dharmadi, Y., 2006. Anaerobic fermentation of glycerol by *Escherichia coli*: a new platform for metabolic engineering. *Biotechnology and Bioengineering*, 94(5), pp.821–829.

Drożdżyńska, A. Leja, K. Czaczyk, K., 2011. Biotechnological production of 1 , 3-propanediol from crude glycerol. *BioTechnologia: Journal of Biotechnology, Computational Biology and Bionanotechnology*, 92(1), pp.92–100.

Durnin, G. *et. al.*, 2009. Understanding and harnessing the microaerobic metabolism of glycerol in *Escherichia coli*. *Biotechnology and bioengineering*, 103(1), pp.148–61.

EMD Biosciences, 2012. *Duet Vectors*, User Protocol TB340 Rev. F 0211JN. Online. Available at: http://www.merckmillipore.com/ZA/en/product/pETDuet™-1-DNA---Novagen,EMD_BIO-71146?ReferrerURL=https%3A%2F%2Fwww.google.com%2F&bd=1.

Fakas, S., Makri, A., Bellou, S., and Aggelis, G., 2009. *Microbial Conversions of Raw Glycerol* 1st ed. G. Aggelis, ed., New York: Nova Biomedical Books.

Fjerbaek, L., Christensen, K. V & Norddahl, B., 2009. A review of the current state of biodiesel production using enzymatic transesterification. *Biotechnology and bioengineering*, 102(5), pp.1298–315.

Food Agriculture and Natural Resources Policy Analysis Network, 2009. Competence Platform on Energy Crop and Agroforestry Systems for Arid and Semi-arid Ecosystems. In *PERFORMANCE EVALUATION OF NATIONAL AND REGIONAL BIOFUELS POLICIES IN SSA*. pp. 1–35.

Förster, A.H. & Gescher, J., 2014. Metabolic Engineering of *Escherichia coli* for Production of Mixed-Acid Fermentation End Products. *Frontiers in Bioengineering and Biotechnology*, 2, p.16.

Fujita, Y. *et. al.*, 2002. Direct and Efficient Production of Ethanol from Cellulosic Material with a Yeast Strain Displaying Cellulolytic Enzymes Direct and Efficient Production of Ethanol from Cellulosic Material with a Yeast Strain Displaying Cellulolytic Enzymes. *Applied and*

environmental microbiology, 26, pp.668–673.

Fukuda, H. *et. al.*, 2008. Whole-cell biocatalysts for biodiesel fuel production. *Trends in biotechnology*, 26(12), pp.668–73.

Gaur, R., Gupta, A. & Khare, S.K., 2008. Purification and characterization of lipase from solvent tolerant *Pseudomonas aeruginosa* PseA. *Process Biochemistry*, 43(10), pp.1040–1046.

Gilder, A. & Mamkeli, M., 2014. Biofuels in South Africa. *Environment Ensight*. Available at: https://www.ensafrica.com/news/biofuels-in-South-Africa?Id=1339 [Accessed March 17, 2016].

Gonzalez, R. *et. al.*, 2008. A new model for the anaerobic fermentation of glycerol in enteric bacteria: trunk and auxiliary pathways in *Escherichia coli*. *Metabolic engineering*, 10(5), pp.234–45.

Greve, N., 2015. DoE goes to ground over mandatory blending of biofuels deadline. *Creamer Media's Engeneering News*, p.1.

Gupta, A. *et. al.*, 2009. Anaerobic fermentation of glycerol in *Paenibacillus macerans*: metabolic pathways and environmental determinants. *Applied and environmental microbiology*, 75(18), pp.5871–83.

Halan, B., Buehler, K. & Schmid, A., 2012. Biofilms as living catalysts in continuous chemical syntheses. *Trends in biotechnology*, 30(9), pp.453–465.

Hara, F., Nakashima, T. & Fukuda, H., 1997. Comparative study of commercially available lipases in hydrolysis reaction of phosphatidylcholine. *Journal of the American Oil Chemists' Society*, 74(9), pp.1129–1132.

Hasan, F., Shah, A.A. & Hameed, A., 2006. Industrial applications of microbial lipases. *Enzyme and Microbial Technology*, 39(2), pp.235–251.

Hasan, F., Shah, A.A. & Hameed, A., 2009. Methods for detection and characterization of lipases: A comprehensive review. *Biotechnology advances*, 27(6), pp.782–98.

He, B.-Q. *et. al.*, 2003. The effect of ethanol blended diesel fuels on emissions from a diesel engine. *Atmospheric Environment*, 37(35), pp.4965–4971.

Hill, J. *et. al.*, 2006. Environmental, economic, and energetic costs and benefits of biodiesel and ethanol biofuels. *Proceedings of the National Academy of Sciences of the United States of America*, 103(30), pp.11206–10.

Ihara, F. *et. al.*, 1992. Requirement in trans of the downstream limL gene for activation of lactonizing lipase from *Pseudomonas* sp. 109. *Journal of Fermentation and Bioengineering*, 73(5), pp.337–342.

IncBio, 2016. Biodiesel and Glycerine Distillation. Available at: http://incbio.com/technologies_biodiesel_glycerine_distillation.html [Accessed March 17, 2016].

Institute for Supply Management, 2015. *Second quarter commodities 2015 report*, New York.

Islam, A. *et. al.*, 2013. Studies on design of heterogeneous catalysts for biodiesel production. *Process Safety and Environmental Protection*, 91(1–2), pp.131–144.

Jaeger, K.-E. *et. al.*, 1994. Bacterial lipases. *FEMS Microbiology Reviews*, 15(1), pp.29–63.

Jaeger, K., 1998. Microbial lipases form versatile tools for biotechnology. *Trends in Biotechnology*, 16(9), pp.396–403.

Jaeger, K.-E. & Eggert, T., 2002. Lipases for biotechnology. *Current Opinion in Biotechnology*, 13(4), pp.390–397.

Jaeger, K.E., Dijkstra, B.W. & Reetz, M.T., 1999. Bacterial biocatalysts: molecular biology, three-dimensional structures, and biotechnological applications of lipases. *Annual review of microbiology*, 53(1), pp.315–51.

Jinwal, U.K. *et. al.*, 2003. Purification and characterization of an alkaline lipase from a newly isolated *Pseudomonas mendocina* PK-12CS and chemoselective hydrolysis of fatty acid ester††CDRI Communication No. 6212. *Bioorganic & Medicinal Chemistry*, 11(6), pp.1041–1046.

Johnson, D.T. & Taconi, K.A., 2007. The glycerin glut: Options for the value-added conversion of crude glycerol resulting from biodiesel production. *Environmental Progress*, 26(4), pp.338–348.

Jose, J., Maas, R.M. & Teese, M.G., 2012. Autodisplay of enzymes--molecular basis and

perspectives. *Journal of biotechnology*, 161(2), pp.92–103.

Joseph, B., Ramteke, P.W. & Thomas, G., 2008. Cold active microbial lipases: some hot issues and recent developments. *Biotechnology advances*, 26(5), pp.457–70.

Joubert, R., 2012. Fuel price to continue upward march. *Farmer's Weekly*. Online. Available at: http://www.farmersweekly.co.za/news.aspx?id=16606&h=Fuel-price-to-continue-upward-march

Katryniok, B. *et. al.*, 2011. Selective catalytic oxidation of glycerol: perspectives for high value chemicals. *Green Chemistry*, 13(8), pp.1960–1979.

Kenar, J., 2007. Glycerol as a platform chemical: Sweet opportunities on the horizon? *Lipid Technology*, 19(11), pp.249–253.

Kousoulidou, M. *et. al.*, 2008. Effect of biodiesel and bioethanol on exhaust emissions. *European Topic Centre on Air Pollution and Climate Change*, 5(February), pp.1–52.

Lam, M.K., Lee, K.T. & Mohamed, A.R., 2010. Homogeneous, heterogeneous and enzymatic catalysis for transesterification of high free fatty acid oil (waste cooking oil) to biodiesel: a review. *Biotechnology advances*, 28(4), pp.500–18.

Lee, C.H. & Lee, K.H., 2007. An experimental study of the combustion characteristics in SCCI and CAI based on direct-injection gasoline engine. *Experimental Thermal and Fluid Science*, 31(8), pp.1121–1132.

Letete, T., 2009. *Multiobjective modelling of biofuel supply systems*. M.Sc.(Chemical Engineering), University of Cape Town.

Letete, T. & Blottnitz, H. von, 2009. Biofuel Policies in South Africa : A critical analysis.Online. Available at: http://www.erc.uct.ac.za/sites/default/files/image_tool/images/119/Papers-2012/12Letete-Blottnitz-biofuel_policies.pdf.

Li, Z. *et. al.*, 2011. Simple defined autoinduction medium for high-level recombinant protein production using T7-based *Escherichia coli* expression systems. *Applied Microbiology and Biotechnology*, 91(4), pp.1203–1213.

Liu, H.-J. *et. al.*, 2007. Microbial production of 1,3-propanediol from glycerol by *Klebsiella*

pneumoniae under micro-aerobic conditions up to a pilot scale. *Biotechnology Letters*, 29(8), pp.1281–1285.

Miller-Klein Associates, 2006. Impact of Biodiesel Production on the Glycerol Market What is glycerol., Online. (October), pp.1–5. Available at: http://www.hgca.com/publications/documents/Impact_of_Biodiesel_Production_on_the_Glycerol_Market.pdf

Morgan, J., 2013. *Carbohydrate Metabolism in Cultured Cells* M. J. Morgan, ed., Springer Science & Business Media, 2013.

Mu, Y., Xiu, Z. & Zhang, D., 2008. A combined bioprocess of biodiesel production by lipase with microbial production of 1, 3-propanediol by *Klebsiella pneumoniae*. *Biochemical Engineering Journal*, 40, pp.537–541.

Murarka, A. *et. al.*, 2008. Fermentative utilization of glycerol by *Escherichia coli* and its implications for the production of fuels and chemicals. *Applied and environmental microbiology*, 74(4), pp.1124–35.

Nagradova, N.K., 2008. *Foldases: Enzymes Catalyzing Protein Folding* N. K. Nagradova, ed., United States: Nova Science Publishers Inc.

Nantel, G. & Proulx, P., 1973. Lipase activity in *E. coli*. *Biochimica et Biophysica Acta (BBA) - Lipids and Lipid Metabolism*, 316(2), pp.156–161.

Narita, J. *et. al.*, 2006. Display of active enzymes on the cell surface of *Escherichia coli* using PgsA anchor protein and their application to bioconversion. *Applied microbiology and biotechnology*, 70(5), pp.564–72.

Nolte, M., 2007. *COMMERCIAL BIODIESEL PRODUCTION IN SOUTH AFRICA : A PRELIMINARY ECONOMIC FEASIBILITY STUDY*. M.Sc. (Chemical Engineering), University of Stellenbosch.

Oroz-Guinea, I. & García-Junceda, E., 2013. Enzyme catalysed tandem reactions. *Current opinion in chemical biology*, 17(2), pp.236–49.

Pagliaro, M. *et. al.*, 2007. Minireviews Glycerol Chemistry From Glycerol to Value-Added Products. , (May 2002), pp.4434–4440.

Partridge, J.D. *et. al.*, 2006. *Escherichia coli* transcriptome dynamics during the transition from anaerobic to aerobic conditions. *The Journal of biological chemistry*, 281(38), pp.27806–27815.

Paulo, G., Mack, M. & Contiero, J., 2009. Glycerol : A promising and abundant carbon source for industrial microbiology. *Biotechnology Advances*, 27(1), pp.30–39.

Pauwels, K., 2008. *Structure/function relationship of the lipase-foldase complex of Burkholderia glumae*. Vrije Universiteit Brussel.

Pencreac'h, G. & Baratti, J.C., 1996. Hydrolysis of p-nitrophenyl palmitate in n-heptane by the *Pseudomonas cepacia* lipase: A simple test for the determination of lipase activity in organic media. *Enzyme and Microbial Technology*, 18(6), pp.417–422.

Pencreac'h, G. & Baratti, J.C., 2001. Comparison of hydrolytic activity in water and heptane for thirty-two commercial lipase preparations. *Enzyme and Microbial Technology*, 28(4–5), pp.473–479.

Pereira, C.O. *et. al.*, 2014. SnSO4 as Catalyst for Simultaneous Transesterification and Esterification of Acid Soybean Oil. *Journal of the Brazilian Chemical Society*, 25, pp.2409–2416.

Quyen, D.T., Schmidt-Dannert, C. & Schmid, R.D., 1999. High-Level Formation of Active *Pseudomonas cepacia* Lipase after Heterologous Expression of the Encoding Gene and Its Modified Chaperone in *Escherichia coli* and Rapid In Vitro Refolding. *Applied and Environmental Microbiology*, 65(2), pp.787–794.

Radiant Insights Inc, 2016. *Glycerol Market Analysis, Service And Price Trend to 2022*, Online. Available at: http://radiantinsightsinc.blogspot.co.za/2016/04/glycerol-market-analysis-service-and.html.

Ragauskas, A.J. *et. al.*, 2006. The Path Forward for Biofuels and Biomaterials. *Science*, 311(5760), pp.484–489.

Ranganathan, S.V., Narasimhan, S.L. & Muthukumar, K., 2008. An overview of enzymatic production of biodiesel. *Bioresource technology*, 99(10), pp.3975–81.

Ribeiro, N. *et. al.*, 2007. The role of additives for diesel and diesel blended (ethanol or biodiesel)

fuels: A review. *Energy and Fuels*, 21(4), pp.2433–2445.

Romero, C.M., Baigori, M.D. & Pera, L.M., 2007. Catalytic properties of mycelium-bound lipases from *Aspergillus niger* MYA 135. *Applied Microbiology and Biotechnology*, 76(4), pp.861–866.

Rosenau, F. & Jaeger, K., 2000. Bacterial lipases from *Pseudomonas*: regulation of gene expression and mechanisms of secretion. *Biochimie*, 82(11), pp.1023–32.

Rosenau, F., Tommassen, J. & Jaeger, K.-E., 2004. Lipase-Specific Foldases. *ChemBioChem*, 5(2), pp.152–161.

Sani, Y.M., Daud, W.M.A.W. & Abdul Aziz, A.R., 2014. Activity of solid acid catalysts for biodiesel production: A critical review. *Applied Catalysis A: General*, 470, pp.140–161.

Schmid, R.D. & Verger, R., 1998. Lipases: Interfacial Enzymes with Attractive Applications. *Angewandte Chemie International Edition*, 37(12), pp.1608–1633.

Schmid, U. *et. al.*, 1999. Highly selective synthesis of 1,3-oleoyl-2-palmitoylglycerol by lipase catalysis. *Biotechnology and Bioengineering*, 64(6), pp.678–684.

Shams Yazdani, S. & Gonzalez, R., 2008. Engineering *Escherichia coli* for the efficient conversion of glycerol to ethanol and co-products. *Metabolic engineering*, 10(6), pp.340–51.

Shangguan, J.-J. *et. al.*, 2011. Expression and Characterization of a Novel Lipase from *Aspergillus fumigatus* with High Specific Activity. *Applied Biochemistry and Biotechnology*, 165(3), pp.949–962.

Sharma, R., Chisti, Y. & Chand, U., 2001. Production, purification, characterization and applications of lipases. *Biotechnology advances*, 19, pp.627–662.

Sheldon, R. a & van Pelt, S., 2013. Enzyme immobilisation in biocatalysis: why, what and how. *Chemical Society reviews*, 42(15), pp.6223–35.

Shi, X. *et. al.*, 2006. Emission reduction potential of using ethanol–biodiesel–diesel fuel blend on a heavy-duty diesel engine. *Atmospheric Environment*, 40(14), pp.2567–2574.

Shibata, H., Kato, H. & Oda, J., 1998a. Random mutagenesis on the *Pseudomonas* lipase activator

protein, LipB: exploring amino acid residues required for its function. *Protein Engineering* , 11(6), pp.467–472.

Shibata, H., Kato, H. & Oda, J., 1998b. Molecular Properties and Activity of Amino-Terminal Truncated Forms of Lipase Activator Protein. *Bioscience, Biotechnology, and Biochemistry*, 62(2), pp.354–357.

da Silva, G.P., Mack, M. & Contiero, J., 2009. Glycerol: a promising and abundant carbon source for industrial microbiology. *Biotechnology advances*, 27(1), pp.30–9.

Sivasamy, A. *et. al.*, 2009. Catalytic applications in the production of biodiesel from vegetable oils. *ChemSusChem*, 2(4), pp.278–300.

Sonnenborn, U. & Schulze, J., 2009. The non-pathogenic *Escherichia coli* strain Nissle 1917 – features of a versatile probiotic. , (October), pp.122–158.

Sotenko, M. V *et. al.*, 2012. Tandem transformation of glycerol to esters. *Journal of biotechnology*, 162(4), pp.390–7.

Sprague, G.F. & Cronan, J.E., 1977. Isolation and characterization of *Saccharomyces cerevisiae* mutants defective in glycerol catabolism. *Journal of bacteriology*, 129(3), pp.1335–1342.

Straathof, A.J.J., Panke, S. & Schmid, A., 2002. The production of fine chemicals by biotransformations. *Current opinion in biotechnology*, 13(6), pp.548–56.

Svanberg, L. *et. al.*, 2013. Pre-crystallization to control the fat crystal structure and its relation to storage stability in dark chocolate. *InsideFood Symposium, 9-12 April 2013, Leuven, Belgium*, (April), pp.9–12. Available at: http://www.insidefood.eu/INSIDEFOOD_WEB/UK/WORD/proceedings/090O.pdf.

Szczęsna Antczak, M. *et. al.*, 2009. Enzymatic biodiesel synthesis – Key factors affecting efficiency of the process. *Renewable Energy*, 34(5), pp.1185–1194.

Tan, T. *et. al.*, 2010. Biodiesel production with immobilized lipase: A review. *Biotechnology advances*, 28(5), pp.628–34.

Terpe, K., 2003. Overview of tag protein fusions: from molecular and biochemical fundamentals to

commercial systems. *Applied Microbiology and Biotechnology*, 60(5), pp.523–533.

Tom, G.D., Viswanath-Reddy, M. & Howe, H.B.J., 1978. Effect of carbon source on enzymes involved in glycerol metabolism in *Neurospora crassa*. *Archives of microbiology*, 117(3), pp.259–263.

TransparencyMarketResearch, 2013. Glycerol market expected to reach $2.1 billion in 2018. *Biodiesel Magazine*. Online. Available at: http://www.biodieselmagazine.com/articles/9004/report-glycerol-market-expected-to-reach-2-1-billion-in-2018.

Trinh, C.T. & Srienc, F., 2009. Metabolic engineering of *Escherichia coli* for efficient conversion of glycerol to ethanol. *Applied and environmental microbiology*, 75(21), pp.6696–705.

Uttatree, S., Winayanuwattikun, P. & Charoenpanich, J., 2010. Isolation and Characterization of a Novel Thermophilic-Organic Solvent Stable Lipase From *Acinetobacter baylyi*. *Applied Biochemistry and Biotechnology*, 162(5), pp.1362–1376.

Veljković, V.B., Avramović, J.M. & Stamenković, O.S., 2012. Biodiesel production by ultrasound-assisted transesterification: State of the art and the perspectives. *Renewable and Sustainable Energy Reviews*, 16(2), pp.1193–1209.

Vorderwülbecke, T., Kieslich, K. & Erdmann, H., 1992. Comparison of lipases by different assays. *Enzyme and Microbial Technology*, 14(8), pp.631–639.

Walker, A.J. & Bruce, N.C., 2004. Combined biological and chemical catalysis in the preparation of oxycodone. *Tetrahedron*, 60(3), pp.561–568.

Wang, B. *et. al.*, 2013. A new solid base catalyst for the transesterification of rapeseed oil to biodiesel with methanol. *Fuel*, 104, pp.698–703.

Wang, J.-X. *et. al.*, 2012. Production of biodiesel through transesterification of soybean oil using lithium orthosilicate solid catalyst. *Fuel Processing Technology*, 104, pp.167–173.

Wang, Z.X. *et. al.*, 2001. Glycerol production by microbial fermentation: a review. *Biotechnology advances*, 19(3), pp.201–23.

West, A.H., Posarac, D. & Ellis, N., 2008. Assessment of four biodiesel production processes using HYSYS.Plant. *Bioresource technology*, 99(14), pp.6587–601.

White, N. & Callahan, C., 2013. Vermont On-Farm Oilseed Enterprises : Production Capacity and Breakeven Economics. Online, (July). Available at: http://www.vsjf.org/assets/files/VBI/VT Oilseed Enterprises_July_2013.pdf.

Xiao, M., Qi, C. & Obbard, J.P., 2011. Biodiesel production using *Aspergillus niger* as a whole-cell biocatalyst in a packed-bed reactor. *GCB Bioenergy*, 3(4), pp.293–298.

Xie, G. *et. al.*, 2008. Esterase SeE of *Streptococcus equi* ssp. equi is a novel nonspecific carboxylic ester hydrolase. *FEMS microbiology letters*, 289(2), pp.181–6.

Xie, W. & Fan, M., 2014. Biodiesel production by transesterification using tetraalkylammonium hydroxides immobilized onto SBA-15 as a solid catalyst. *Chemical Engineering Journal*, 239, pp.60–67.

Yang, F., Hanna, M. a & Sun, R., 2012. Value-added uses for crude glycerol--a byproduct of biodiesel production. *Biotechnology for Biofuels*, 5(1), p.13.

Yazdani, S.S. & Gonzalez, R., 2007. Anaerobic fermentation of glycerol: a path to economic viability for the biofuels industry. *Current opinion in biotechnology*, 18(3), pp.213–9.

Young, C.L., Britton, Z.T. & Robinson, A.S., 2012. Recombinant protein expression and purification: A comprehensive review of affinity tags and microbial applications. *Biotechnology Journal*, 7(5), pp.620–634.

12 APPENDIX

12.1 Gene optimisation and syntheses

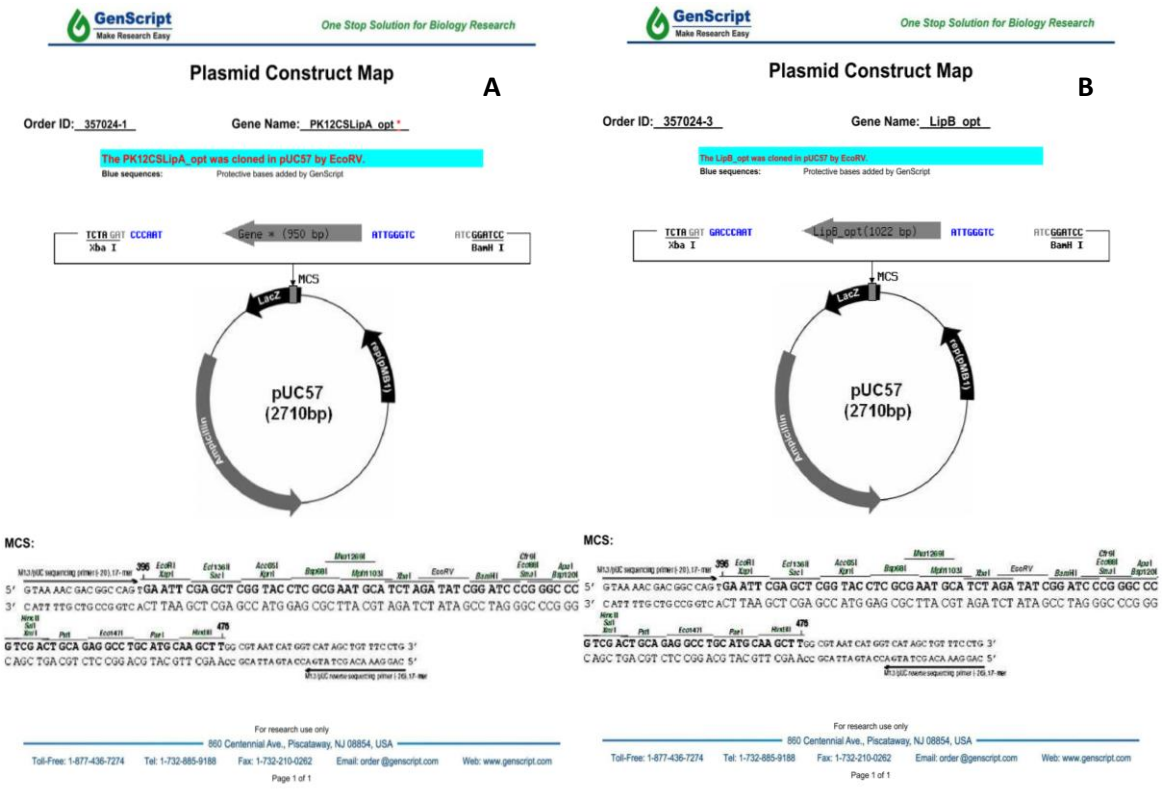


Figure: Genes (LipA and LipB) optimised and synthesised by GenScript®. (A) LipA, (B) LipB. Genes were delivered as shown in the maps above, cloned into a pUC57 vector.

12.2 LipA sequences

Original sequence:

>ENA|AAM14701|AAM14701.1 *Pseudomonas mendocina* **LipA** : Location:1..936

ATGAACAAGAACAAAACCTTGCTCGCCCTCTGTCTCGGAAGCGCCCTCGCGCTTTCCGGT
CAGGCATTCGCTGCCACCGGCAGCGGCTATACCGCCACGAAGTACCCAATCGTCCTCACC
CACGGCATGCTGGGTTTCGACAGCCTATTGGGCATCGACTACTGGTACGGCATCCCCAGC
GCTTTGCGCCGTGACGGCGCGCAGGTCTACATCACCGAAGTCAGCCAACTCAACACTTCC
GAACTGCGTGGCGAGGAACTGCTGGCCCAGGTCGAGGAAATCGTCGCCATCAGCGGCAA
GCCGAAGGTCAACCTGATCGGCCACAGCCACGGCGGACCGACCATCCGTTACGTGGCAG
GCGTGCGGCCGGACCTGATCGCCTCGGTCACCAGCGTCGGCGCGCCACACAAGGGCTCG
GACGTCGCCGACCTGATCCGCAAGGTTCCCGAGGGTTCATCCGGTGAGGCCATAATTGCC
GGCTTGGTGAACGCCATGGGCGCGTTCATCAACTTCGTCTCCGGCAGTTCCAGCACCGCT

CCGCAGAACTCCCTGGGTTCGCTGGAATCGCTCAACAGCGAGGGCGCGGCCCGCTTCAA
TGCCAAGTTCCCTCAAGGCATACCGACCACCGCGTGCGGCGAAGGCGCCTACAAGGTCA
ACGGCGTGCGCTACTACTCCTGGAGCGGCACCAGCCCACTGACCAATCCACTGGACGTG
AGCGACGCCATGATGGGCGCCGGCTCGCTGGCCTTCAGCGGACCCAATGACGGGCTGGT
CGGACGCTGCAGCTCGCACCTGGGGATGGTGATCCGCGACGACTACCGCATGAACCATC
TGGACGAGGTCAACCAGTTCATGGGGCTGACCAGCCTGTTCGAGACCGATCCGGTCAGC
GTCTACCGCCAGCACGCGAACCGATTGAAGAACGCGGGGCTCTGA

Codon optimised sequence (from GenScript®):

GGATCCATGAATAAAAATAAAACGCTGCTGGCTCTGTGTCTGGGCTCGGCACTGGCTCTG
TCGGGTCAGGCATTTGCGGCTACGGGCTCAGGTTATACCGCCACGAAATACCCGATTGTG
CTGACCCACGGCATGCTGGGTTTTGATTCGCTGCTGGGCATTGACTATTGGTACGGTATC
CCGTCAGCTCTGCGTCGCGATGGTGCACAGGTCTATATCACCGAAGTGTCGCAACTGAAC
ACGAGCGAACTGCGTGGTGAAGAACTGCTGGCCCAGGTGGAAGAAATTGTTGCAATCTC
CGGCAAACCGAAAGTGAATCTGATTGGTCATTCACACGGCGGTCCGACCATCCGTTACGT
GGCTGGCGTTCGCCCGGATCTGATTGCTTCCGTCACGTCAGTGGGTGCACCGCACAAAGG
TTCTGATGTTGCAGACCTGATCCGCAAAGTCCCGGAAGGCAGCTCTGGTGAAGCAATTAT
CGCTGGCCTGGTGAACGCGATGGGTGCCTTTATTAATTTCGTTAGTGGCAGTTCCTCAAC
CGCACCGCAGAACTCGCTGGGCAGCCTGGAATCTCTGAACAGTGAGGGTGCGGCCCGTT
TTAATGCAAAATTCCCGCAAGGTATCCCGACCACGGCATGCGGCGAAGGTGCATATAAA
GTTAACGGCGTCCGCTATTACTCTTGGAGTGGCACCAGCCCGCTGACGAATCCGCTGGAT
GTTAGTGACGCAATGATGGGTGCTGGTTCCCTGGCATTCTCAGGTCCGAATGATGGCCTG
GTCGGTCGTTGTTCGAGCCATCTGGGTATGGTTATTCGTGATGACTACCGCATGAACCAC
CTGGACGAAGTTAATCAATTTATGGGTCTGACCAGCCTGTTCGAAACGGACCCGGTTAGC
GTTTATCGTCAACATGCCAATCGCCTGAAAAATGCTGGTCTGTGAGCGGCCGC

12.3 LipB sequences

>ENA|AY091666|AY091666.1 Pseudomonas mendocina LipA (lipA) and LipB (lipB) genes, complete cds

GATCACACCAGAAGGCGAGGCCCGGCTGCGCGCCGAATTGCACGAACTGTGGCATGTCA
GGCGACCACAGGTTACCCAGTCGGTCAGCGAAGCCGCCGCCCAGGGCGACCGTTCGGAA
AACGCCGAGTACACCTACGGCAAGAAAATGCTGCGCGAGATCGACAGCCGTGTTCGCTT
TCTGACCAAGCGTCTGGAAAAGCTGAAAGTCGTCAGCGAACGACCCAGCGACCCCAACA
AGGTGTACTTCGGTGCCTGGGTGACGCTCGAGGATGAAGACGGTGAGCAGGCGCGCTAC

CGCATCGTCGGTCCCGATGAGCTGGACCTGCGGCAGGGCATGATCAGCATCGATTCGCC
GCTGGCTCGTGCGCTGGTGGGCAAAGCGCTGGACGCCGAGGTGCAGGTGCAAACGCCGA
CCGGGACAAAGCTCTGGTACGTCGTCGCCATCGATTACCCATGACCAGACAGTCAGATA
CAGAATTTTAGTCACGATAATCGCCGATCATGCAGACTTTAAACGCACAAGTTCTGTGAA
AAATCCAGATCATCACATAATCACCCACTCCGGCGTTTCGCTTCGTAACACGCACGCCCA
ACCCGCCTGATAGCGCAAGGCTACCCGCATCGTTGCGATCCGCCAGTTAGAGCGGACGC
TGCCGAGTGGGTCGGCTCTGGCACGATTGCTGCGCTGACGAGGCCGCAGTACGCGCCAC
GCGCGGTGAACGGCAAGGGACTGCCCCGAAAGCCCGATTCACAATCGAAGAGTGCGTCC
ATGAACAAGAACAAAACCTTGCTCGCCCTCTGTCTCGGAAGCGCCCTCGCGCTTTCCGGT
CAGGCATTCGCTGCCACCGGCAGCGGCTATACCGCCACGAAGTACCCAATCGTCCTCACC
CACGGCATGCTGGGTTTCGACAGCCTATTGGGCATCGACTACTGGTACGGCATCCCCAGC
GCTTTGCGCCGTGACGGCGCGCAGGTCTACATCACCGAAGTCAGCCAACTCAACACTTCC
GAACTGCGTGGCGAGGAACTGCTGGCCCAGGTCGAGGAAATCGTCGCCATCAGCGGCAA
GCCGAAGGTCAACCTGATCGGCCACAGCCACGGCGGACCGACCATCCGTTACGTGGCAG
GCGTGCGGCCGGACCTGATCGCCTCGGTCACCAGCGTCGGCGCGCCACACAAGGGCTCG
GACGTCGCCGACCTGATCCGCAAGGTTCCCGAGGGTTCATCCGGTGAGGCCATAATTGCC
GGCTTGGTGAACGCCATGGGCGCGTTCATCAACTTCGTCTCCGGCAGTTCCAGCACCGCT
CCGCAGAACTCCCTGGGTTCGCTGGAATCGCTCAACAGCGAGGGCGCGGCCCGCTTCAA
TGCCAAGTTCCCTCAAGGCATACCGACCACCGCGTGCGGCGAAGGCGCCTACAAGGTCA
ACGGCGTGCGCTACTACTCCTGGAGCGGCACCAGCCCACTGACCAATCCACTGGACGTG
AGCGACGCCATGATGGGCGCCGGCTCGCTGGCCTTCAGCGGACCCAATGACGGGCTGGT
CGGACGCTGCAGCTCGCACCTGGGGATGGTGATCCGCGACGACTACCGCATGAACCATC
TGGACGAGGTCAACCAGTTCATGGGGCTGACCAGCCTGTTCGAGACCGATCCGGTCAGC
GTCTACCGCCAGCACGCGAACCGATTGAAGAACGCGGGGCTCTGACGCAGCCGTTTCCTT
GAACCAGGCCGGGATCATCGATCCCGGCCGCTACCGAAAGGCGAGTCCATGAGCAGATC
CATCCTTCTGTTGCCGCTGGCCATCGCGCTGGGCCTGGGCTTCTTTATCGCCCGGCCCGAA
TCCACCGTGACGCCGGTGGCAGAAGCACCCGCATCGTCTCCCGCCGCCAACCTCACTGCC
GCTCGTCCTGCCCAGCGCACAGCGACCGGCGCGGCACCGCAGGTCATGGCGAAGCTGCC
CGCCTCCTTCAAGGGCACCGAGGTCGACGGCCAGTTCCAGCTGGACGCCGCCGGCAACC
TGATCATCGGTCCAGAGCTGCGTCAGCTGTTCGACTACTTCCTCAGCGCCATTGGCGAGG
AGCCGCTCAAACAGAGCATCGAGCGCCTGCGGCGCCATATCGCTGCGCAATTGCCGGAG
CCTGCCCAGGCGCAGGCACTTGCCGTGCTCAACCAATATCTCAACTACAAGCGCCAACTC
GTTGATTTCGAAGCGCAGCATCCTCGGGTTGCGGACCTCGCCTCGATGCGGGACCGGTTG
AGCGCCGTACGAGCGCTGCGCGCGCACGCGTTCGATCCGGCGATTCACCAGGCGTTTTTC
GGCCTGGAAGAAGCCTATGACCATTTCAGCCTGGAGCGGTTGGCCATCCGCTTCGATCCC
GCGCTGGACAGCGATGCCAAGGGTCGCGCCATCGACCAGCTGCGAGCCGGGCTGCCCGC
TGAACTGCAGGACCTGCTGATACCCCAGCTGCAGACCGAACTGCGTGAGCAGACCACCG

CCCTGCTGGCGAACGGAGCGGGTCCACAGCAGCTGCGGCAGCTGCGCCAACAACTGGTC
GGCAGCGAGGCAGCGGATCGGTTGGAGGCACTGGATCTGCAACGACGGCAGTGGCAGC
AGCGCGTCGCCAGCTACCAGCAGGAGCGTACCCGTATCGAAACCGCCCGCGGGCTGGAT
GAGGTCGAACGCCGTGCCGCCGTCGAACGGCTTGAAGCACAGCGCTTCAGCGACAGTGA
GCGCCTGCGTCTGCTCGCGGTTGTGCAGGAGGATCGGACTCGCTGAGCGAGTCAGTTGGC
GGCGGTCTTGCGGTCCGCCTCCAGCAGATAGCGTTCGCGCTGGTAGGCCAGGTAGTACTT
GTTGACGCTGTTGACGTAGGCCACGACTCCCATGCCGACCGTTTCCATGGCGATGCGCTC
GACCTGGAAGAACCACTGGTCCGGGTTGAGGCCGCGCCGCCTGGCTTCGGCGCGCATGC
TCTGCACGCGCTGCGGCCCCAGGTTGTAGGCAGCGAGGATGAACGCCATGCGCTCGCGC
TCGTTCAACCGCGGGCTGGCGAAATGGTTGCGACGGATATTGGCCAGGTACCTGGCGCT
GGCCTGCACATTGTTGTCCAGCTGCTGGACGTTGCTCACGCCCATTGCGCGCGCGGTCGC
CGGCGTCACCTGCATCAGGCCGGTGGCACCGCCTGCGCCTCGTGCGGCGGGGTTGAGCG
TCGACTCCTTGAACGCCAGCGCGGCCAGATTCAGCCAGTCCAGCTCGATCTGCTCGGCGT
AGCGCTGCAGGGTCGGGCGGACCTTTTCCAGGCGCTGGCGGCCAACCCCAGTGGATACT
GCACCTTGTACAGTCGCCGGTAGACCCGTTCGAAGGCTGCATCCTGATTGTCGGGAAGGT
CATAGTCCTTCAGGAACCGATCGGCACTGGCCCGGAGCATGCTGGCCTCCTTGCGCACGA
ACCAGTGCATGCTGGTCTTCTCGCCAAGACTCAGGTGCTGCTCGATGCGCAGCTTCGGCA
TGACCTTGGCCCAGCGCTGGGCGATGGTCTGCTCGACGACTGTCGCCGGGTAGACCCCGG
CCTGCACCATCTCCAGCACATCCTCCACCGCCAGCGTCGGGTCGACCCACTCGGCGACAA
TGGGGGCCAGCTTGCGCTCCATCAGCTGCTTGTTCAGCTGCGCCAGTGCGGGCCCGGCCG
CGCTGCCCGGCGGCAGCGCCAGGCTGCGCCCGGAGAGCTGTTCGAGGCGCTGGTAGCGC
GGCCCACCCTGGCGGCTGACCAGCACCAGGGCAACGTCGCTGACCACCGGTCGGCTGCG
GCTGATGCCCTTCATACCGGACTGTGGAAGCAGCTCCCCAGGTGCAACCAGATCGGCGG
CACGTCGATGAGCCGCTTCGAGGAAGTTCTCGACAATATCTTCATCGGCCGCCGGGAAG
GCGCAGCGCTGTACCAGCGTATCTTCGTCGTCTCGGCCTACAGCGGCATGACCAACCTGC
TGCTGGAGCACAAGAAGACCGGCGAGCCCGGCGTCTACCAACGCTTCGCCGATGCGCAG
AGCGAAGGTGCCTGGCGCGAAGCGCTGGAGGGTGTGCGCCAGCGCATGCTCGCCAAGAA
CGCCGAGCTGTTCAGTTCCGAGTACGAACTGCACGCCGCCAACCAGTTCATCAACTCGCG
CATCGACGATGCCAGCGAGTGCATGCACAGCCTGCAGAAGCTTTGCGCCTACGGCCACTT
CCAGCTCTCCGAACACCTGATGAAGGTGCGCGAGATGCTCGCTTCCCTCGGCGAAGCCCA
CAGCGCCTTCAACTCGGTGCTGGCGCTCAAGCAGCGCGGCGTCAACGCGCGCCTGGCCG
ACCTCACCGGCTGGCAGCAGGAAGCACCGCTGCCGTTCGAGGAGATGATTTCCAGCCAC
TTCGCCGGCTTCGACTTCAGCCGCGAACTGGTGGTCGCCACCGGTTACACCCATTGCGCC
GAAGGCCTGATGAACACCTTCGATC

Protein Sequence: (Translation acc. no.: AAM14702.1).

MSRSILLLPLAIALGLGFFIARPESTVTPVAEAPASSPAANLTAARPAQRTATGAAPQVMAKLP
ASFKGTEVDGQFQLDAAGNLIIGPELRQLFDYFLSAIGEEPLKQSIERLRRHIAAQLPEPAQAQ
ALAVLNQYLNYKRQLVDFEAQHPRVADLASMRDRLSAVRALRAHAFDPAIHQAFFGLEEAY
DHFSLERLAIRFDPALDSDAKGRAIDQLRAGLPAELQDLLIPQLQTELREQTTALLANGAGPQ
QLRQLRQQLVGSEAADRLEALDLQRRQWQQRVASYQQERTRIETARGLDEVERRAAVERLE
AQRFSDSERLRLLAVVQEDRTR

Sequence available on (http://www.uniprot.org/uniprot/Q8RKT5).

The sequence was back-translated using the EMBL BackTransSeq with *E. coli* K-12 (high) codon table:

ATGTCTCGTTCTATCCTGCTGCTGCCGCTGGCGATCGCGCTGGGTCTGGGTTTCTTCAT
CGCGCGTCCGGAATCTACCGTTACCCCGGTTGCGGAAGCGCCGGCGTCTTCTCCGGCG
GCGAACCTGACCGCGGCGCGTCCGGCGCAGCGTACCGCGACCGGTGCGGCGCCGCAG
GTTATGGCGAAACTGCCGGCGTCTTTCAAAGGTACCGAAGTTGACGGTCAGTTCCAG
CTGGACGCGGCGGGTAACCTGATCATCGGTCCGGAACTGCGTCAGCTGTTCGACTACT
TCCTGTCTGCGATCGGTGAAGAACCGCTGAAACAGTCTATCGAACGTCTGCGTCGTCA
CATCGCGGCGCAGCTGCCGGAACCGGCGCAGGCGCAGGCGCTGGCGGTTCTGAACCA
GTACCTGAACTACAAACGTCAGCTGGTTGACTTCGAAGCGCAGCACCCGCGTGTTGC
GGACCTGGCGTCTATGCGTGACCGTCTGTCTGCGGTTCGTGCGCTGCGTGCGCACGCG
TTCGACCCGGCGATCCACCAGGCGTTCTTCGGTCTGGAAGAAGCGTACGACCACTTCT
CTCTGGAACGTCTGGCGATCCGTTTCGACCCGGCGCTGGACTCTGACGCGAAAGGTC
GTGCGATCGACCAGCTGCGTGCGGGTCTGCCGGCGGAACTGCAGGACCTGCTGATCC
CGCAGCTGCAGACCGAACTGCGTGAACAGACCACCGCGCTGCTGGCGAACGGTGCGG
GTCCGCAGCAGCTGCGTCAGCTGCGTCAGCAGCTGGTTGGTTCTGAAGCGGCGGACC
GTCTGGAAGCGCTGGACCTGCAGCGTCGTCAGTGGCAGCAGCGTGTTGCGTCTTACC
AGCAGGAACGTACCCGTATCGAAACCGCGCGTGGTCTGGACGAAGTTGAACGTCGTG
CGGCGGTTGAACGTCTGGAAGCGCAGCGTTTCTCTGACTCTGAACGTCTGCGTCTGCT
GGCGGTTGTTCAGGAAGACCGTACCCGTTAA

Codon optimised sequence (GenScript®):

GGATCCATGTCACGCTCCATCCTGCTGCTGCCGCTGGCTATCGCACTGGGTCTGGGTT
TCTTCATCGCACGCCCGGAATCGACGGTTACGCCGGTGGCAGAAGCTCCGGCGAGCT
CTCCGGCAGCAAACCTGACCGCAGCTCGTCCGGCACAACGTACCGCTACGGGTGCAG
CACCGCAGGTTATGGCAAAACTGCCGGCCAGTTTTAAAGGCACGGAAGTCGATGGCC
AGTTCCAACTGGACGCAGCTGGCAATCTGATTATCGGTCCGGAACTGCGTCAGCTGTT
TGATTATTTCCTGTCAGCGATTGGTGAAGAACCGCTGAAACAGTCGATTGAACGTCTG
CGTCGCCATATCGCAGCACAGCTGCCGGAACCGGCACAGGCACAAGCTCTGGCAGTC
CTGAACCAGTATCTGAATTACAAACGTCAACTGGTCGATTTTGAAGCACAGCACCCG
CGCGTGGCTGATCTGGCAAGTATGCGTGACCGTCTGTCCGCAGTTCGTGCACTGCGTG
CACATGCATTCGATCCGGCAATTCACCAGGCGTTTTTCGGCCTGGAAGAAGCCTACGA
TCATTTTAGCCTGGAACGTCTGGCCATTCGCTTCGACCCGGCACTGGATTCTGACGCG
AAAGGCCGTGCCATCGATCAACTGCGCGCAGGTCTGCCGGCTGAACTGCAGGACCTG
CTGATCCCGCAGCTGCAAACCGAACTGCGTGAACAGACCACGGCTCTGCTGGCAAAC
GGTGCAGGTCCGCAGCAACTGCGTCAGCTGCGCCAGCAACTGGTGGGCTCCGAAGCA
GCTGATCGTCTGGAAGCGCTGGACCTGCAGCGTCGCCAATGGCAGCAACGCGTTGCG
AGCTATCAGCAAGAACGTACCCGCATCGAAACGGCCCGCGGTCTGGATGAAGTGGAA
CGTCGCGCGGCCGTTGAACGTCTGGAAGCGCAGCGCTTCAGTGATTCGGAACGCCTG
CGCCTGCTGGCAGTCGTCCAAGAAGACCGTACCCGCTAAGCGGCCGC

Translation of GenScript® sequence:

GSMNKNKTLLALCLGSALALSGQAFAATGSGYTATKYPIVLTHGMLGFDSLLGIDYWYG
IPSALRRDGAQVYITEVSQLNTSELRGEELLAQVEEIVAISGKPKVNLIGHSHGGPTIRYVA
GVRPDLIASVTSVGAPHKGSDVADLIRKVPEGSSGEAIIAGLVNAMGAFINFVSGSSSTAP
QNSLGSLESLNSEGAARFNAKFPQGIPTTACGEGAYKVNGVRYYSWSGTSPLTNPLDVSD
AMMGAGSLAFSGPNDGLVGRCSSHLGMVIRDDYRMNHLDEVNQFMGLTSLFETDPVSV
YRQHANRLKNAGL*AA